NASA CONTRACTOR REPORT
FINAL TECHNICAL REPORT

ADVANCED RADIATOR CONCEPTS UTILIZING HONEYCOMB PANEL HEAT PIPES

CONTRACT NAS 9-16581
W-30746

PREPARED FOR

NATIONAL AERONAUTICS AND SPACE ADMINISTRATION
LYNDON B. JOHNSON SPACE CENTER
HOUSTON, TX 77058

BY
G. L. FLEISCHMAN
S. J. PECK
H. J. TANZER

OCTOBER 1987

HUGHES AIRCRAFT COMPANY
ELECTRON DYNAMICS DIVISION
3100 WEST LOMITA BOULEVARD
P.O. BOX 2999
TORRANCE, CA 90509-2999

FOREWORD

This final report was prepared by the Hughes Aircraft Company, Electron Dynamics Division, for the NASA Johnson Space Center.

The purpose of this program was to determine the feasibility of using advanced honeycomb panel heat pipes as reliable, lightweight, and highly efficient radiators for future space station applications. The scope of this program included the design, fabrication, testing, and delivery of two prototype heat pipe panels, which are 24 inches (0.61 m) wide by 120 inches (3.0 m) long. The first panel was fabricated from stainless steel, and the second panel was fabricated from aluminum. This report describes the results of this development program.

This program was conducted in accordance with the Statement of Work in NASA Contract NAS9-16581. Mr. G.L. Fleischman was the Hughes, Electron Dynamics Division, Project Manager, while Mr. A. Basiulis served as both administrative and technical adviser at Hughes. Mr. H.J. Tanzer was responsible for the stainless steel honeycomb panel heat pipe design and analysis. It was manufactured to Hughes specifications by Astech Division of TRE Corporation, Santa Ana, California. Mr. S.J. Peck was responsible for the aluminum panel heat pipe design, analysis, fabrication, and testing. Technical direction was provided by Mr. J.G. Rankin, Technical Representative, NASA Johnson Space Center.

TABLE OF CONTENTS

TABLE OF CONTENTS (Continued)

LIST OF ILLUSTRATIONS

LIST OF ILLUSTRATIONS (Continued)

LIST OF ILLUSTRATIONS (Continued)

LIST OF TABLES

1.0 SUMMARY

The feasibility of fabricating and processing moderate temperature range (-20 to 65°C) lightweight heat pipe panels for advanced space radiator applications was investigated. Both a stainless steel honeycomb heat pipe panel and an aluminum heat pipe panel were developed.

An all-welded stainless steel honeycomb panel was the first prototype panel to be built. Methanol was selected as the working fluid because of its favorable thermal performance and vapor pressure characteristics over the temperature range of interest. It is also compatible with the stainless steel envelope material. The design goal was to build a 3.0 by 0.6 m (120.0 by 24.0 inch) heat pipe panel that would dissipate 1000 watts under 1-g test conditions.

The as-built configuration of the stainless steel prototype unit measured 3.0 m long by 0.6 m wide by 6.4 mm thick (120.0 by 24.0 by 0.25 inches) and weighed 9.2 kg/m^2 (1.9 lbm/ft^2), including the fluid fill. Test results using methanol as the working fluid demonstrated a maximum heat transport capacity of 600 watts at 50°C with a 25.4 mm (1.0 inch) heater along the center line of the panel. The heat pipe panel was isothermal to within ±1.5°C throughout the entire active surface. This performance fell short of the design goal of 1000 watts, primarily because the vapor holes were punched in every other crimp of the honeycomb core ribbon material, rather than every crimp as originally designed. However, analysis with a model correlated to the as-built panel test results predicts that the 1000-watt goal can be exceeded by simply including the correct number and distribution of vapor holes in the core ribbon material.

After the successful demonstration of the stainless steel honeycomb panel, a follow-on program was initiated by NASA-Johnson Space Center (JSC) to extend the panel heat pipe concept to lighter weight aluminum materials. A design goal of 7.0 kg/m^2 (1.43 lbm/ft^2) was selected for this effort.

During the preliminary design phase of this follow-on program, it was determined that an aluminum honeycomb panel design could not be fabricated in the

same manner as the stainless steel panel. Therefore, an alternative formed design approach was selected.

The formed design consists of two grooved facesheets: One facesheet is flat, and the other facesheet is formed into a dimpled pan. These facesheets are then resistance welded together. The end result is a heat pipe panel constructed with only three piece-parts: two facesheets and a fill tube. The grooves provide the necessary capillary pumping. Acetone was selected as the working fluid because of its favorable thermal characteristics and low vapor pressure over the -20 to 65°C temperature range. Methanol, which was used in the stainless panel, is not compatible with aluminum.

The aluminum prototype consists of 10 individual 0.6 by 0.3 m (24.0 by 12.0 inch) formed design panels. The ten individual panels (modules) are welded together, edge to edge, to form one large panel. The as-built panel dimensions are 3.1 m wide by 0.6 m long by 6.4 mm thick (122.0 by 24.0 by 0.15 inches). The panel weighs 7.1 kg/m^2 (1.46 lbm/ft^2), including the fluid fill. Test results using acetone as the working fluid demonstrated 1000 watts at 70°C with no evidence of dryout. Because the test facility heat sink was limited to this power level, it was not possible to determine the maximum transport capability. Individual panel ΔTs varied from a low of 0.1°C to a high of 7.7°C. The average panel ΔT was 2.3°C.

2.0 INTRODUCTION

Future space stations and space platforms will require highly efficient radiator systems for dissipation of several kilowatts of waste heat.[1] These radiator systems must be lightweight and simple to fabricate in space environments. The radiator system should consist of as few parts as possible to minimize payload weight and the amount of on-orbit assembly and repair. To meet these goals, NASA initiated the development of a space radiator system known as the Space Constructible Radiator (SCR). In an initial study on manned platforms[2] and an extension that focused on unmanned platforms,[3] development of constructible radiator technology was judged to have significant potential for heat rejection system-level improvements. This includes high-capacity heat pipes, efficient "plug in" contact heat exchangers, and lightweight efficient radiator fins.[4]

As the performance of large transport heat pipes continues to increase, a corresponding improvement must be made in the efficiency of longer radiating fins in order to take advantage of the heat pipe's maximum transport potential. Longer fins will, in turn, minimize the total number of transport heat pipes required for a given system size. The purpose of this program was to investigate the feasibility of using the honeycomb panel heat pipe concept[5] as a reliable, lightweight, and highly efficient space radiator fin.[6] The program objective was to design, fabricate, test, and evaluate a representative segment of a full-size radiator fin. The program consisted of two phases:

I. Stainless steel honeycomb panel development
II. Lightweight aluminum panel development.

The stainless steel heat pipe panel development is described in detail in References 6, 7, and 8. This report summarizes the stainless steel panel results and describes the work performed in the development of lightweight aluminum heat pipe radiator panels. The design goals were as follows:

- Operating temperature range: -20^{o} to $65^{o}C$ (-4.0^{o} to $149^{o}F$)
- Heat Rejection Requirements: 1000 watts
- Panel Size: 3.0 by 0.6 m (120.0 x 24.0 inches)
- Weight: ≤ 7.0 kg/m^2 (1.43 lbm/ft^2).

3.0 DESIGN CONCEPT

As the modular SCR system is presently perceived, a high-capacity transport heat pipe will receive waste heat from the central heat aquisition system of the space station and transport the heat to the heat pipe fins, which will then radiate the heat to space. The advantage of a heat pipe radiator fin over a solid radiator is that the heat pipe radiator has a fin efficiency (η_f) of approximately 1.0. Both radiator system weight and surface area can be minimized by the use of heat pipe fins.

Figure 3-1 illustrates the advantage of an aluminum heat pipe fin ($\eta_f \sim 1.0$) versus a solid aluminum fin ($\eta_f \sim 0.9$). This graph shows that, for high heat dissipation loads in space environments, large fin surface areas will be required. Moreover, for solid fin lengths (L_f) over 12.5 cm (4.9 inch) the heat pipe fin will radiate more heat and weigh significantly less than a solid fin.

First order performance and weight tradeoffs are illustrated in Figure 3-2 and Table 3-1 for various radiator system configurations having a total surface area of 18.6 square meters. Figures 3-2a and 3-2b show that the radiator with heat pipe fins dissipates 10 percent more heat and weighs on the order of 16.0 kg less than the radiator with solid fins. This corresponds to 21.7 kg/kW for the radiator with heat pipe fins versus 28.2 kg/kW for solid fins. The heat pipe radiator is lighter because fewer transport heat pipes and interface heat exchangers are required.[4,9] If the heat pipe fin length is increased to 0.95 m, as shown in Figure 3-2c, the overall radiator weight will be 22.8 kg lighter than with solid fins. This additional weight savings occurs because of shorter transport heat pipes. Note that the transport heat pipes in Figures 3-2b and 3-2c must be larger and, therefore, heavier per unit length in order to transport the total heat load. It was assumed for this analysis that the transport pipes in Figures 3-2b and 3-2c were twice as heavy per unit length as those in Figure 3-2a. However, the interface heat exchangers, which couple each heat pipe evaporator to the spacecraft thermal bus coolant loop, were assumed to be identical in weight for all three cases. No allowance was made for higher temperature drops due to the increased heat flux across structural interfaces

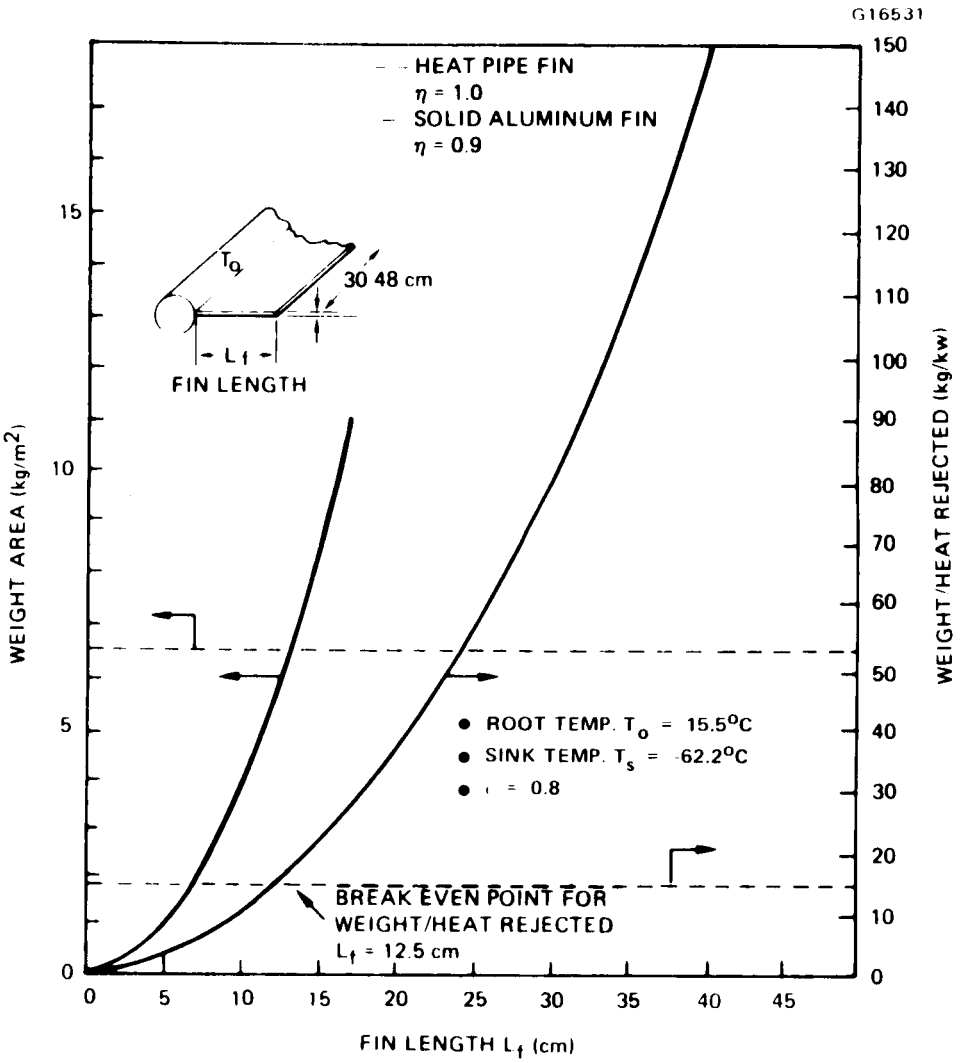

Figure 3-1 Comparison of heat pipe fin performance versus solid aluminum radiator fin.

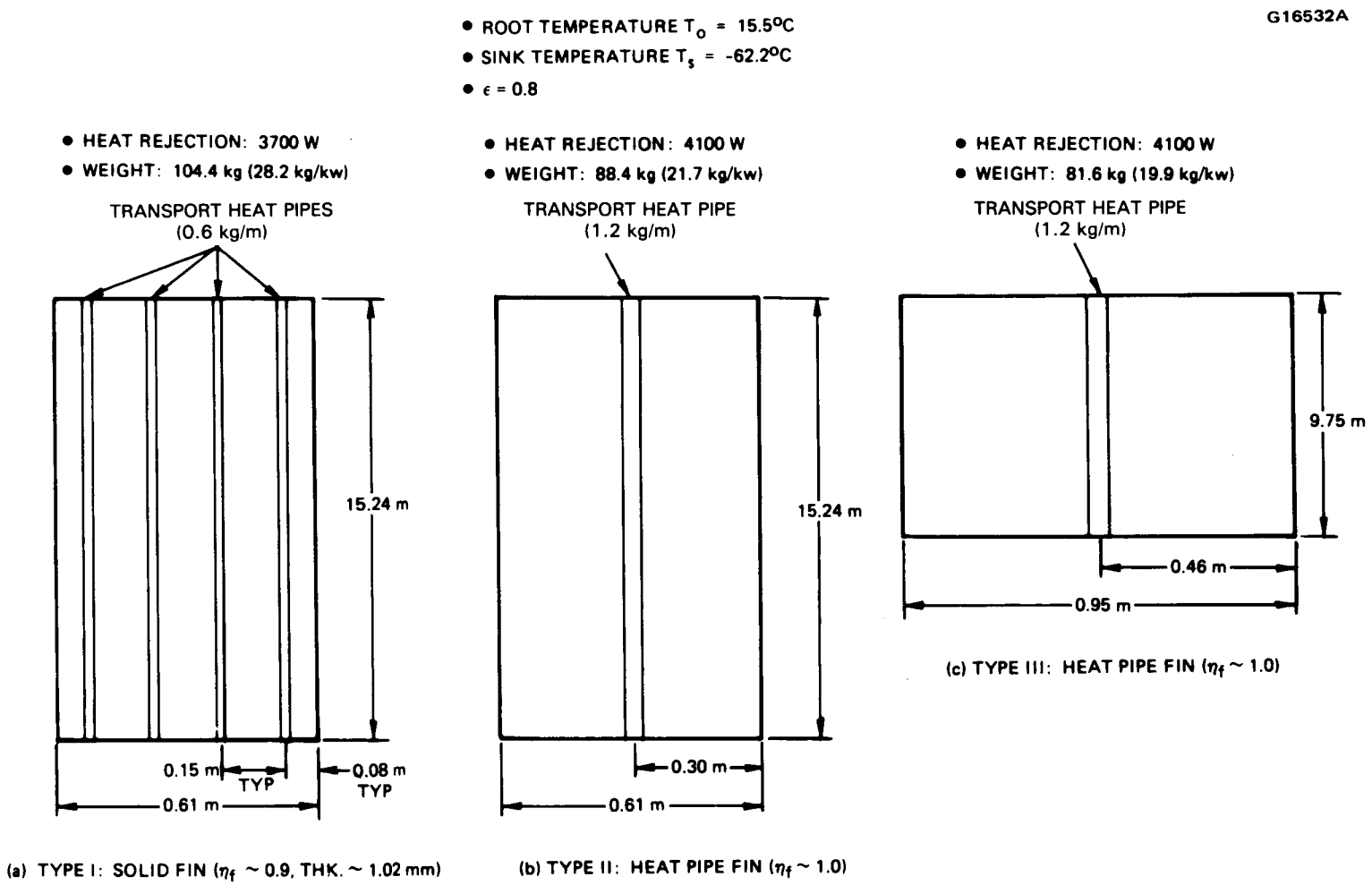

Figure 3-2 Radiator fin trade-offs for a surface area of 18.6 m^2.

TABLE 3-1

SUMMARY OF RADIATOR COMPONENT WEIGHTS (kg)

Component	Fin Type		
	I	II	III
Fin	25.4	59.0	59.0
Transport Heat Pipes	33.6	18.1	11.3
Interface Heat Exchanger	45.4	11.3	11.3
Total Weight	104.4	88.4	81.6

in Figures 3-2b and 3-2c. Nevertheless, it can be concluded from this simplified analysis that the heat pipe fin has both a weight and area advantage over the solid fin. The use of long heat pipe fins allows shorter and fewer transport heat pipes, as well as fewer interface heat exchangers, for a given radiator system.

4.0 STAINLESS STEEL HONEYCOMB PANEL DEVELOPMENT

The stainless steel honeycomb heat pipe panel development is described in detail in References 6, 7, and 8. This section provides a summary of the design, fabrication, and test performance of the prototype heat pipe radiator panel.

4.1 CONCEPTUAL DESIGN

The heat pipe panel, shown schematically in Figure 4-1, consists of a wickable honeycomb core, internally wickable facesheets, and an appropriate working fluid. Evaporation of the working fluid occurs at any section of the panel exposed to heating. Vapor will flow to a cooler region where it condenses, and the condensate will return to the evaporator by means of capillary pumping action of the wick structure. The honeycomb cells can be notched at both ends, to allow intercellular liquid flow along the faces, and perforated to allow intercellular vapor flow. The intercellular communication of liquid and vapor is necessary to ensure heat pipe action, both in the plane of the panel and through its depth. The primary mode of heat transfer can be either transverse (face-to-face) or longitudinal (in-plane), depending on the wickable core design.

4.2 MANUFACTURING TECHNOLOGY STATUS

The technology and commercial equipment are available to construct all-welded, machine-assembled honeycomb panels.[10] At present, such panels are constructed and formed into various shapes for use in aircraft, missile, and ship frames. The honeycomb structure can be manufactured from any weldable material (excluding aluminum), up to 1.22 m (48 inches) wide in any reasonable length, with a minimum overall thickness of 6.35 to 25.4 mm (0.25 to 1.0 inch), in a variety of cell and channel sizes from 6.35 to 12.70 mm (0.25 to 0.50 inch) and shapes with different facesheet thicknesses. The basic panel is readily producible into components by cutting, stretch-forming, drawing, welding, and riveting.

For the honeycomb panels to function properly as heat pipes, the internal surfaces must be fabricated from porous materials or have porous materials attached to the internal surfaces. The structure consists of two internally

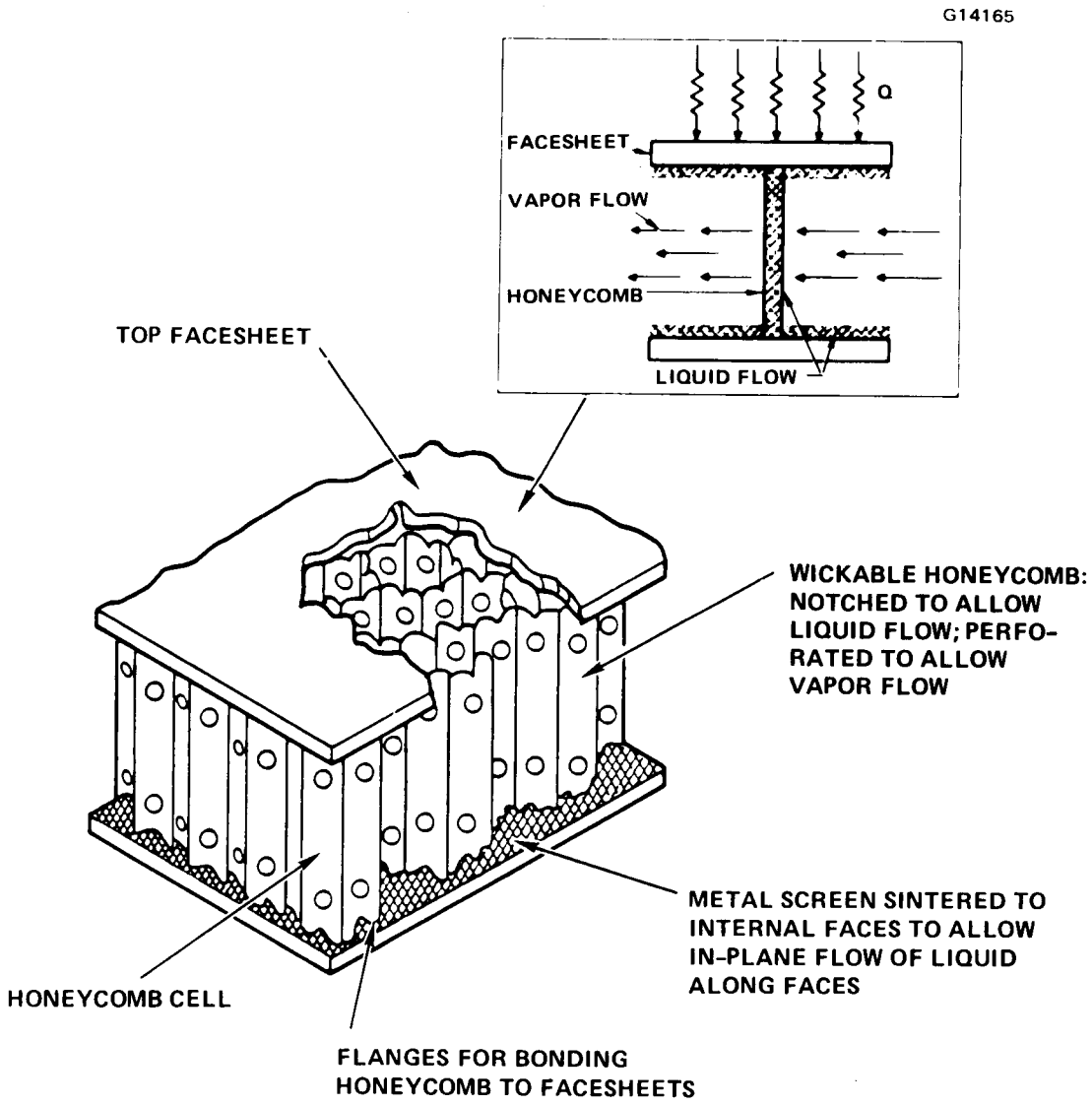

Figure 4-1 Honeycomb heatpipe panel concept.

wickable faces bonded to perforated, wickable honeycomb core material. Calculations and previous experiments with piece parts have led to the development of machine-fabricated, wickable honeycomb subscale liquid metal test panels for thermal stress reductions in NASA Scramjet Engines.[11,12] Various test samples and prototype panels were built to evaluate alternative construction methods, to perform proof-pressure and weld-integrity testing, to verify heat pipe processing techniques, and to do performance testing. Evaluation of options resulted in final design and fabrication of 0.15 m^2 by 0.03 m thick (6.0 by 6.0 by 1.14 inches) test panels, constructed entirely of stainless steel materials. Two designs for the honeycomb core were built: a foil-gauge sintered screen material, and a metal screen sintered to foil-gauge sheet material. The former design offers increased wicking capability, and the latter provides stronger structural design. Details of final panel construction (welding of sidewalls), cleaning and processing procedures, and experimentally determined wick parameters (capillary radius, r_c, and permeability, K) for porous core materials are reported in Reference 11. Table 4-1 outlines current manufacturing limits on the honeycomb heat pipe panel design.

4.3 DESIGN DETAILS AND CONSTRAINTS

As a result of experimental work reported previously,[11] certain design details and test data were established, which could be used as a baseline. The entire honeycomb panel is fabricated using an automated procedure for simultaneously resistance welding corrugated honeycomb core ribbons to each other (in the case of cells) and to both facesheets, forming a 6.35, 9.52, or 12.70 mm (0.25, 0.375, or 0.5 inch) hexagonal cell or channel configurations. Core ribbon details are shown in Figure 4-2. A sketch of the heat pipe honeycomb panel and associated component parts is shown in Figure 4-3.

The honeycomb panel manufacturer is machine limited to a maximum uninterrupted length of 3.0 m (120 inch). Beyond that, sections can be welded together to produce any longer length desired. The initial break in panel continuity,

TABLE 4-1

MANUFACTURING LIMITS* FOR HONEYCOMB PANEL MATERIAL

Facesheet

- Longest piece before welding: 0.64 m (48 inches)

Honeycomb Panel

- Materials: stainless steel, titanium
- Longest section before welding: 3.0 m (120 inches)
- Panel width: 0.64 m (48 inches)
- Core depth: 6.35 to 50.8 mm (0.25 to 2.0 inches)
- Core ribbon thickness: 0.15 mm (0.006 inch) maximum
- Cell or channel sizes: 6.35, 9.52, and 12.70 mm (0.25, 0.375, and 0.5 inch)
- Facesheet thickness: 0.25 to 0.76 mm (0.010 to 0.030 inch)

*Dictated by materials supplier and panel manufacturer

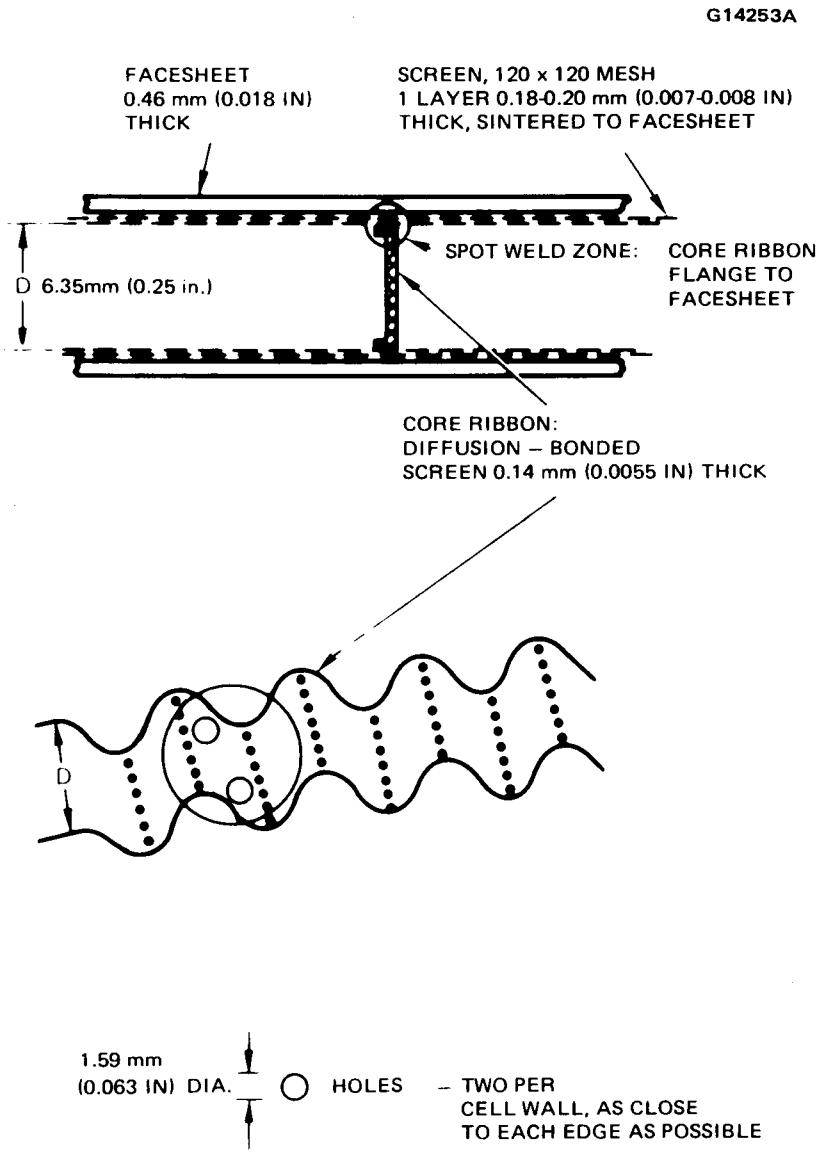

Figure 4-2 Core ribbon details.

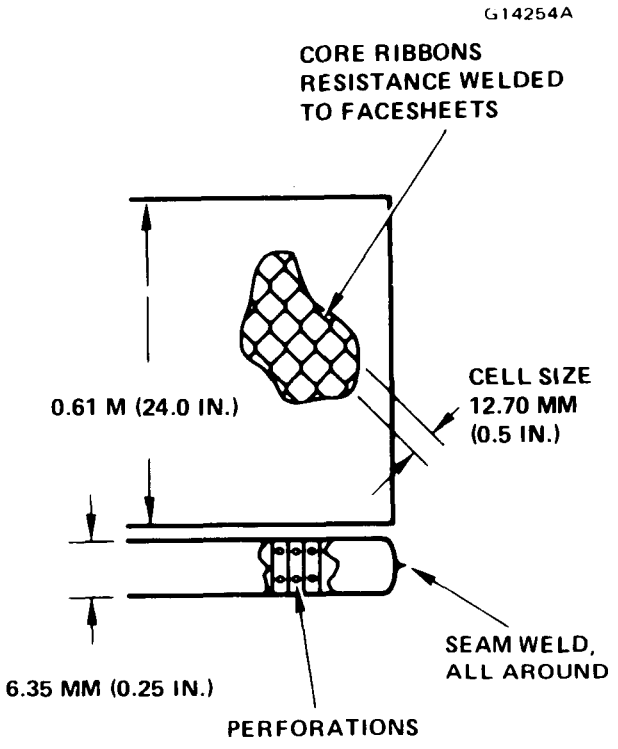

Figure 4-3 Sketch of heat pipe honeycomb panel.

however, is created by weld joining of facesheet subsections. The sintered facesheet fabricator produces a maximum standard length of 1.22 m (48 inches), which dictates that honeycomb panel weld seams shall occur at least every 1.22 m (Figure 4-4).

Since the heat flow is in the same direction as the weld seam, and since the core ribbon crosses the welds to provide liquid communication, the detrimental effect on heat pipe performance is minimized. Conventional plasma butt welding will produce a seam width of approximately 2.38 mm (0.094 inch). Electron beam welding can reduce the facesheet wick destruction zone to an absolute minimum, and was therefore the preferred method.

Final design parameters are summarized in Table 4-2. Performance calculations[8] based on this design verified that the panel can meet the 1000 watt heat transport requirement. These performance predictions are plotted in Figure 4-5 as a function of operating temperature.

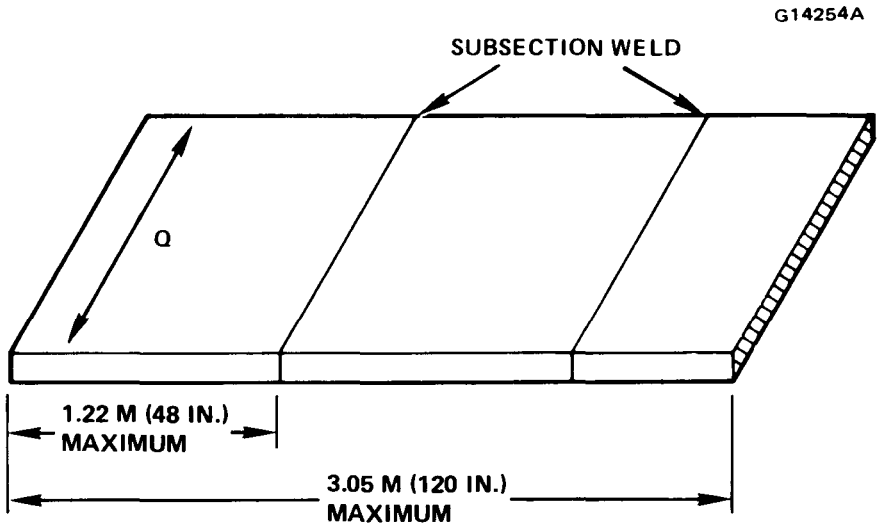

Figure 4-4 Panel weld seams.

TABLE 4-2

DESIGN SUMMARY FOR STAINLESS STEEL HONEYCOMB RADIATOR PANEL

Selected design parameters

- All stainless steel construction
- Facesheet thickness: 0.46 mm (0.018 inch)
- Wire mesh laminate for core ribbon
- Overall length of panel: 3.0 m (120 inches)
- Overall panel width: 0.60 m (24 inches)
- Core ribbon depth (D): 6.35 mm, (0.25 inch)
- Core ribbon hole pattern:
  Two 1.59 mm (0.063 inch) holes per cell wall
- Honeycomb cell size: 12.70 mm (0.5 inch)
- Facesheet wick layers: 1
- Working Fluid: Methanol

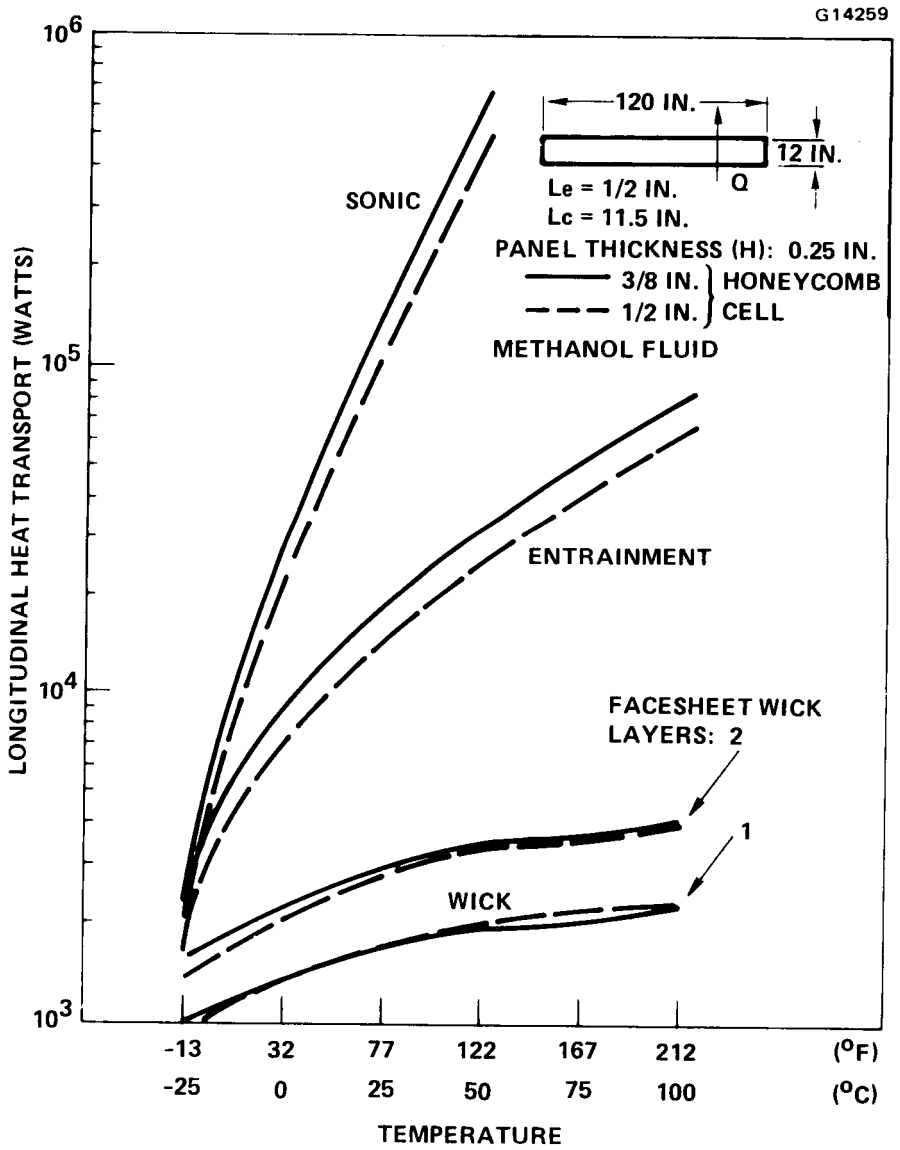

Figure 4-5 Performance limits versus temperature for 6.35 mm (0.25 in.) thick honeycomb cell panel.

4.4 FABRICATION

The following section describes the assembly steps required for stainless steel honeycomb panel fabrication.

4.4.1 Diffusion Welded Material

As previously described, the facesheet material consists of one layer of 120 by 120 mesh 316 SST screen, diffusion bonded (sintered) to one layer of 0.46 mm (0.018 inch) thick 316 SST sheet. Figure 4-6 is a cross section of the facesheet/sintered wick interface. The largest available stock sizes for this material are 1.2 by 0.6 m (48 by 24 inches) and 0.9 by 0.9 m (36 by 36 inches) due to vacuum furnace size limitations. To achieve a finished panel width of 0.6 m (24 inches), the panel welder requires a starting facesheet width of at least 0.7 m (0.05 m extra at both edges for "grabbing" the panel during the weld operation). Therefore, the 0.9 by 0.9 m sintered stock was used. This facesheet material, as originally received, was unacceptable because of the presence of small, sharp depressions. The material was reworked by flattening it in a rolling machine. However, the material had to be trimmed to 0.91 by 0.66 m (36 by 26 inches). It follows, then, that the final panel would consist of five sections joined together to create a total length of 3.0 m (120 inches); in other words, welds would occur every 0.66 m (26 inches), rather than every 1.2 m (48 inches) as originally planned.

The core ribbon material consists of sintered 316 SST twilled-weave, wire mesh laminate (165 by 1400 mesh), which is 1.67 mm (0.0055 inch) thick. Sheets measuring 1.2 by 0.6 m (48 by 24 inch) were prepared.

4.4.2 Core Ribbon Fabrication

The ribbon material was cut into thin strips (1.2 m long), crimped, corrugated, and then folded 90^{o} at both 1.2 m (48 inches) edges to form miniflanges. Holes (perforations) were punched into the ribbon with small dies. After some experimentation, the panel welder settled on the inclusion of two 1.59 mm (0.063 inch) diameter holes, which were located very near the miniflanges at the top and

E4938

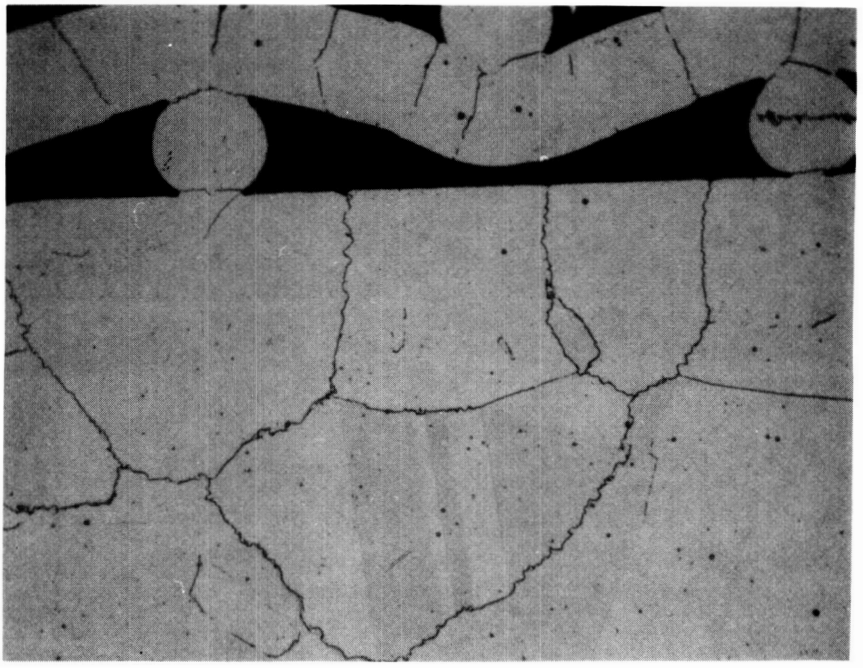

Figure 4-6 Cross section of facesheet/sintered wick interface (250X).

bottom of every second cell face (vapor flow area through the honeycomb cells is the summed open area from two faces per cell). A photograph (Figure 4-7) of the finished core ribbon shows the holes punched on alternating cell walls. However, the actual vapor flow area was only 75 percent of that originally desired. Also, vapor flow was constrained to a diagonal direction through the panel, or a 41 percent increase in travel length from the straight direction.

Liquid transport is affected by the location and spacing of spot welds in its flow path. An increase of miniflange to facesheet spot weld spacing was requested. However, the actual extent of this increase is unclear. Upon close examination of a finished panel specimen, variance in spotweld consistency makes it difficult to establish a percentage factor for the "open" wick cross-sectional area. The initial estimate of a 25 percent porous zone may be optimistic. Thermal transport capacity is sensitive to this available wicking flow area. However, spot welds at core ribbon cell wall interfaces (see Figure 4-2) were eliminated entirely (as requested), and this should increase transport capacity contribution of the core wick.

4.4.3 Panel Facesheet Joining

Electron beam welding of the facesheet sections was originally planned, but due to cost and time constraints, the panel fabricator elected to use butt welding (GTAW). Four butt welds of this type were used for welding five facesheet sections into an overall length of 3.0 m (120 inches). Note that these welds are in the transverse direction parallel to the liquid flow path. Moreover, the core ribbon material crosses these welds to provide liquid flow communication.

4.4.4 Final Panel Fabrication

Figure 4-8 is a close-up photograph of the internal honeycomb structure with one facesheet removed. The sintered core material (ribbons), perforated holes for vapor and liquid communication among the cells, and facesheet wick sintered to the facesheet material can be seen in this photograph. Spotwelds for attaching the core ribbon to the facesheets and a facesheet butt weld are also visible.

E4939

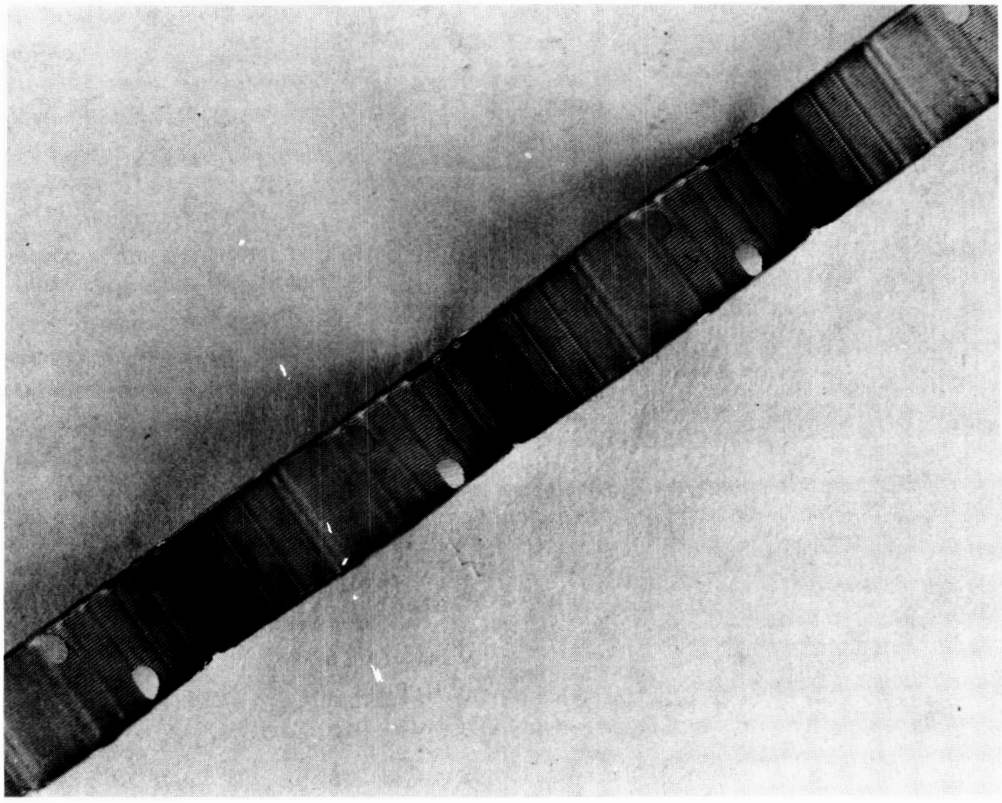

Figure 4-7 Core ribbon material after crimping.

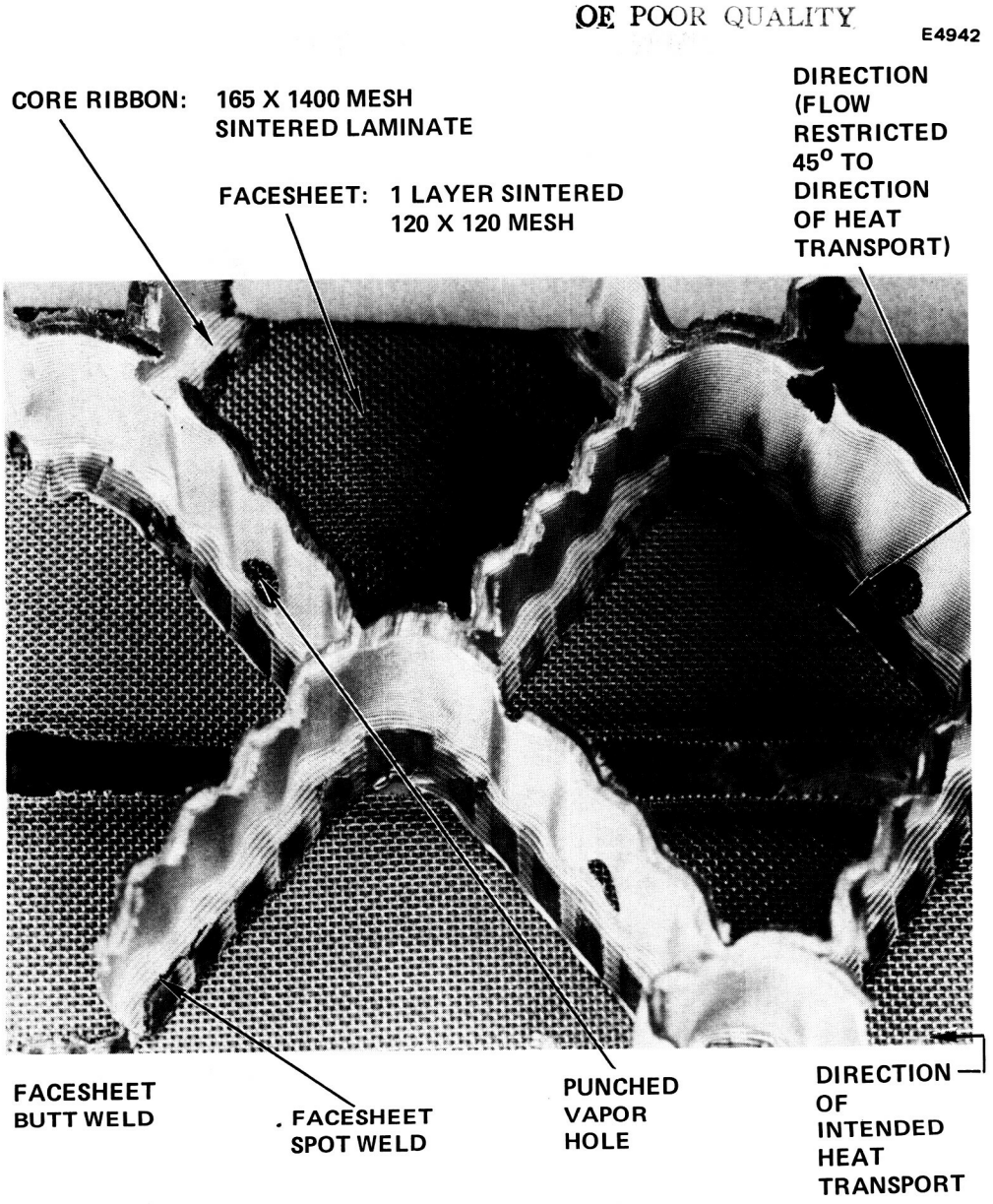

Figure 4-8 Close-up of internal honeycomb structure.

After fabrication and trimming of the honeycomb panel material to size (0.6 by 3.0 m), a rolled edge was formed, completely encircling the panel. The edge was butt-fusion (GTAW) welded all around to produce a leak-tight seal (Figure 4-9). A 6.35 mm (0.25 inch) diameter hole was drilled at the center of one short (0.6 m) edge, and a 6.35 mm (0.25 inch) diameter by 0.3 m (12 inches) length fill tube was welded in place. This technique resulted in a single edge weld, rather than two welds, plus additional piece parts for the edges as originally envisioned. The completed panel is shown in Figure 4-9.

4.5 PROCESSING PROCEDURES

After fabrication was completed, the panel was subjected to a leak test by internally pressurizing the panel to 5 psig using helium, and checking for leaks with a high-speed sniffer probe attached to a Veeco^{TR} mass spectrometer leak detector. No leakage was detected.

Following this leak test, the panel was vacuum baked at a temperature of approximately 65^{o}C for a period of 261 hours. Electrical resistance heater tapes were bonded to the external surfaces to provide an elevated temperature during bakeout. The panel outlet pressure was on the order of 10^{-5} Torr during the entire bakeout period.

After bakeout, the panel was then processed. First, 0.518 kg (1.14 lbm) of methanol was vacuum distilled into an evacuated stainless steel cylinder. This cylinder was then connected to a valve attached to the honeycomb panel, which was evacuated. Next, the methanol was drained into the panel and the panel was degassed. The degassing was accomplished by placing a 76.2 mm (3.0 inches) thick layer of open cell polyurethane foam underneath and on top of the panel, and cooling by pouring liquid nitrogen onto the top layer. When the panel was sufficiently cooled (<-40^{o}C), the fill valve was opened to vacuum to vent the gases.

E4943

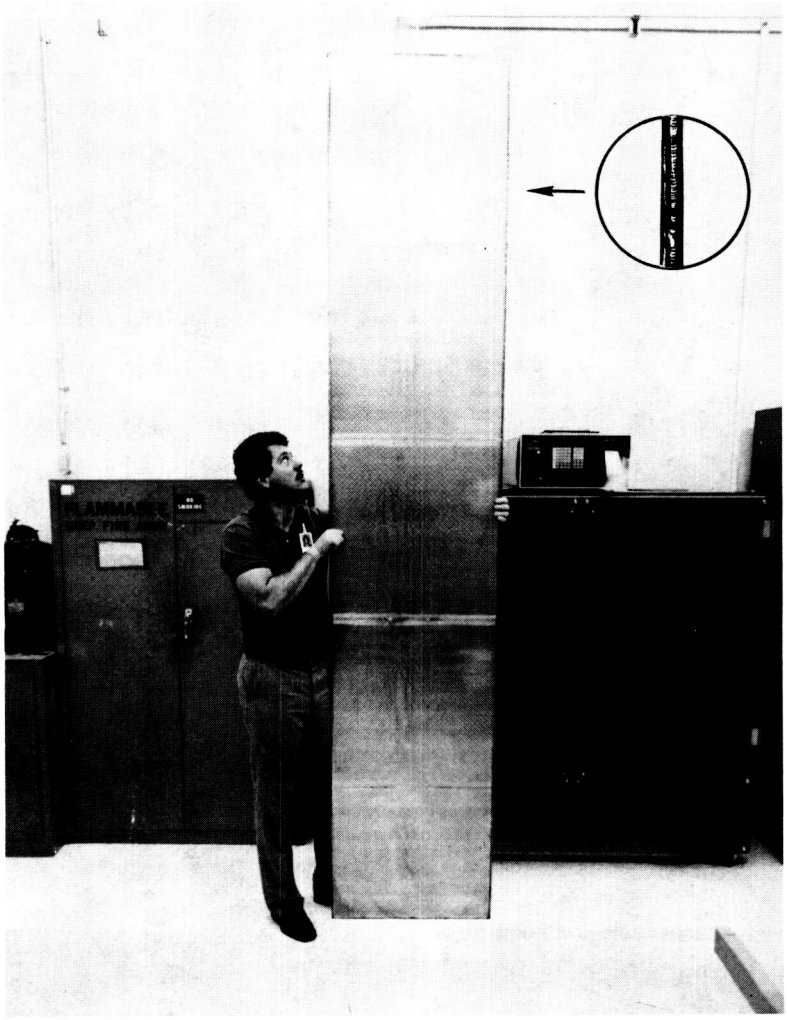

Figure 4-9 Completed honeycomb panel

4.6 TEST PERFORMANCE

Preliminary performance testing and checkout of the honeycomb panel heat pipe was conducted in laboratory ambient air. For testing over the temperature range of -20 to 65°C, however, the panel was installed in a special test station. The test station, methods, and heat transport performance test results are described in the following paragraphs.

4.6.1 Test Setup

Figure 4-10 is a photograph of the test station designed for testing the honeycomb panel performance over the temperature range -20 to 65°C. Referring to the sketch in Figure 4-11, it can be seen that the heat sink is provided by six 0.2 m (8 inches) wide flanged aluminum extrusions with 25.4 mm (1.0 inch) diameter liquid nitrogen (LN_2) coolant passages. Three extrusions are placed above the test panel and three below for heat rejection from both sides of the panel. The test panel is centered approximately 76.2 mm (3 inches) from the flanged surfaces of the heat sinks, using a total of eight adjustable Plexiglas support pegs. The test setup was enclosed in a 3.4 m long by 0.8 m wide by 0.6 m high (132 by 30 by 24 inches) Plexiglas chamber. Note that this is not a vacuum chamber, and heat transfer from the heat pipe to the heat sink is by radiation, conduction, and natural convection through the surrounding air.

Thirty chromel-constantan (Type E) thermocouples were spot-welded directly to the panel surface at the locations shown in Figure 4-12. Thermocouples on the bottom surface are placed directly underneath the top ones. Note, however, that there are no thermocouples underneath the four circled ones (Figure 4-12). The reason for this is that a thirty-channel strip chart recorder was selected for recording the data. Since there are no edge effects associated with these locations, it is felt that the top thermocouples are sufficient.

Heat input was provided by four strips of Clayborne Labs heater tape (E-16-2) wired in parallel. For initial testing, the heat input zone was a 25.4 mm (1 inch) wide strip running the entire length of the panel (3.0 m), as shown in Figure 4-12. This approach simulates the honeycomb panel being used as a

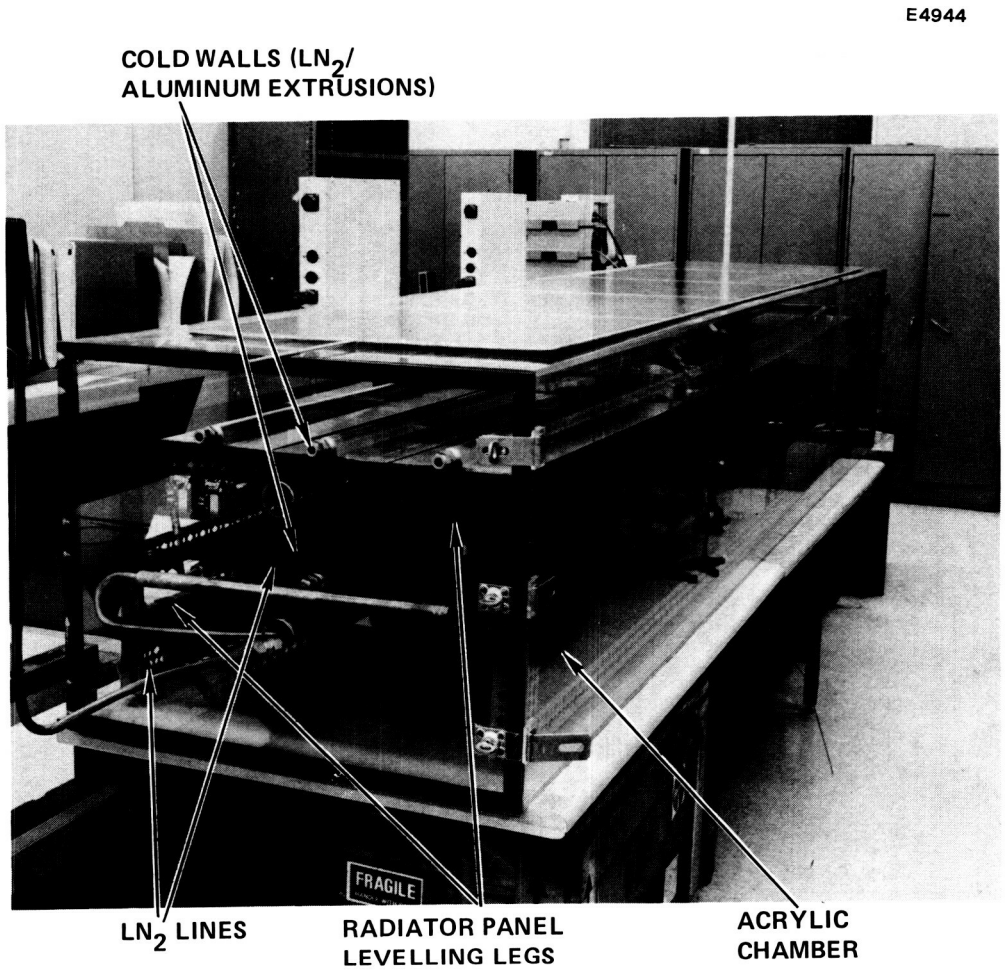

Figure 4-10 Performance test set-up.

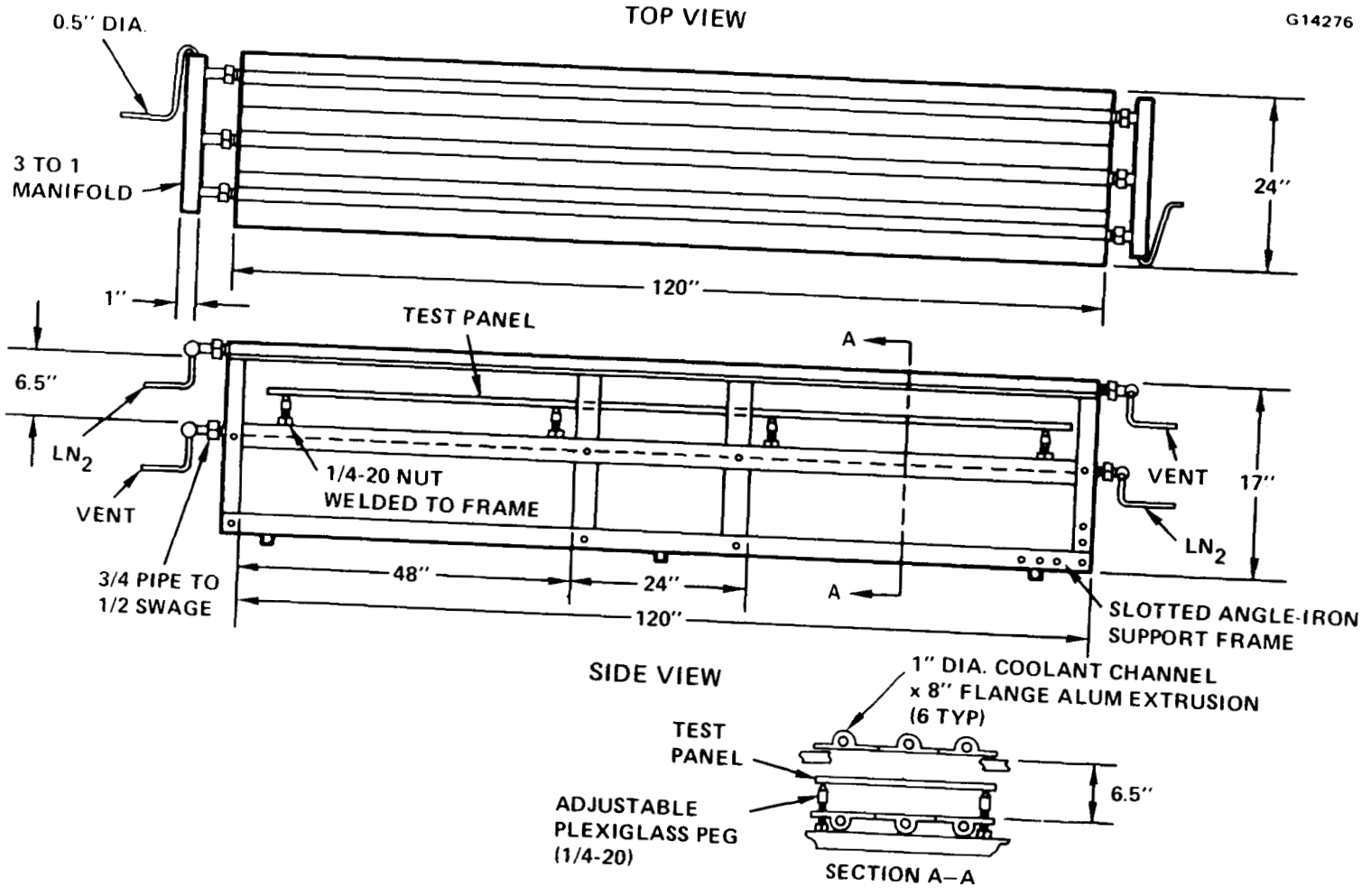

Figure 4-11 Schematic diagram of test station.

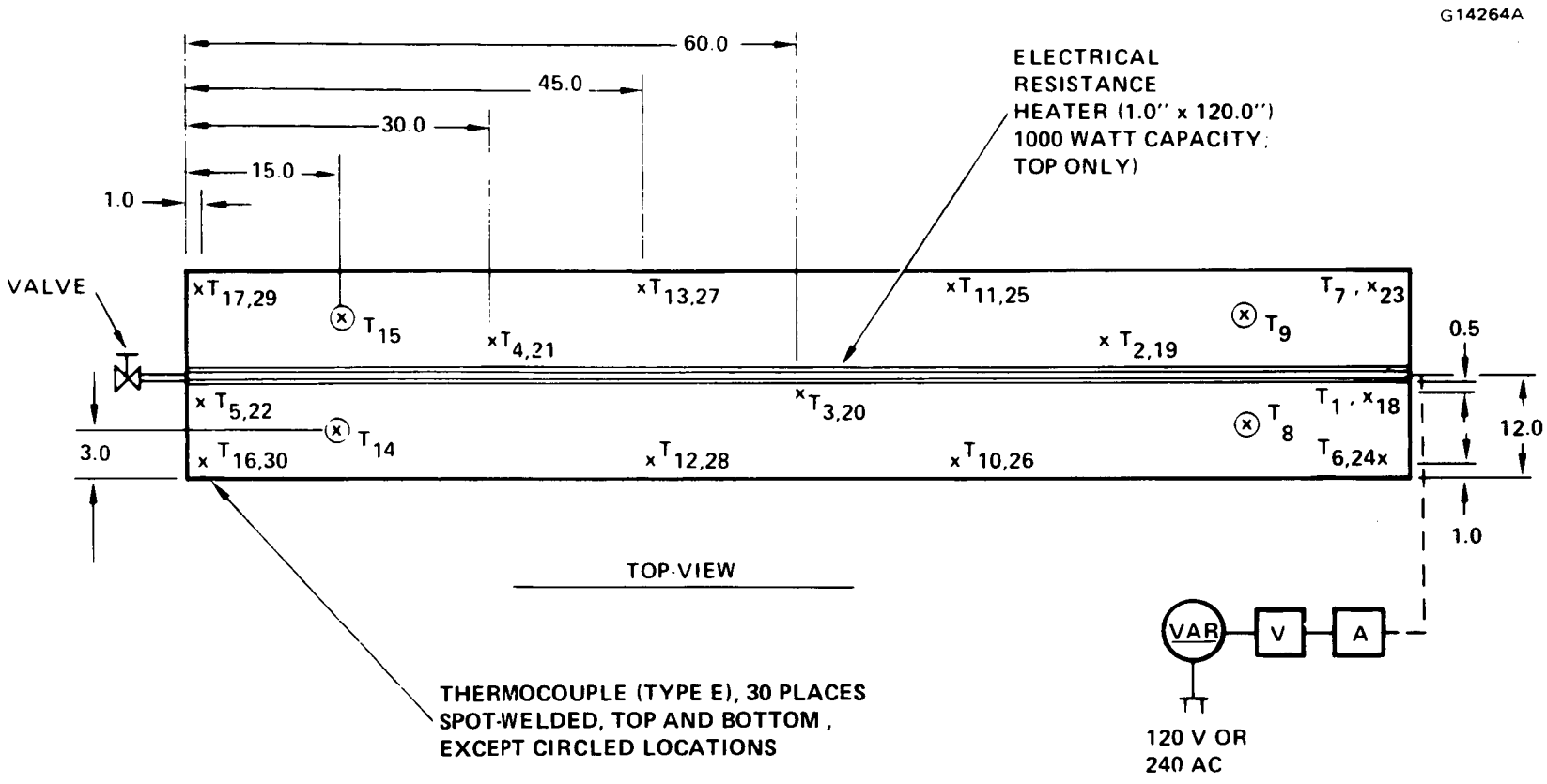

NOTES:

1. CIRCLED THERMOCOUPLES ON TOP ONLY
2. $T_{a,b}$; WHERE a = TOP TC NO. AND b = BOTTOM TC NO.
3. INSTRUMENTATION IS SYMMETRICAL, EXCEPT AS NOTED
4. DIMENSIONS IN INCHES

Figure 4-12 Honeycomb panel performance test instrumentation.

high efficiency radiator fin in conjunction with a high-capacity axial transport heat pipe or coolant loop.

4.6.2 Performance Testing Over the Temperature Range -20 to 65°C

The honeycomb panel heat pipe was installed in the test chamber (Figures 4-10 and 4-11) and a cold test was performed. First, only the lower cold wall was turned on. With 100 watts input to the panel, the temperature was lowered approximately 15°C in 1 hour. When the lower cold wall was turned off and the upper one turned on, the panel was cooled an additional 22°C in one-half hour. This translates into a cooling rate three times higher than that observed with the lower cold wall. This indicates that natural convection coupling between the panel and the upper cold wall was significantly higher than for the lower cold wall, as would be expected. The surface temperature of the panel varied by ±2.1°C. When the power was increased to 120 watts, dryout was observed.

For high-temperature operation, the upper and lower cold walls were not used. The interior air temperature of the chamber was heated by ducting the exhaust air from an environmental chamber into the test chamber. A small fan was provided inside to distribute the air uniformly. The panel held 500 watts with a surface temperature variation of ±2.2°C. A dryout was observed at 550 watts.

High and low temperature test results can be seen in Figure 4-13, along with computer predictions for the as-built honeycomb panel.[8] The correlated model was then used to predict the performance of upgraded honeycomb panels, which have adequate vapor communication. Two additional cases are shown in Figure 4-14. The upper curve shows the increase in as-designed panel performance, which incorporates a four-fold increase in vapor flow area and 50 percent open liquid flow area at facesheet spotwelds. Leveling of the curve is a result of the relative significance of vapor as compared to liquid pressure drops at lower temperatures. However, to meet the design goal of 1000 watts over the entire operating temperature range shown in the upper curve, it is necessary to incorporate the lower flow resistance of honeycomb channels. Both cases use combined tortuosity factors of 0.8 (Figure 4-13), which is very conservative for the channel design.

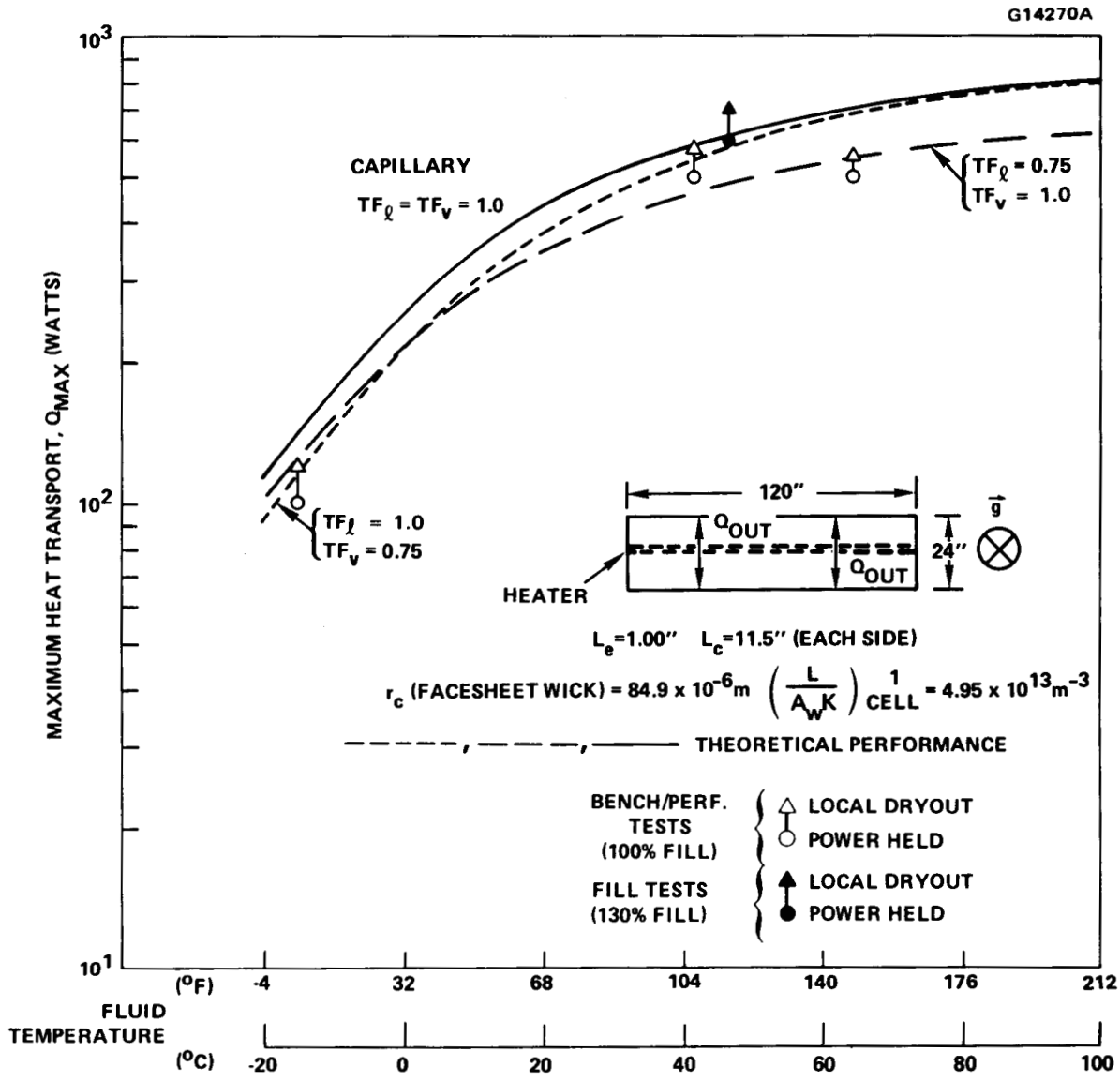

Figure 4-13 Data correlation: thermal transport limitation.

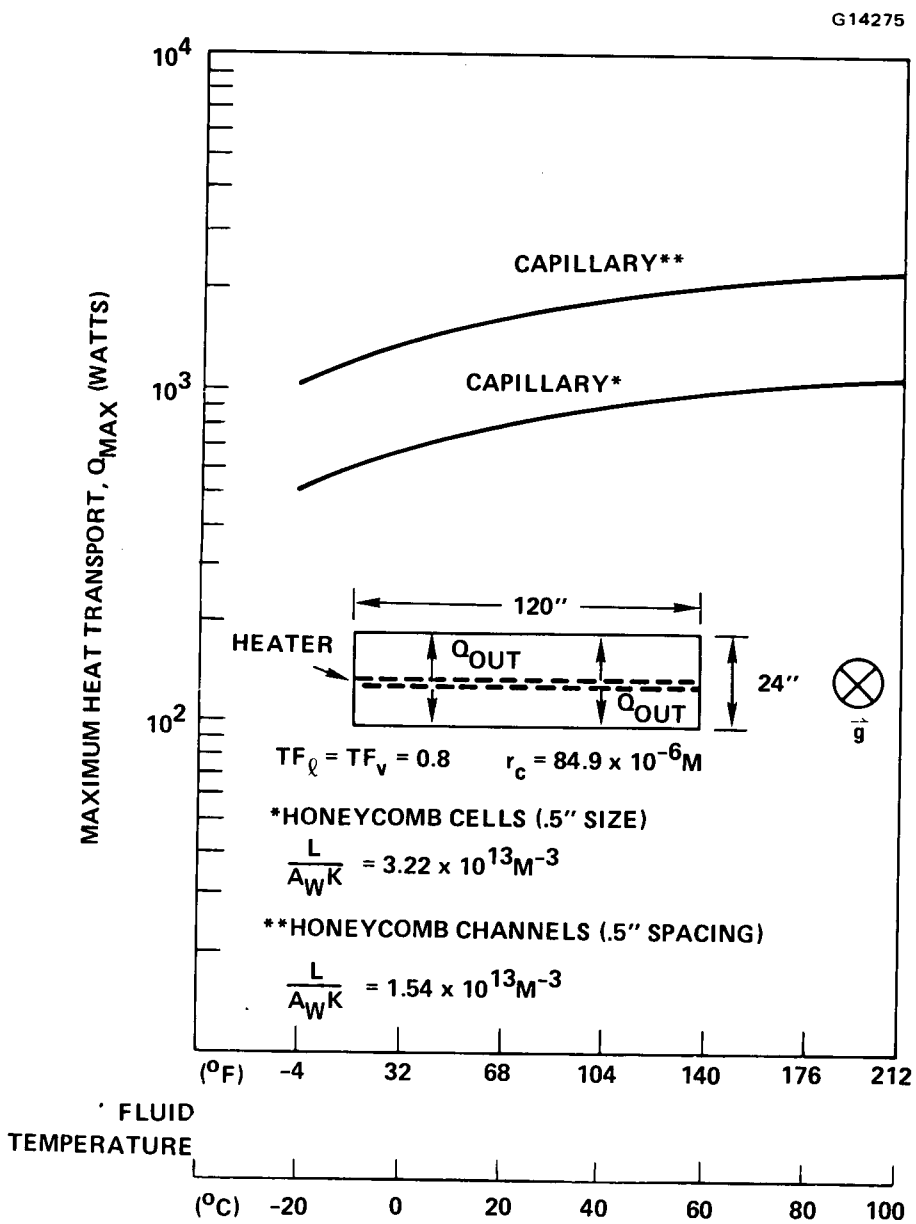

Figure 4-14 Predictions for as-designed and increased capacity design using correlated model.

4.6.3 Liquid Fill Test

After completion of the low and high temperature performance test, the panel was removed from the test chamber and connected to the process station. An additional 50 grams of methanol were added to the panel in order to start the liquid fill test. This corresponds to a 10 percent increase in the liquid fill.

After reprocessing, the panel was placed in the test chamber and retested. Input power of 400 watts was applied to the panel, with no evidence of excess liquid. The surface temperature varied by only $\pm 2.2^{\circ}C$. Since no evidence of an excess in fluid was observed, the panel fill was again increased by 10 percent.

This time, the panel was tested on the bench in order to facilitate the detection of excess liquid by tilting in various directions. When the methanol fill was increased to 120 percent, the performance was essentially the same as 100 and 110 percent, i.e., there was no evidence of excess liquid at 400 watts heat input. This shows that the panel was relatively insensitive to an underfill. The fill was then increased by 10 percent again, to 130 percent. At this time, it was decided to perform a maximum power test to determine whether the additional fill had any effect on the heat transport capacity.

The maximum power increased to 600 watts, with only a $3.0^{\circ}C$ ΔT over the entire active surface of the panel. At 700 watts, the ΔT increased to $11^{\circ}C$, which was considered to be a dryout. However, the panel recovered when the power was reduced to 400 watts. Results are plotted in Figure 4-13.

There was evidence of excess liquid in the corner where thermocouples 6 and 24 are located (see Figure 4-12). In order to check this, the opposite corner (7, 23) was lowered.

Thermocouple No. 6, which is on the upper surface, responded instantaneously, and thermocouple No. 24, on the bottom surface, slowly recovered also. This test was not conclusive, however, because this corner (6, 24) has been known

to trap liquid at the lower fills. In this case, however, thermocouples 17 and 29 slowly started to decrease in temperature with time. When this corner (17, 29) was tilted upward, there was a rapid recovery, indicating the presence of excess liquid in the panel.

It was concluded from these tests that a fill of 125 percent represents the optimum fill for this panel. This amounts to approximately 0.65 kg (1.43 lbm) or 355 g of methanol per square meter (0.07 lbm/ft^2).

4.6.4 Tilt Test

Next, the heater was removed from the centerline of the panel and placed along one edge in order to perform the tilt test. The heater was bonded to the top surface just inboard of thermocouple Nos. 6, 10, 12, and 16 (see Figure 4-12). The purpose of this test was to demonstrate that the panel does operate properly, even against a positive gravity loading. One side of the panel was always gravity aided, with the heater in the center, regardless of which direction the panel was tilted. Note, however, that a factor of four reduction in maximum heat transport is to be expected in this configuration. This is because all of the heat input must be transported over the full width of the panel. When the heater was in the center, only half of the heat load was required to be transported over one half of the panel. Therefore, with no tilt and the heater located on the edge of the panel, maximum heat transport should be 150 watts.

This test was performed with the panel outside the test chamber, using the room temperature ambient air as the heat sink. The tilt test results are plotted in Figure 4-15. In all cases, thermocouple Nos. 10 and 12 were the first to indicate dry-out, followed by thermocouple Nos. 26 and 28. The lower data points represent steady-state heat transport capability over a period of at least one hour, whereas the upper points indicated a temperature difference of greater than 10°C between any two temperatures on the panel, i.e., dryout.

Although the maximum heat transport is lower than expected, these results verify the ability of the panel wicking system to successfully perform against

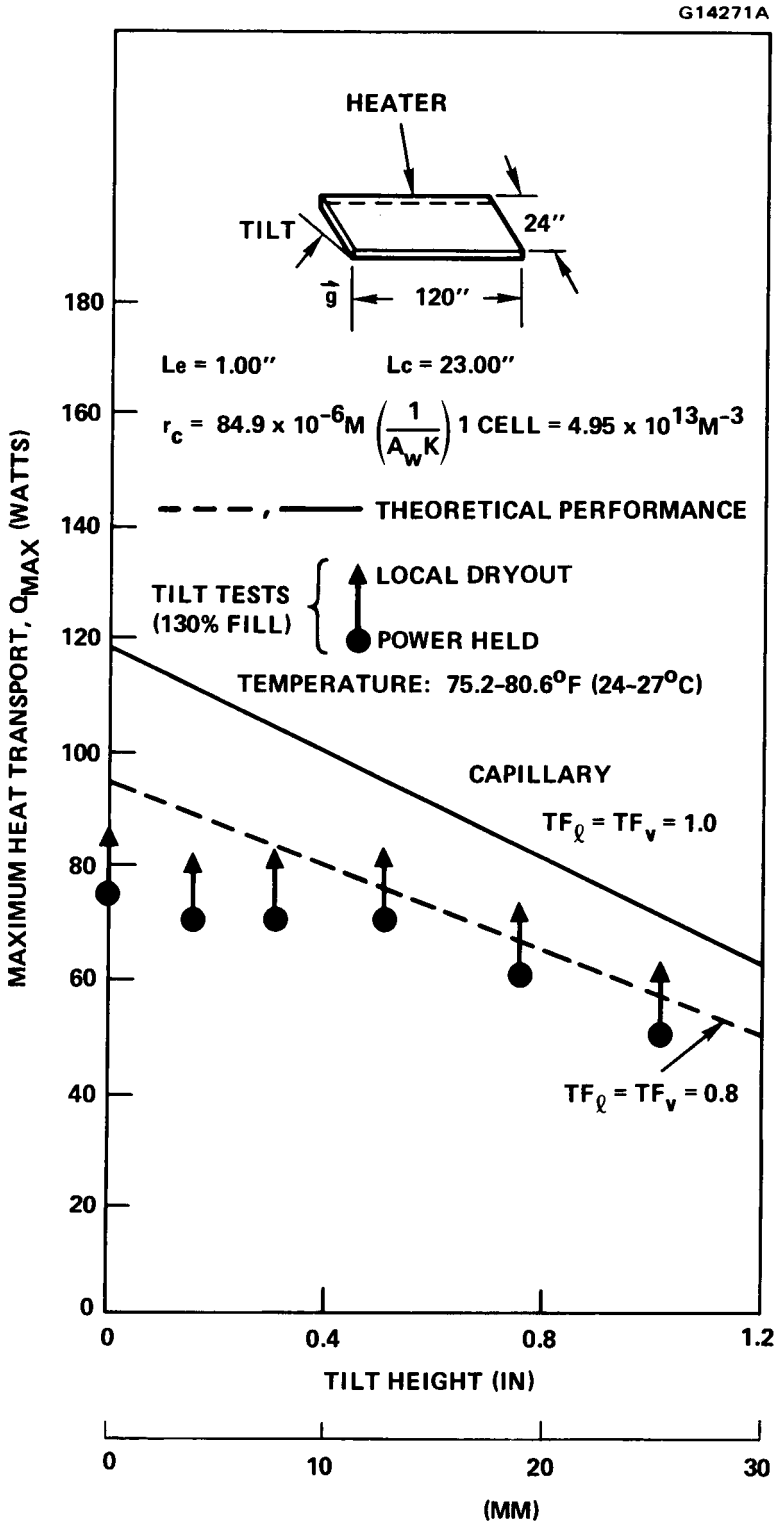

Figure 4-15 Data correlation: tilt test performance.

an adverse gravity field. Because the curve "levels off" at low values of tilt, however, it is concluded that the reduced performance is due to a higher than expected vapor pressure drop. See Reference 8 for a more detailed discussion.

4.6.5 Burst Pressure Test

The burst pressure test was performed on a subscale 0.14 by 0.14 m (5.50 by 5.50 inches) honeycomb panel. This sample was identical in materials and construction to the large thermal performance test panel. It was also constructed at the same time as the large panel. The test sample was helium leak checked before pressurizing.

Figure 4-16a shows the five locations where the sample thickness was measured. (Note that location No. 5 is not at the center, but at a point conveniently measured with technician's calipers.) First, the thickness was measured in the free unpressurized state and recorded on the data sheet. The panel was then placed in a safety chamber and pressurized with ultrapure nitrogen in 50 psig increments. After holding the pressure for ten minutes, the panel thickness was measured and recorded. The test data are summarized in Table 4-3. Between each pressure point, the sample was removed from the test chamber and helium leak checked to verify continued structural integrity.

At 200 psig, a maximum deflection of 0.25 mm (0.01 inch) was observed. This deflection relaxed to only 0.23 mm (0.009 inch) when the pressure was vented to atmosphere, indicating permanent deformation. The sample was repressurized to 250 psig where, after approximately five minutes, the panel failed (Figure 4-16b). Subsequent examination of the panel, with a borescope inserted through the fill tube, revealed that the sintered wire core material had failed adjacent to the spot welds. Upon failure of the core material, the unit expanded, like a "pillow." A leak check revealed two small leaks, one in the seam and one adjacent to the seam weld in a corner.

G14267

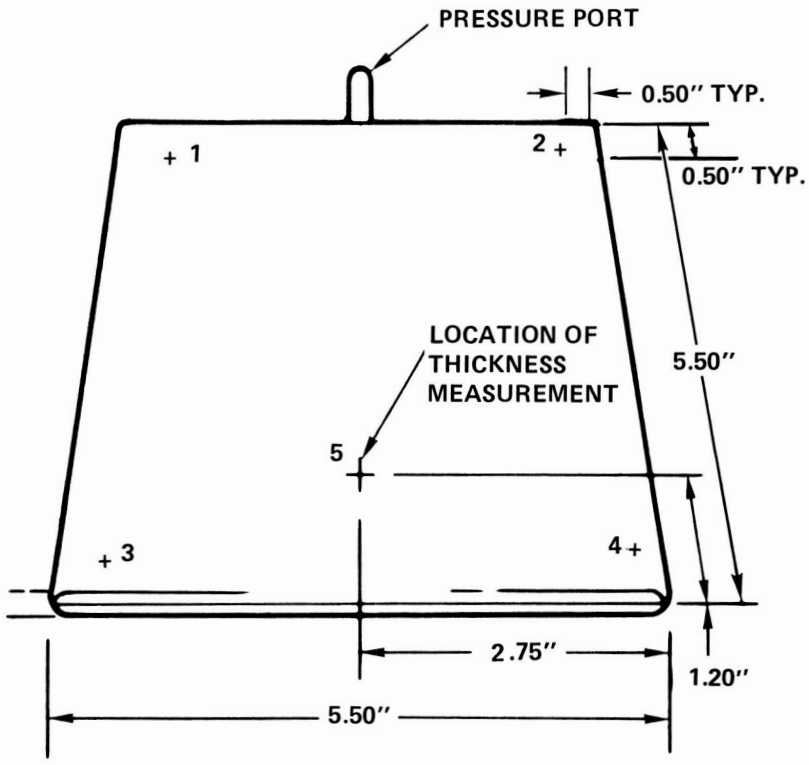

A. BURST PRESSURE TEST SAMPLE DIAGRAM SHOWING MEASUREMENT LOCATIONS.

E4945

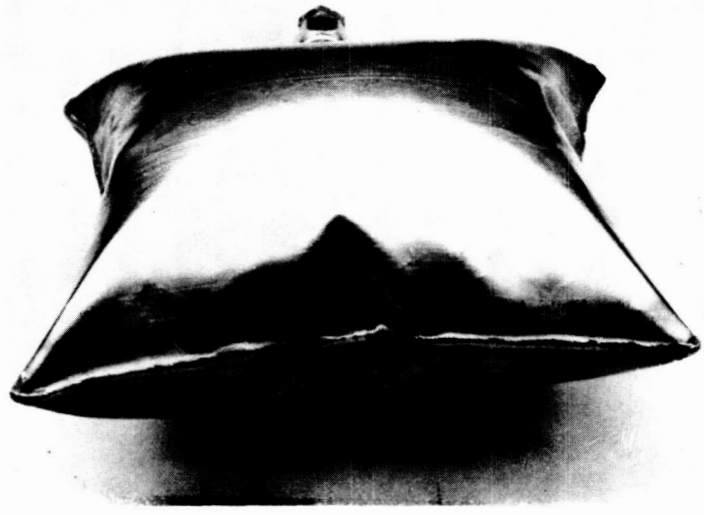

B. BURST PRESSURE TEST RESULT

Figure 4-16 Burst pressure test.

TABLE 4-3

SUMMARY OF BURST PRESSURE DATA

Pressure (psig)	Thickness (inches)					Comments
	1	2	3	4	5	
0	0.311	0.310	0.311	0.311	0.314	
50	0.312	0.307	0.311	0.312	0.312	With pressure
100	0.311	0.309	0.312	0.312	0.314	With pressure
150	0.313	0.310	0.314	0.314	0.317	With pressure
200	0.316	0.315	0.318	0.321	0.322	With pressure
0	0.315	0.312	0.316	0.320	0.319	
250	--	--	--	--	--	Unit failed

5.0 ALUMINUM PANEL DEVELOPMENT

The stainless steel honeycomb panel heat pipe, as previously described, was successfully machine-fabricated and tested for space radiator applications. The second phase of this program was to demonstrate the technology for fabricating a lighter weight aluminum heat pipe panel. The program consisted of identifying the various manufacturing methods and fabricating developmental units. Based on the fabrication and test results of these developmental units, a 3.0 by 0.6 m (120.0 by 24.0 inches) prototype aluminum radiator panel was built. The design requirements for the lightweight aluminum panel were identical to those of the stainless steel honeycomb panel.

During the development of the aluminum panel heat pipe, the following areas were investigated:

1. Modification of existing stainless steel honeycomb construction techniques and equipment for aluminum panel fabrication.

2. Investigations into alternative panel designs.

Key features such as joining methods, core structure, wick structure, working fluid, thermal performance, vapor pressure containment, and modular design trade-offs were addressed during the above investigations.

5.1 FLUID COMPATIBILITY

The first area of investigation was material and fluid compatibility. A survey of various fluids compatible with aluminum was taken, and three of the most promising fluids were chosen for further study. These fluids were ammonia, Freon-11™, and acetone. Note that methanol, which was used in the stainless steel panel, is not compatible with aluminum. It was decided that ammonia, because of its good thermal transport properties (Figure 5-1), would be the best choice. Because of ammonia's high vapor pressure (Figure 5-2), however, it is not suitable for flat-panel heat pipes. Freon was also found to have a high vapor pressure, but its major drawback was its poor heat transport

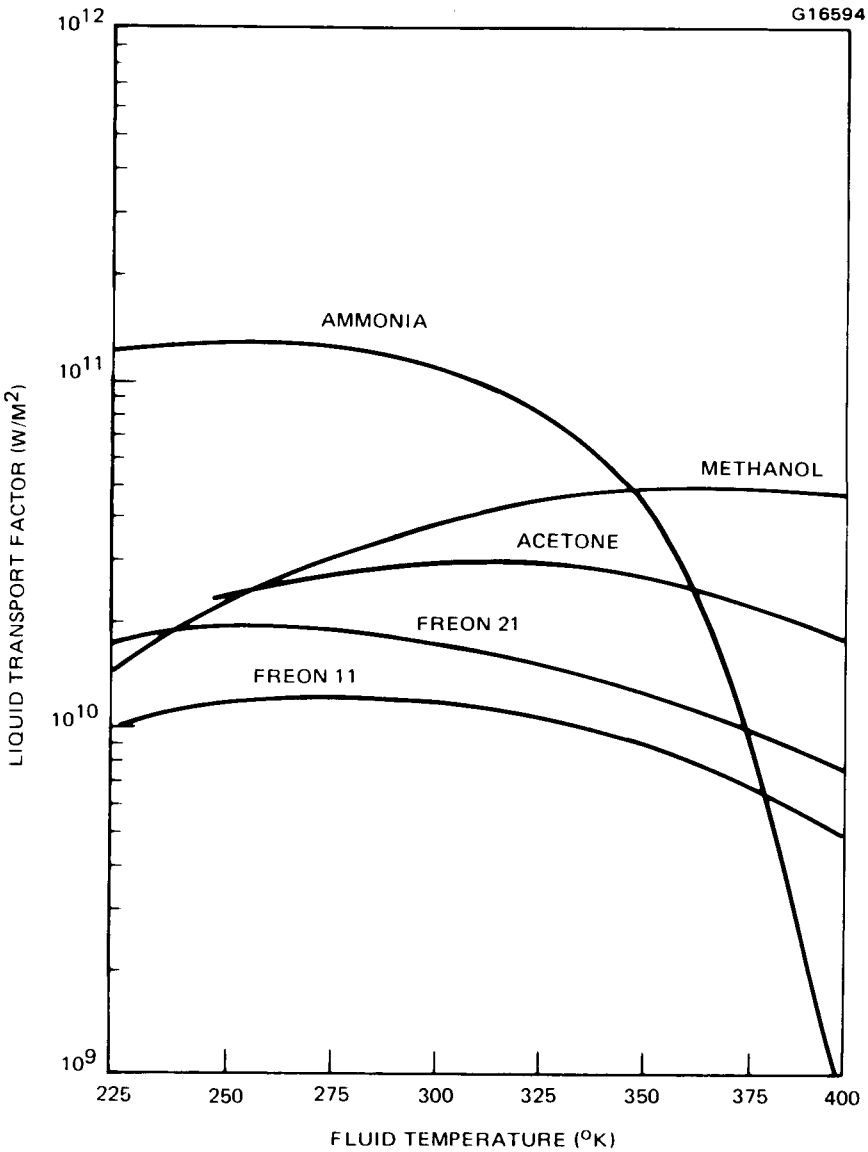

Figure 5-1 Figure of merit for various heat pipe fluids.

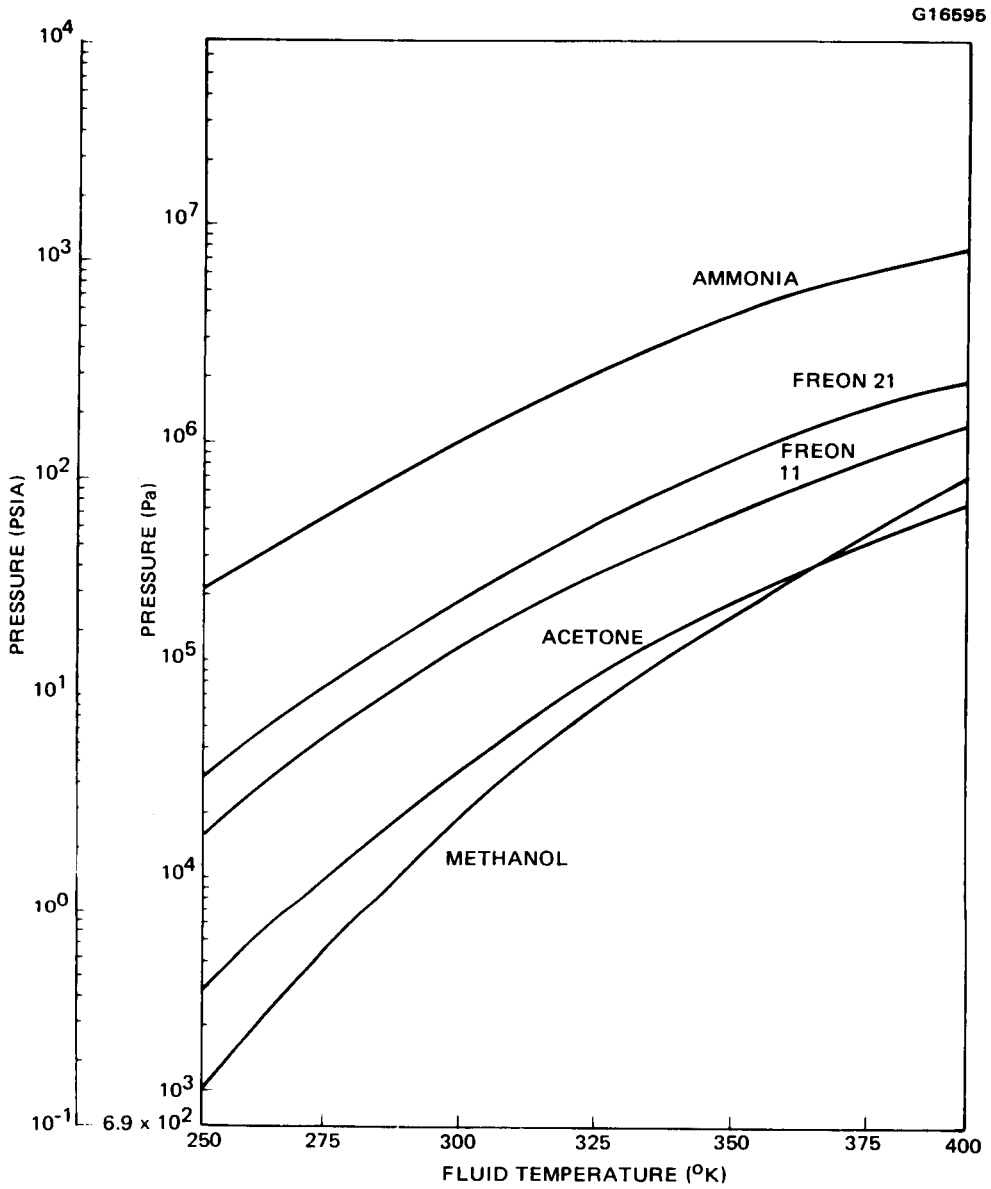

Figure 5-2 Pressure and temperature data for various heat pipe working fluids.

properties; acetone remained the only viable alternative. The heat transport properties of acetone were acceptable, and its vapor pressure was low. Because a literature search gave conflicting results for the compatibility of aluminum and acetone, it is felt that life testing will be necessary to verify compatibility.

5.2 DESIGN CONCEPTS

During the preliminary fabrication/design phase, the stainless steel honeycomb panel manufacturer, Astech Division of TRE Corp., Santa Ana, California, was contacted in regard to modification of existing techniques and equipment to produce an aluminum panel. It was found that Astech could not manufacture an aluminum panel in the same manner that the previous stainless steel honeycomb panel was fabricated.

In addition, the sintering (diffusion welding) vendor for the stainless steel panel, Michigan Dynamics, a subsidiary of United Technologies, Garden City, Michigan, was contacted. It was found that they had no experience in sintering aluminum screen either to itself or to facesheets to produce aluminum honeycomb materials. Sintering, i.e., the metallurgical joining of metal surfaces by applying heat and pressure to cause an actual transfer of atoms at the joint interface of aluminum, is difficult because the oxide film found on aluminum inhibits the diffusion of atoms at the interface joint.

After determining that the aluminum honeycomb panels could not be fabricated using existing techniques and equipment developed for stainless steel, it was concluded that new panel configurations would be required. Evaluation of each panel design consisted of a thermal/structural analysis and subscale developmental panel fabrication and testing. The prototype panel design was based on subscale panel fabrication and test results.

A preliminary design analysis showed that reliability and manufacturing could be enhanced by using a modular panel design. It was decided that the prototype panel would consist of ten individual 0.6 by 0.3 m (24.0 by 12.0 inches) modules. These modules were to be attached together, edge-to-edge, to form one 3.0 by

0.6 m (120.0 by 24.0 inches) panel. This modular approach has the advantage of providing redundancy and, therefore, high system reliability to micrometeoroid and/or space debris damage.

Several methods of panel fabrication were investigated. Various welding techniques, including resistance, electron beam (EB), and tungsten-inert-gas (TIG) welding along with fluxless aluminum brazing, were investigated.

After preliminary design investigations were completed, the following panel concepts were selected for fabrication and test:

1. Brazed panel
2. Formed panel
3. Channel core panel.

The design, fabrication, and testing details for each of the above approaches are described in the following sections.

5.3 BRAZED PANEL

5.3.1 Design and Analysis

The brazed design concept consists of two facesheets and a frame, as shown in Figure 5-3. Various wick configurations, as shown in Figure 5-4, are inserted into the frame to provide for capillary wicking. Both facesheets are lined with a wick material, and additional wick material is placed in the channels, as shown, to provide for liquid communication between the top and bottom facesheets. After wick insertion, the cover facesheets are mated with the frame, and the panel is then vacuum brazed. The end result is a leak-tight structure.

The thermal transport requirements for the 3.0 by 0.6 m (120.0 by 24.0 inch) prototype panel were 1000 watts with a 25.4 mm (1.0 inch) wide center heater over the temperature range of -20 to 65°C. For the developmental units, the panel size was reduced to 0.6 by 0.3 m (24.0 by 12.0 inch). The equivalent thermal transport requirement for this panel size was 100 watts.

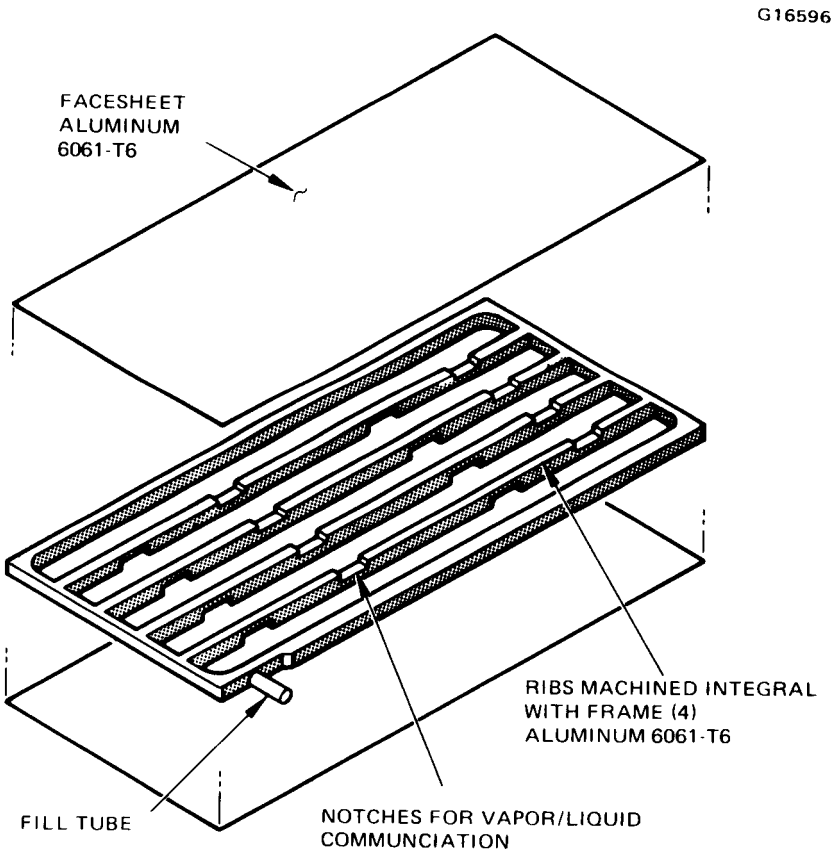

Figure 5-3 Brazed design panel.

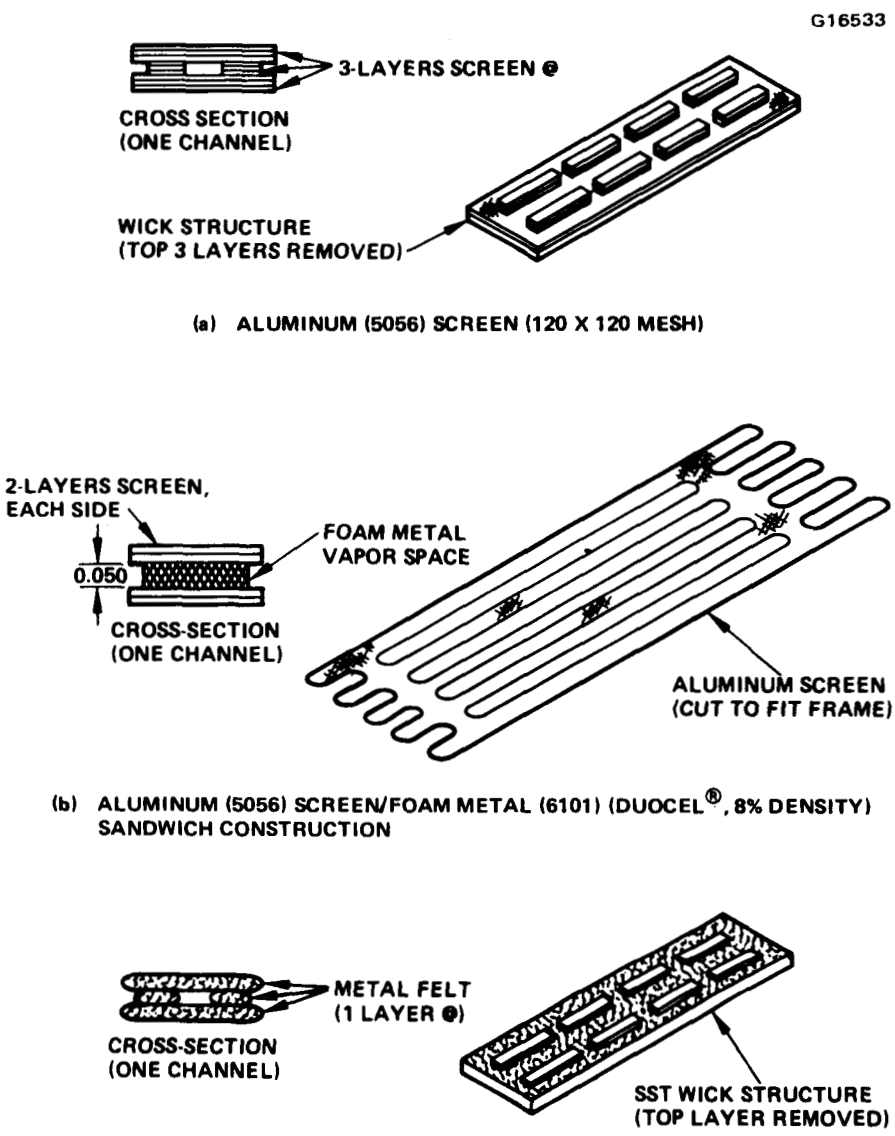

Figure 5-4 Wick configurations - brazed design.

Figure 5-5 shows the results of a heat transport computer analysis[13] performed on the IBM PC-XT for the brazed design. The wick configuration used for this analysis consists of three layers of 120 by 120 mesh screen on each facesheet.

In addition to thermal performance, structural considerations are of primary concern with flat panel heat pipes. A structural analysis[14] was performed on each subscale design. Both maximum stress and deflections were examined. For this analysis, a maximum operating internal panel pressure of 13.5×10^4 Pa (19.6 psia) corresponding to a temperature of $65^{\circ}C$ ($149^{\circ}F$) for acetone was used. It was assumed that the external panel pressure was zero, as in a vacuum environment. A proof pressure factor of 1.5 and burst pressure of 2.5 times the maximum operating pressure were used for design and ambient testing of the developmental panel at Hughes. Results of the structural analysis for the brazed design are shown in Table 5-1. Facesheet deflections and stress were based on a 0.81 mm (0.032 inch) wall thickness.

5.3.2 Fabrication

To evaluate the brazed design concept, three assemblies each with a different wick configuration (Figure 5-4) were fabricated. The objective was to determine the optimum wick design for maximum thermal transport.

Wick fabrication was the first step in panel assembly. The wick design in Panel No. 1 was an all-aluminum mesh wick, as shown in Figure 5-4a. The individual layers of screen were sewn together with fine stainless steel wire (0.25 mm dia.). Small pieces were inserted to interconnect the five channels. Panel No. 2 had two layers of aluminum screen on each facesheet held in place with Duocell^R aluminum foam metal. As illustrated in Figure 5-4b, the foam metal fills the entire vapor space and provides structural support. Its effect on the vapor flow pressure drop is not significant, since it is a very open pore structure with a porosity of 92 percent. Panel No. 3 utilizes stainless steel sintered metal felt as the wick structure, as shown in Figure 5-4c. The advantage of this approach is that the individual wick pieces can be spot

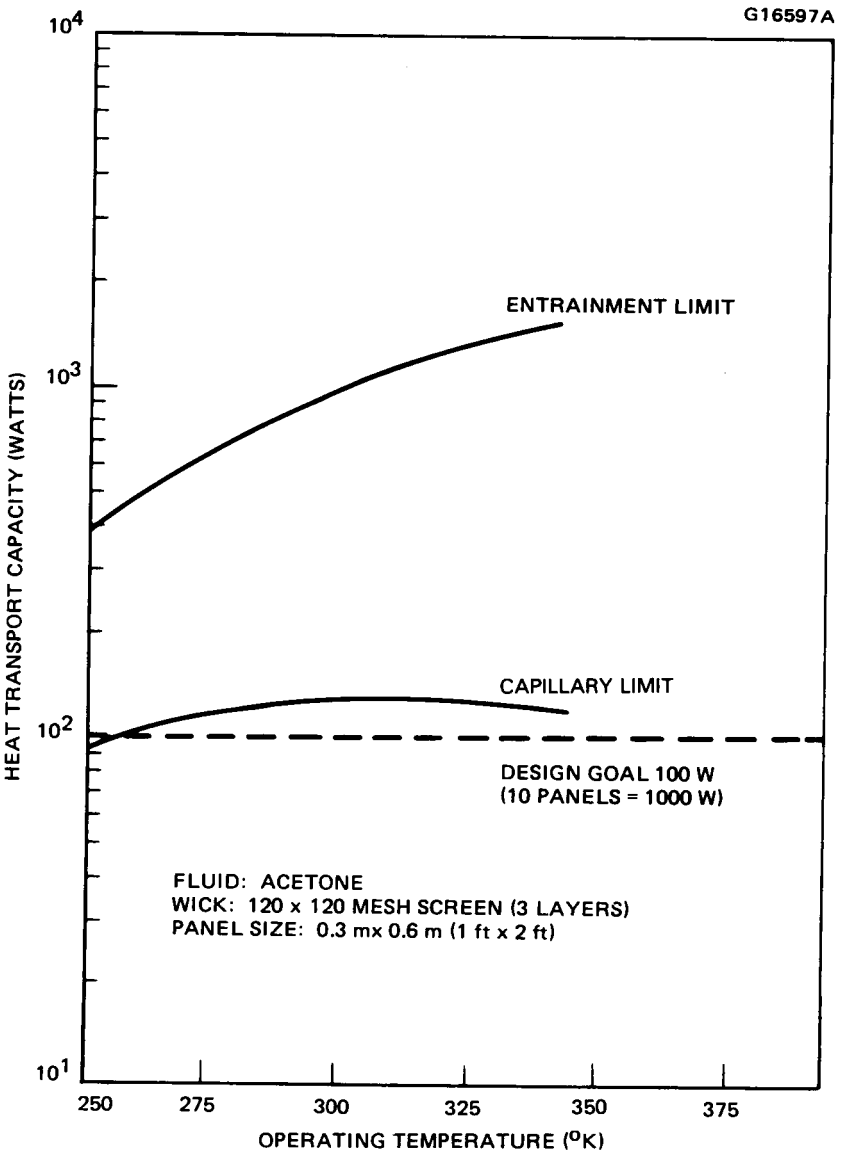

Figure 5-5 Performance prediction brazed design.

TABLE 5-1

MAXIMUM STRESS AND DEFLECTION IN BRAZED DESIGN PANEL
AS A FUNCTION OF INTERNAL PRESSURE
(WALL THICKNESS = 0.81 mm, 0.032 inch)

Pressure Pa x 10^5 (psia)	Deflection mm (in)	Stress N/m^2 (lb/in^2)
1.31*	0.0206	4.56×10^7
(19)	(0.00081)	(6,608)
3.31	0.0508	1.15×10^8
(48)	(0.0020)	(16,695)
3.51	0.0559	1.22×10^8
(51)	(0.0022)	(17,738)
8.75	0.1372	3.04×10^8
(127)	(0.0054)	(44,173)

*Maximum operating pressure 1.31×10^5 Pa (acetone)

welded together. Again, the wicks in each channel were interconnected across the gaps in the ribs of the frame structure (Figure 5-3).

After the wick assemblies were completed, the panels were prepared for vacuum brazing. This process involves exposing the braze joint to the action of magnesium in a vacuum environment to promote bonding. In this case, the faying surfaces of the ribbed frames (Figure 5-3) were first plated with a copper alloy to enhance this bonding process. Each unit was then assembled and placed in a braze fixture. The units were then vacuum brazed. After brazing was completed, each panel was helium leak checked. Panel No. 2 was the only panel that was leak tight after the first braze cycle. Panel Nos. 1 and 2 were rebrazed twice, but could not be repaired.

Figure 5-6 is a photograph of the brazed panel Unit No. 2 which was successfully brazed. The panel is 0.25 m by 0.12 m by 4.1 mm thick (10.0 by 5.0 by 0.16 inches) and weighs 7.0 kg/m^2 (1.43 lbm/ft^2), including the weight of the fluid. The dry weight is 6.5 kg/m^2 (1.34 lbm/ft^2). It should be noted that

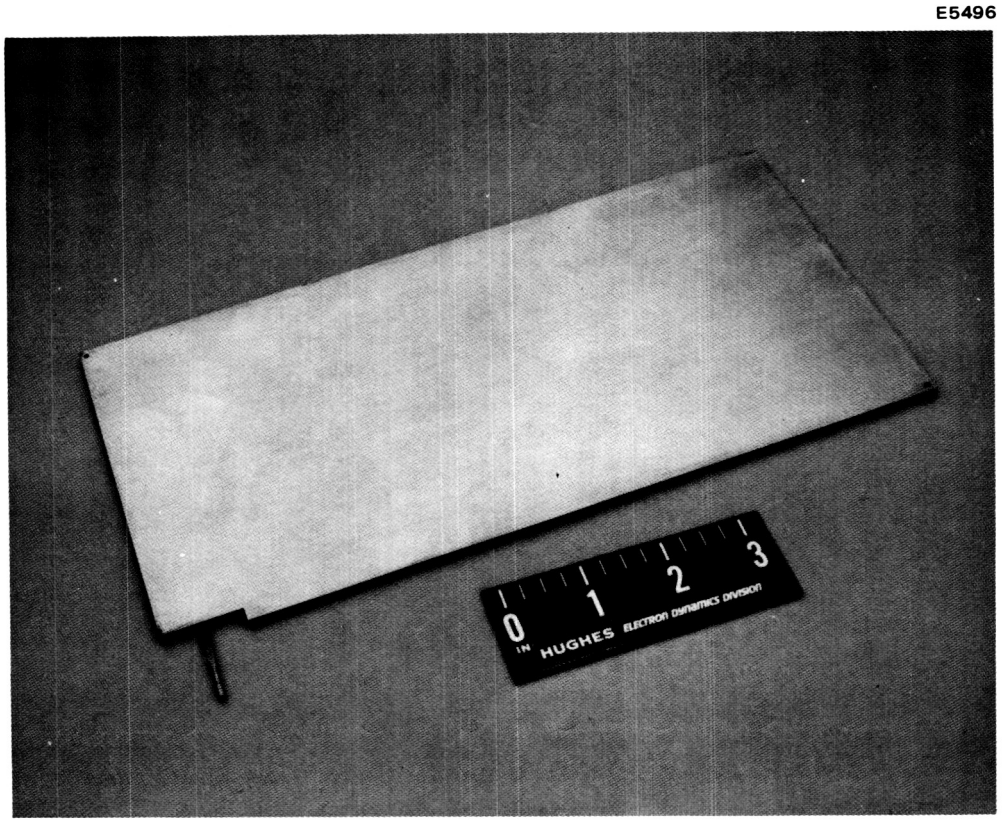

Figure 5-6 Completed brazed panel Unit No. 2.

the size of the brazed subscale unit was limited by the furnace size (0.36 by 0.22 x 0.41 m) of the vacuum brazing vendor.

5.3.3 Thermal Performance Testing

Brazed Unit No. 2 was processed with 17 grams of high performance liquid chromatography (HPLC) grade acetone (99.998 percent pure). The panel was instrumented per Figure 5-7. The edge heater was then tilted 3.17 mm (0.125 inch) above the opposite edge, and the panel was tested in ambient air. Initially, 10 watts of electrical power was applied to the edge heater. Both natural convection and forced fan air cooling were used. Power was then increased to 80 watts, at which point dryout was observed. The test was then repeated with 6.35 mm (0.25 inch) tilt. The panel held approximately 50 watts before dryout occurred. Figure 5-7 shows the corresponding temperature data for the 3.17 mm and 6.35 mm tilts.

5.4 FORMED PANEL

5.4.1 Design and Analysis

The formed design is illustrated in Figure 5-8. This design consists of two facesheets; one sheet is flat, and the other is formed into a dimpled pan. Internal wicking is provided by capillary grooves machined directly into these facesheets. The flat sheet has grooves running lengthwise, whereas the grooves on the formed facesheet are perpendicular to those in the flat sheet. The purpose of this cross-groove design is to provide a two-dimensional liquid flow pattern for nonsymmetrical heating and/or cooling loads without the need for additional wicks. Liquid communication between the top and bottom surfaces is provided by the liquid fillets, which form naturally at each dimple location and around the edges. The end result is a heat pipe panel constructed of only three piece parts, including the fill tube; capillary wicking and structural support are integral with the facesheets themselves. The panel is resistance (seam and spot) welded together, as shown in Figure 5-8.

The formed design uses capillary grooves to provide the required capillary pumping. Computer runs on the IBM PC-XT were made to observe the effect of

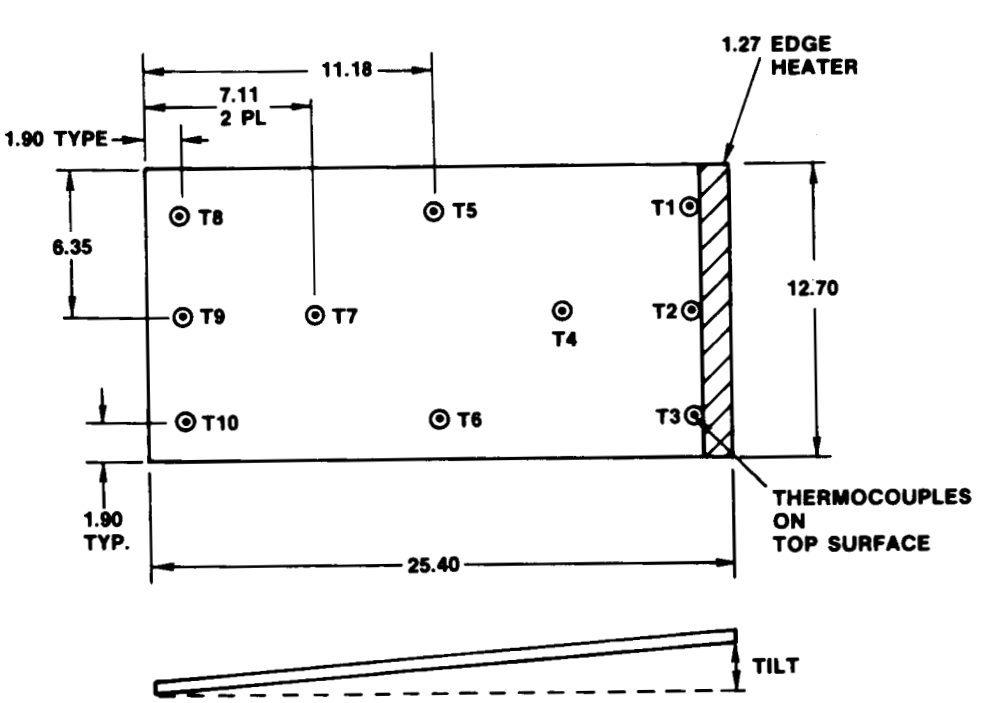

Figure 5-7 Brazed design thermal performance test results.

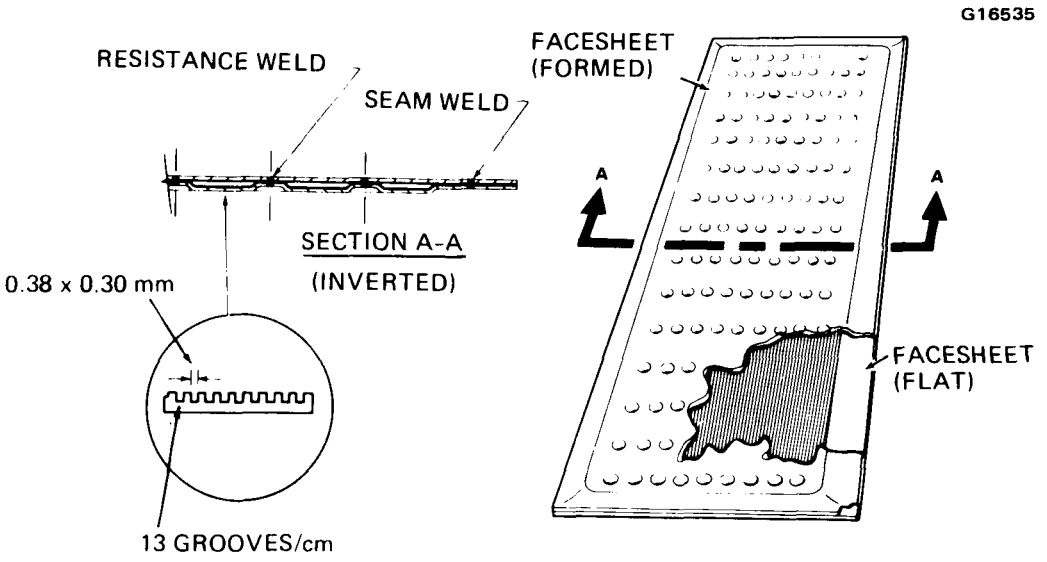

Figure 5-8 Formed design panel.

groove depth and width on thermal performance.[13] Results of a typical run are shown in Figure 5-9. It was found that 0.38 mm wide by 0.30 mm deep (0.015 by 0.012 inch) grooves with a pitch of 0.76 mm (0.030 inch) would meet the performance requirement of 1000 watts over the temperature range of -20 to 65°C.

The estimated maximum stress and deflections in the facesheets of the formed design panel are shown in Figures 5-10 and 5-11. These curves are functions of internal pressure and wall thickness (t) for a dimple spacing of 25.4 mm (1.0 inch).[14] Yield stresses for aluminum 6061-T6 and 5052-H34 are indicated in Figure 5-10. From this analysis, it was determined that a wall thickness of 1.01 mm (0.040 inch), excluding the capillary grooves, would provide an adequate margin of safety.

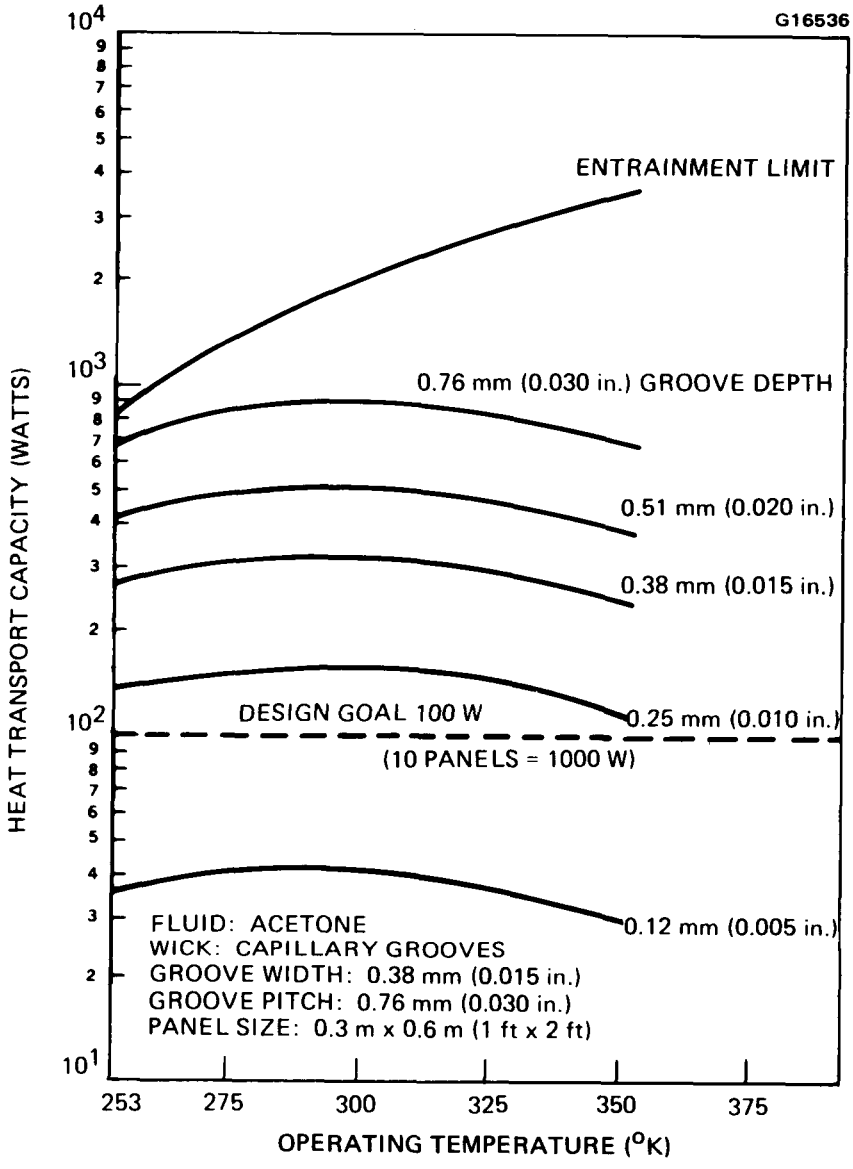

Figure 5-9 Thermal performance prediction for a vapor space height of 2.54 mm (0.10 inch).

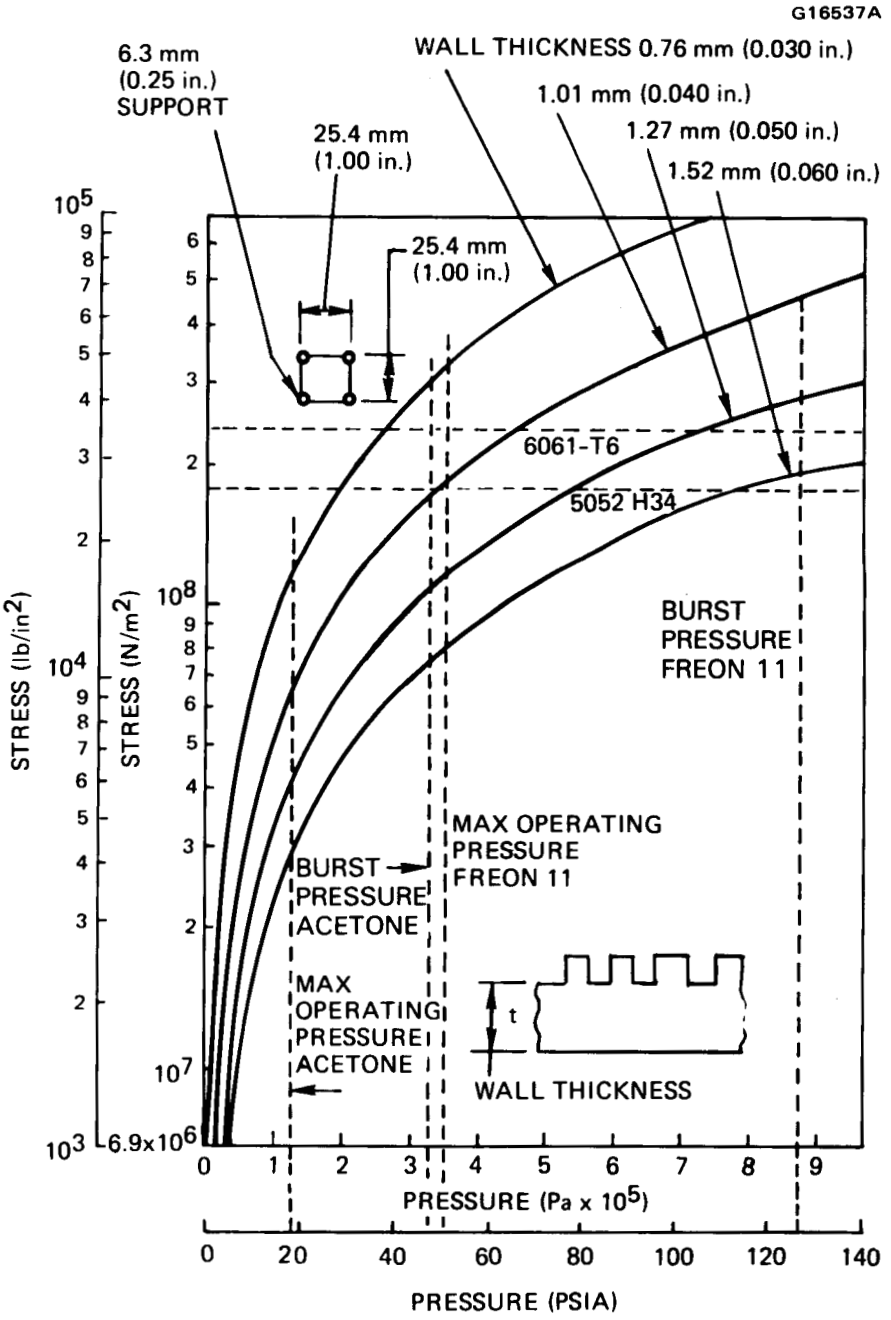

Figure 5-10 Maximum stress in panel as a function of internal pressure.

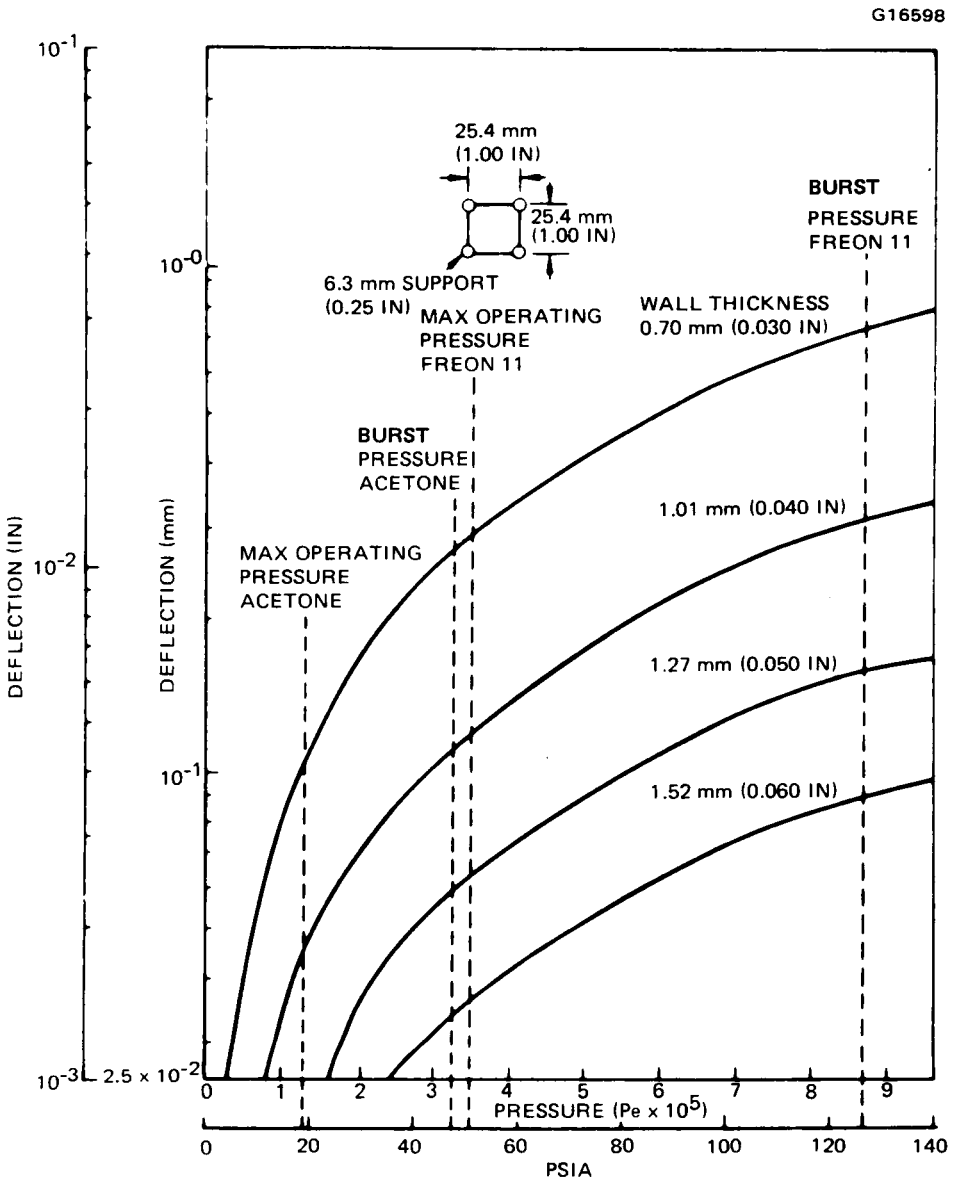

Figure 5-11 Maximum deflection in formed panel as a function of internal pressure.

5.4.2 Fabrication

The formed and welded panel design is really quite simple (Figure 5-8). It consists of only three piece parts:

- Flat grooved facesheet
- Formed grooved facesheet
- Stainless steel/aluminum transition joint fill tube.

Originally, 1.27 mm (0.050 inch) thick 5052-H34 aluminum alloy sheet material was selected as facesheet material because of its excellent welding and forming properties. Because of its tendency to gum up the slitting saws used for cutting the grooves, however, 6061-T6 aluminum alloy was substituted for the facesheet material. Figures 5-12a and 5-12b are photographs of the machined grooves. The as-built groove geometry was 0.38 wide by 0.30 mm deep (0.015 by 0.012 inch) with a groove pitch of 0.76 mm (0.030 inch).

The grooved facesheet material was annealed to the T0 condition to allow forming of the dimpled pan. After forming, the facesheet was straightened and then heat treated back to the T6 condition for strength.

Welding was the final step in fabrication of the panel. The aluminum/stainless steel fill tube (Figure 5-13) was first TIG welded into place on the formed facesheet. Next, the flat and formed facesheets were sandwiched together and resistance welded (spot welded) at the dimple areas (220 spot welds). The final step was to run a resistance weld (seam weld) around the edge of the panel. Figure 5-14 is a photograph of the completed panel. It is 0.6 m by 0.3 m by 3.81 mm thick (24.0 by 12.0 by 0.15 inches) and weighs 6.93 kg/m^2 (1.42 lbm/ft^2), including the weight of the working fluid (wet weight). The dry weight is 6.73 kg/m^2 (1.38 lbm/ft^2).

5.4.3 Thermal Performance Testing

The following series of tests was performed on the formed panel in order to characterize its performance.

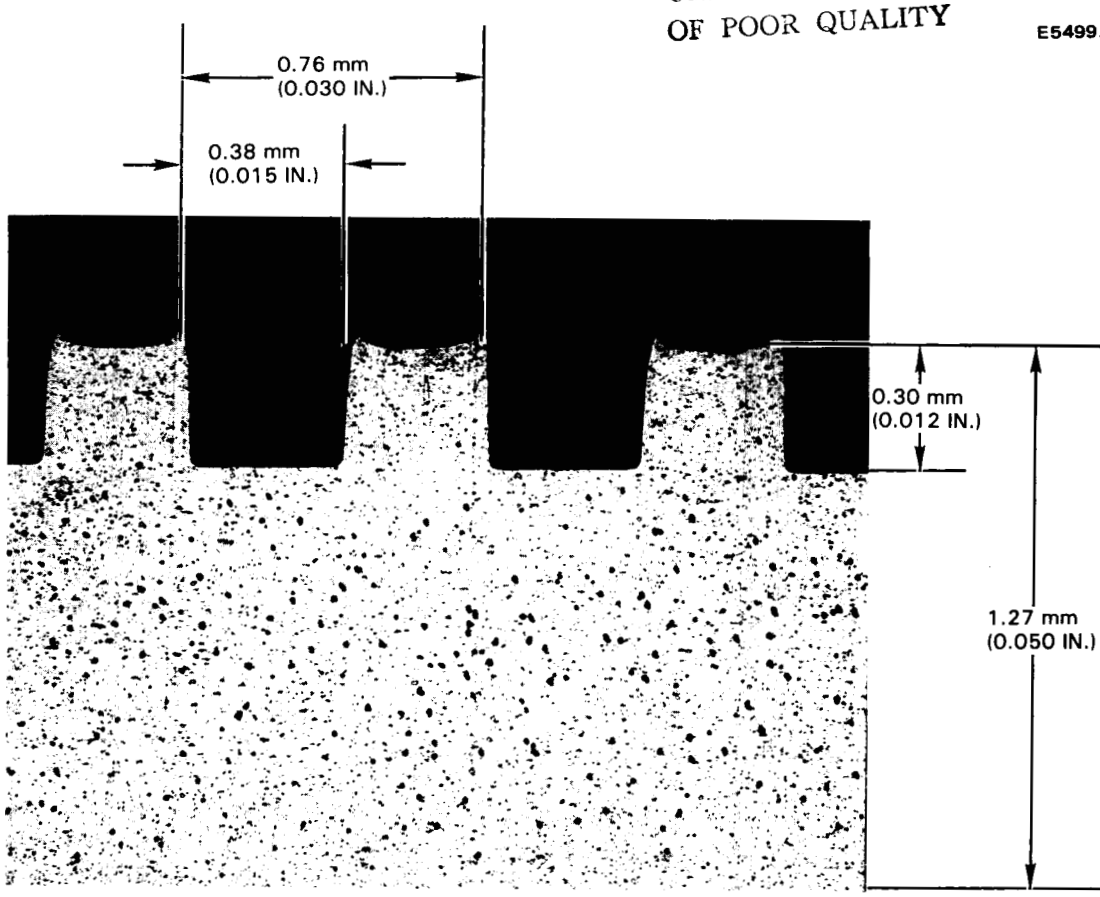

(a) PHOTOMICROGRAPH OF GROOVE CROSS-SECTION (GROOVE DEPTH 0.30 mm).

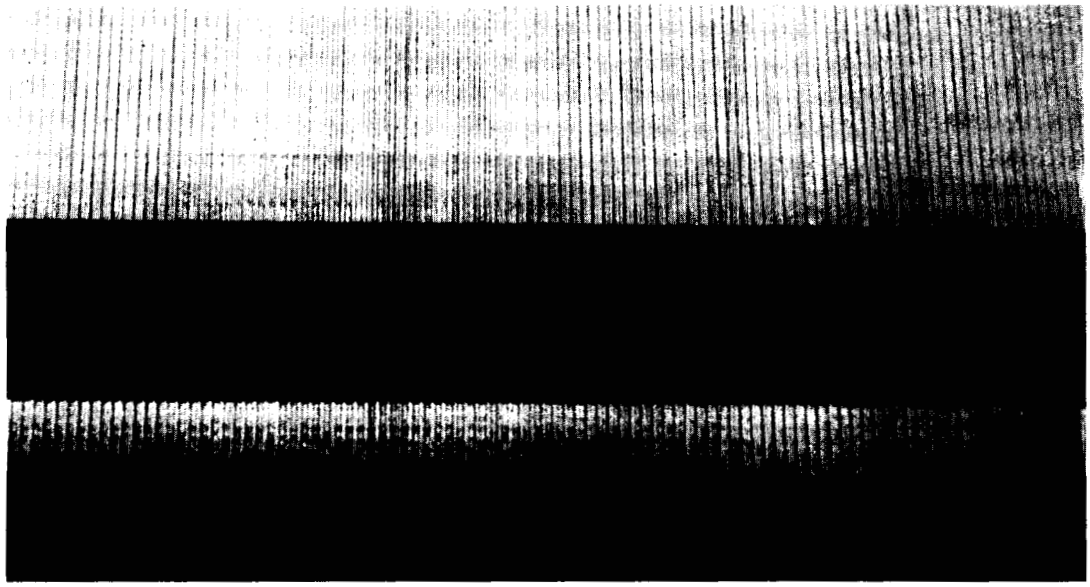

(b) CLOSE-UP OF GROOVED FACESHEET

Figure 5-12 Machined capillary grooves in panel facesheet.

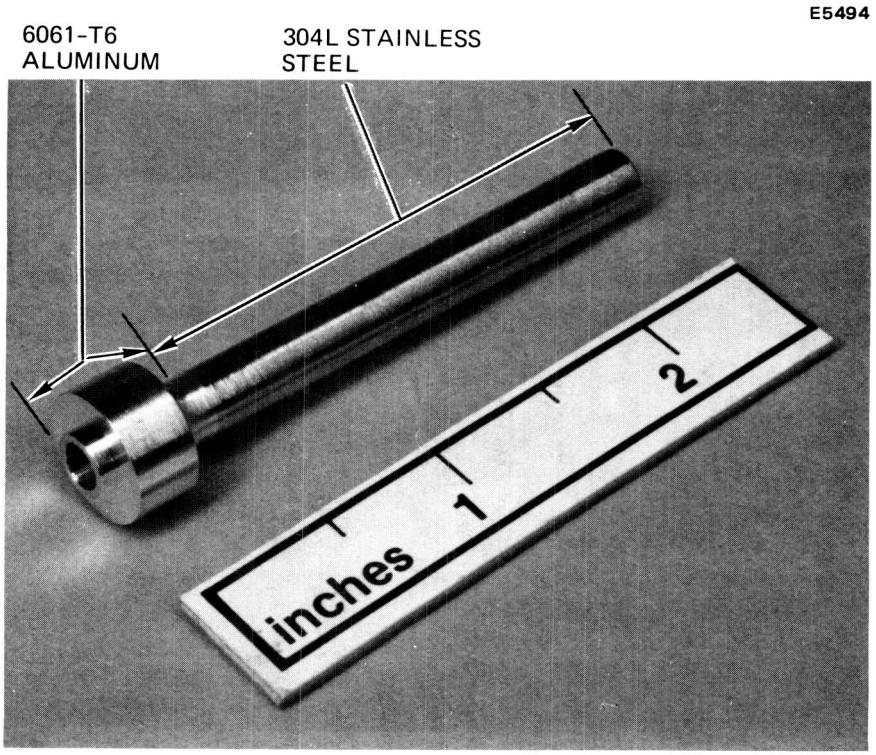

Figure 5-13 Stainless steel/aluminum transition joint fill tube.

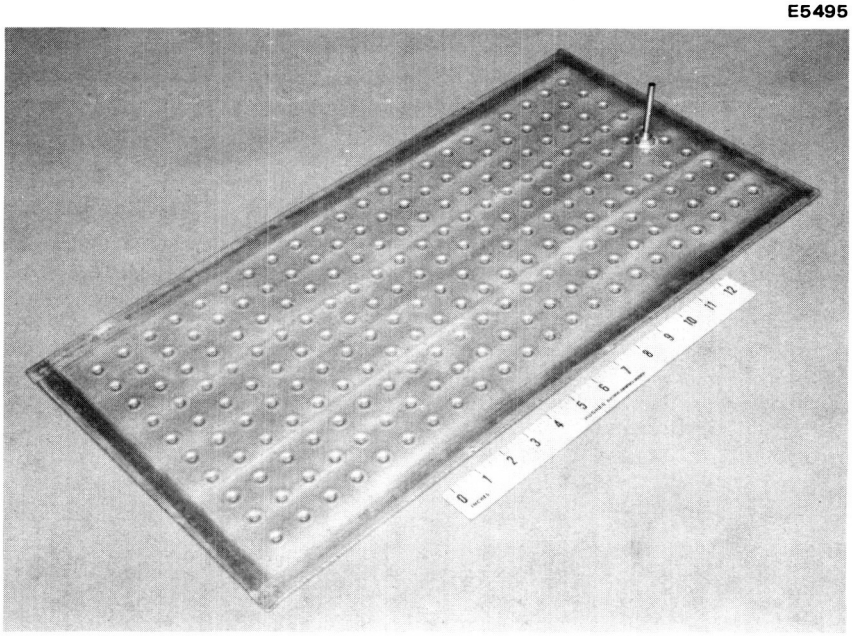

Figure 5-14 Completed formed panel.

- Liquid fill test
- High/low temperature performance test
- Tilt tests
- Simulated failure test

Liquid Fill Test - The purpose of the liquid fill test was to determine the required fill for the formed panel design. The panel was initially filled with 30.0 g of HPLC grade acetone and instrumented per Figure 5-15. Input power of 100 watts was then applied to the center heater with ambient air cooling to see if signs of excess fluid (cold spots) would appear. None could be found. The test was then repeated with fills of 110 percent (33 g), 120 percent (36 g), and 130 percent (39 g) of the original fill. Testing showed no signs of excess fluid. The fill was then increased to approximately 150 percent (44 g). Testing showed that excess fluid was present. Fluid was then removed from the panel in approximately 1 gram increments until no signs of excess fluid could be detected. The fill was finally optimized at 38.5 g based on a 60°C operating temperature.

High/Low Temperature Performance Tests - After the fill was optimized empirically with 38.5 g of acetone, high and low temperature performance testing was started. The panel was instrumented per Figure 5-15 and leveled to within ±1.3 mm (0.050 inch). High temperature performance testing at 60°C (140°F) consisted of applying 100 W of power to the center heater and looking for evidence of dryout. Both ambient air and fan cooling were used. The power was increased in 10-watt increments until evidence of dryout was detected. Test results (Figure 5-16 and 5-17) show that the panel held approximately 120 W (equivalent to 1200 W for a 3-m panel) before dryout occurred at 140 W. The panel was then placed in an environmental chamber and leveled to within ±1.3 mm (0.050 inch). The panel was then performance tested at -20°C (-4°F). Test results show that the panel held approximately 40 W (equivalent to 400 W for a 3-m panel) before dryout occurred at 50 W.

In order to obtain a better correlation of the actual test results with predicted results, the original computer model was upgraded. The original thermal performance model assumed that all grooves were fully primed and that the

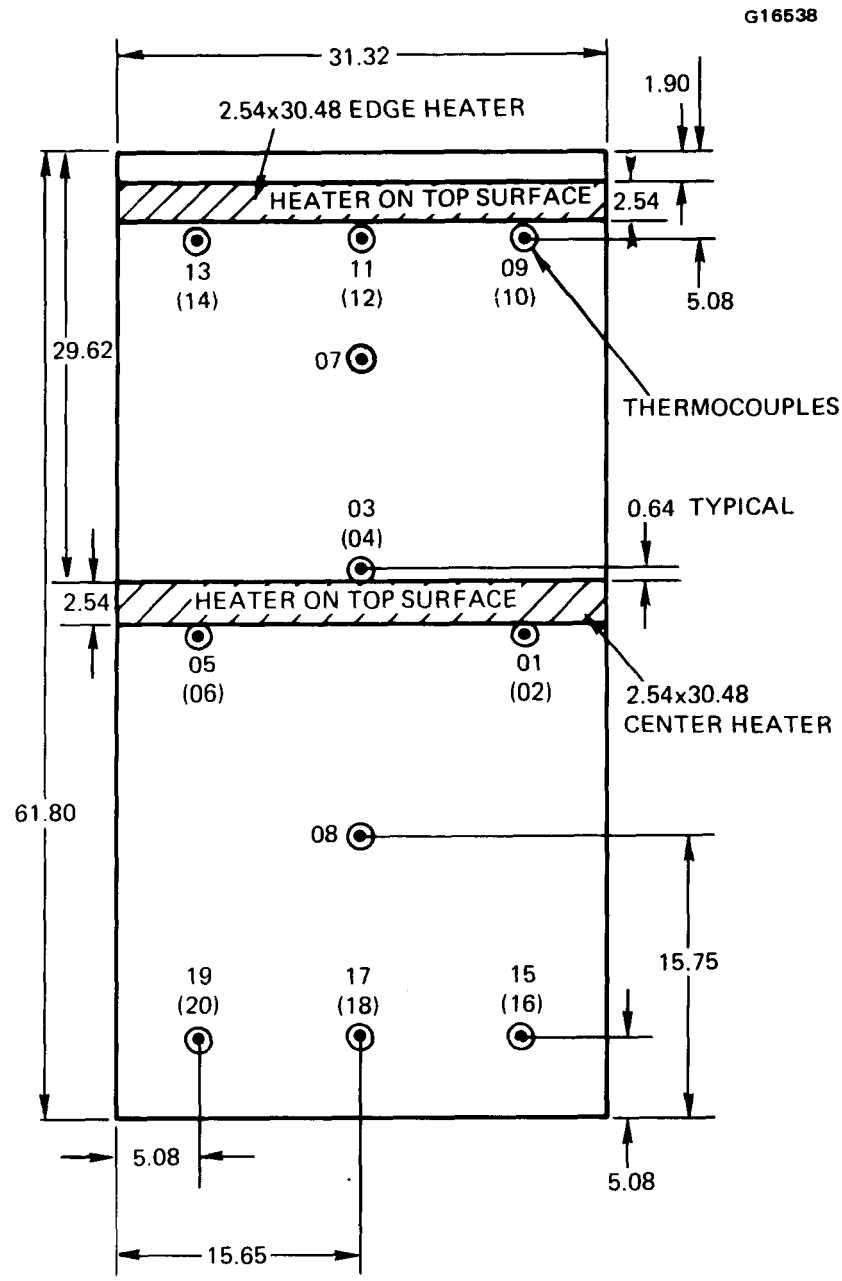

NOTE: 1) NUMBERS IN PARENTHESES INDICATE THERMOCOUPLES ON BOTTOM SURFACE.
2) DIMENSIONS IN CENTIMETERS.

Figure 5-15 Test instrumentation.

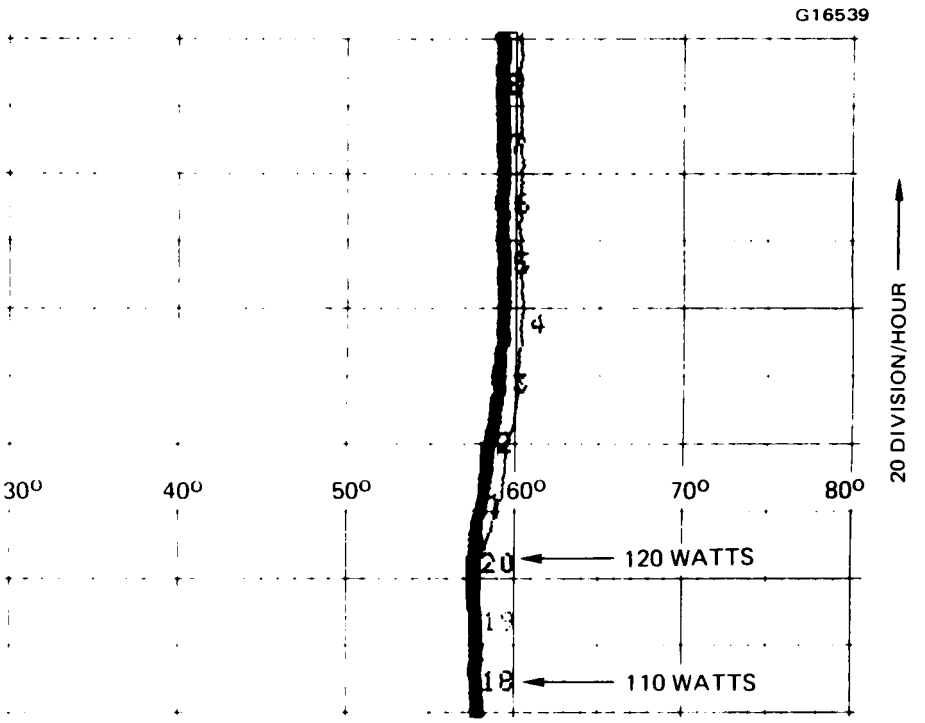

Figure 5-16 High temperature performance test data at 60°C (140°F).

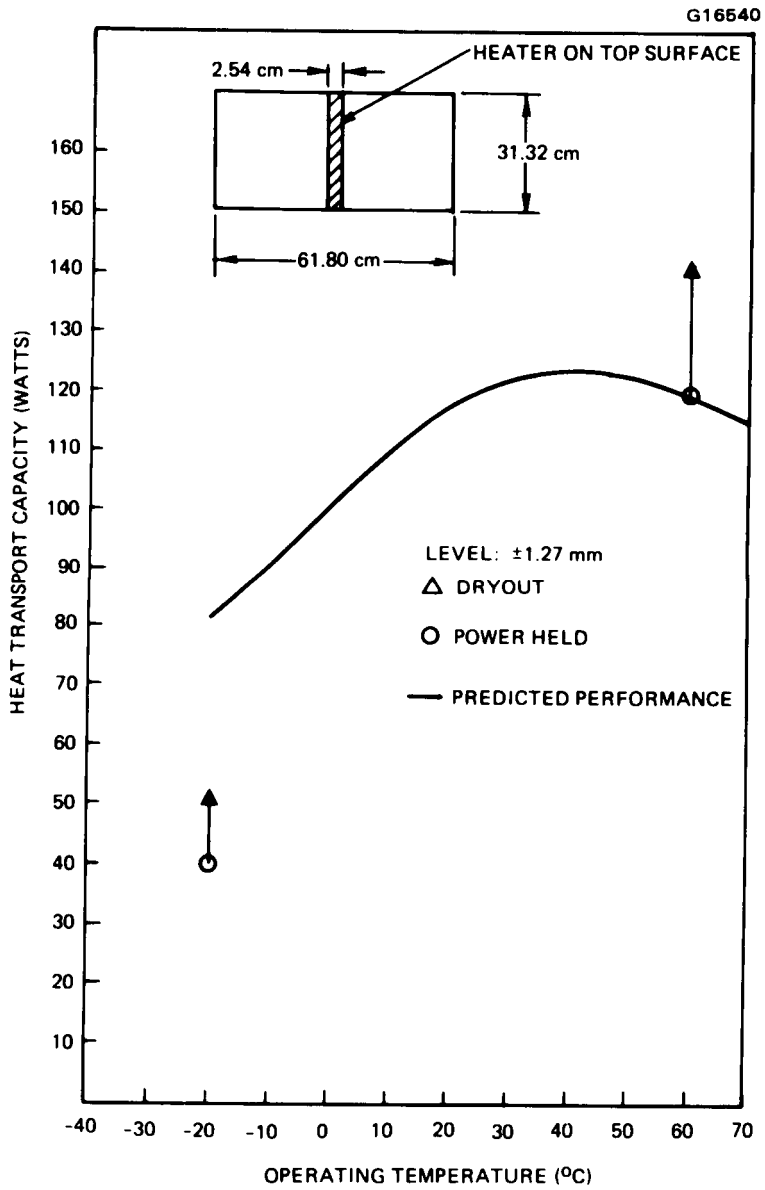

Figure 5-17 Thermal performance and data correlation.

flow area and permeability were constant along the entire groove length. In reality, the grooves are not fully primed, and both the flow area and permeability vary along the pumping length of the groove. These variations are caused by meniscus recession in the grooves. The upgraded thermal performance model accounts for this meniscus recession by using an average flow area and permeability. This average groove area was obtained by matching the test performance at 60°C (140°F) as indicated in Figure 5-17. Subsequent predictions at other temperatures and tilt angles were also based on this value for the groove area. It is seen in Figures 5-17 and 5-18 that the predicted results, using the upgraded model, correlate fairly well with the actual results. Note that the actual low temperature performance was lower than predicted. This is because the panel fill was optimized for a 60°C operating temperature. For the -20°C test, the panel was underfilled (due to fluid shrinkage) by about 13 percent.

Tilt Tests - In both the high and low temperature performance tests, the panel was level within ±1.27 mm (0.050 inch). To investigate the effect of adverse tilt on panel performance, two types of tilt tests were used. The first test consisted of "bowing" the panel sides 3.18 mm (0.125 inch) lower than the middle and then initially applying 25 W to the center heater with ambient air cooling. Power was increased until evidence of dryout was observed. The panel held about 60 W (equivalent to 600 W for a 3 m panel) before dryout occurred. The heaters were then moved from the center location to the edge (Figure 5-15). The panel was then leveled within ±1.27 mm, and heater power (5 W) was applied with ambient air cooling. The power was increased until dryout was observed. The panel held 30 watts before dryout occurred at 35 watts. This was repeated with tilts of 3.18 and 6.35 mm (0.12 and 0.25 inch).

Results are plotted in Figure 5-18. It should be noted that the results do correlate with previous test data. Using heat pipe theory, one would expect a factor of four reduction in heat transport when the center heater is moved to the edge. Test data show that the panel held 120 watts with the center heater and 30 watts with the edge heater. From these results, one can see the factor of four reduction in power. Note that the upgraded computer model correlates well with actual test results (Figure 5-18).

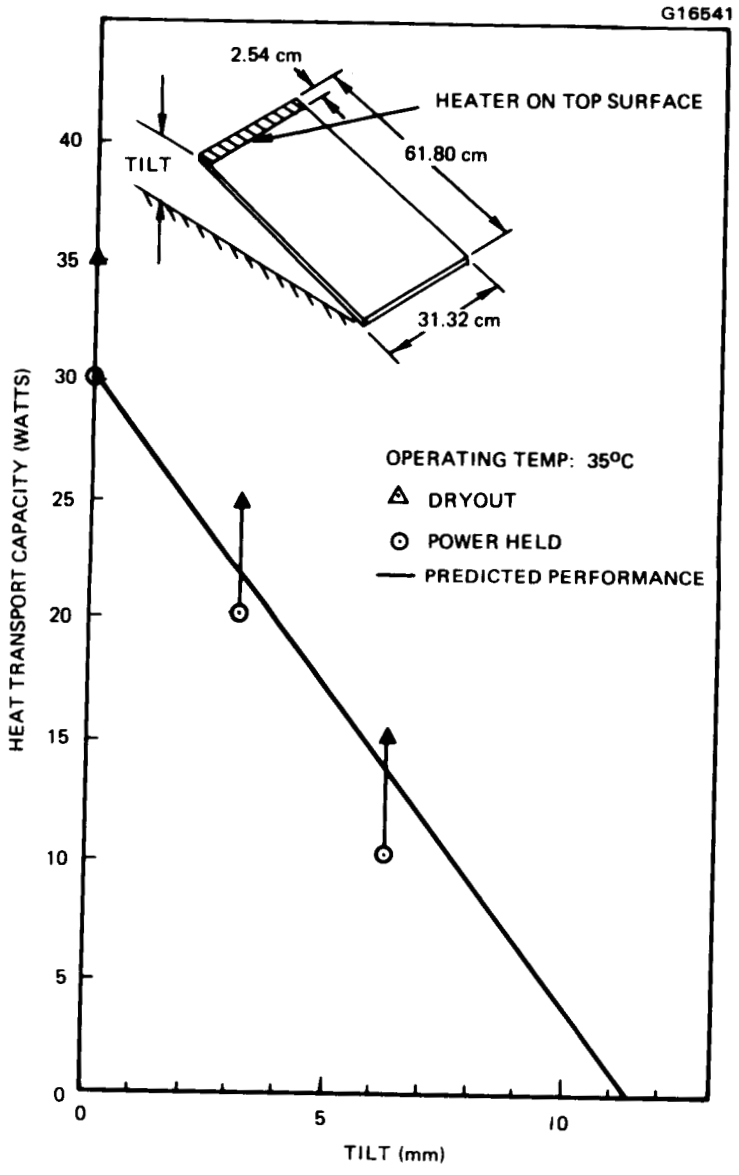

Figure 5-18 Tilt test performance and data correlation at 35°C (95°F).

Simulated Failure Test - The purpose of the failure test was to simulate a heat pipe panel failure. The objective was to compare the temperature profiles between a charged heat pipe panel and an uncharged panel. Before testing began, the formed design heat pipe panel was drained of acetone and instrumented per Figure 5-15, using the center heater. The panel was then placed in the environmental chamber. Various powers were input to the panel, and temperature data were recorded. It can be seen from the results in Figure 5-19 that the uncharged panel acts as a solid fin. When temperature data from an uncharged panel are compared to a charged panel (Figure 5-16), a dramatic

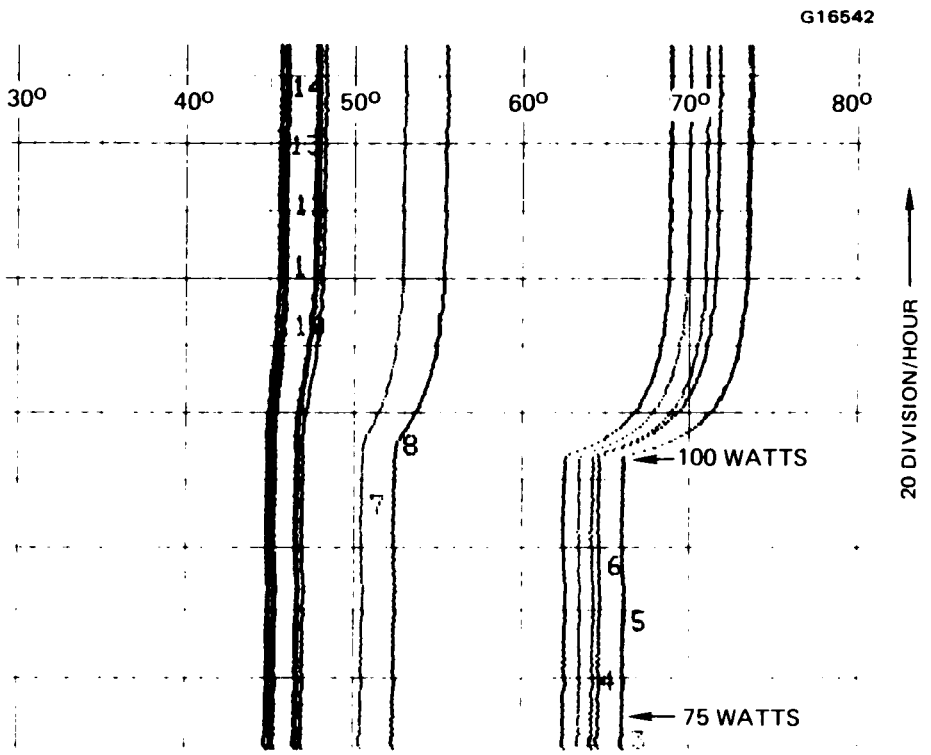

Figure 5-19 Solid aluminum fin performance-simulated panel failure.

difference in temperature profiles can be observed. These results clearly show the advantage of a heat pipe radiator panel over a solid fin radiator. The fin efficiency of the heat pipe panel is approximately 1.0.

5.5 CHANNEL CORE PANEL

5.5.1 Design and Analysis

The channel core design, as illustrated in Figure 5-20, is similar to the stainless steel honeycomb panel design, except that the core structure is a triangular channel configuration rather than cellular. This open channel design has the advantage of reduced vapor flow resistance, which results in higher thermal performance in comparison with the honeycomb design. The core material provides structural support and liquid communication between the top and bottom facesheets while the facesheets are grooved to provide capillary pumping. This particular panel design has the potential of being the lightest weight. This is because the facesheet thickness can be reduced as a result of the internal truss support provided by the core material.

The channel core design, like the formed design, has capillary grooves machined into the facesheets to provide capillary pumping and liquid distribution throughout the panel surfaces. As a first approximation, then, the heat transport analysis for the channel core is the same as for the formed design. Although this approach neglects the contribution of liquid flow along the core structure, and the larger vapor flow area of the channel core panel, the performance predictions (Figure 5-9) are conservative. Subsequent results have shown that the vapor space is not a major effect over the range of interest.

As previously mentioned, the channel core design has the potential of being lighter in weight than the brazed or formed designs. However, there is a practical limit to how thin the facesheets can actually be made, because of manufacturing limitations. Facesheets deflection and stress analysis results for a 51-mm (0.020-inch) wall thickness, excluding the capillary grooves, are summarized in Table 5-2.[14] Additional tradeoffs will be needed in the future to further optimize the facesheet thickness and core dimensions.

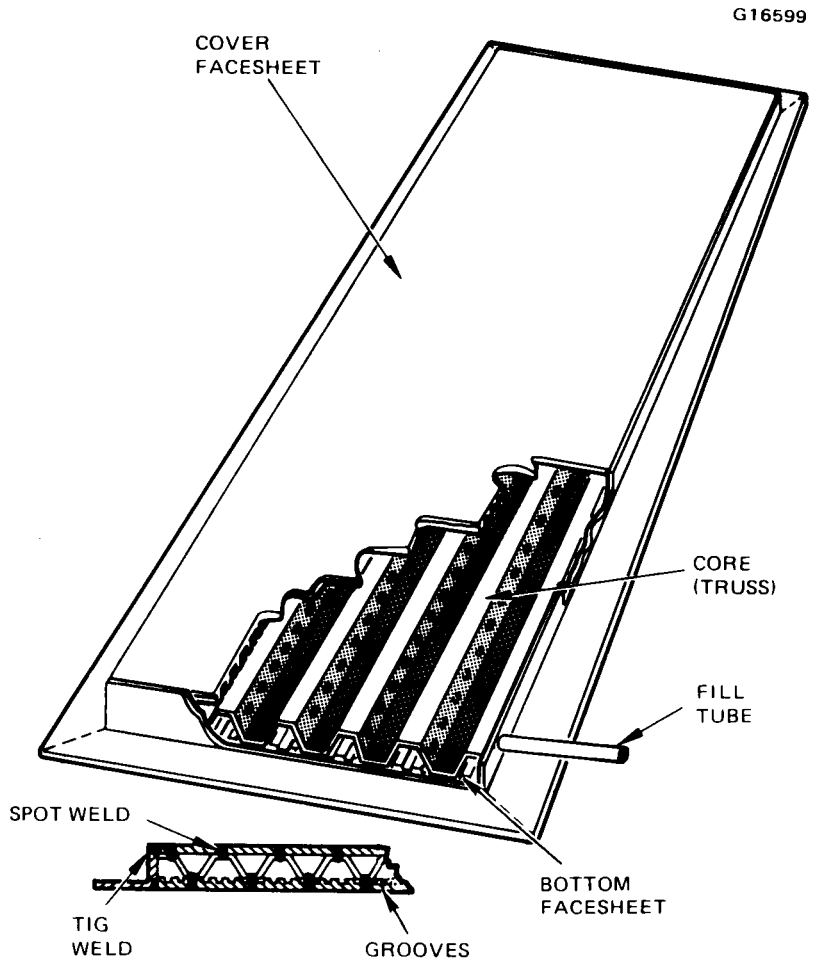

Figure 5-20 Channel core design panel.

TABLE 5-2

MAXIMUM DEFLECTION AND STRESS IN CHANNEL CORE DESIGN PANEL AS A FUNCTION OF INTERNAL PRESSURE (WALL THICKNESS = 0.51 mm, 0.020 inch)

Pressure Pa x 10^5 (psia)	Deflection mm (in)	Stress N/m^2 (lb/in^2)
1.31*	0.0102	4.09×10^7
(19)	(0.0004)	(5,937)
3.31	0.0254	1.03×10^8
(48)	(0.0010)	(15,000)
3.51	0.0279	1.09×10^8
(51)	(0.0011)	(15,937)
8.75	0.0686	2.73×10^8
(127)	(0.0027)	(39,687)

*Maximum operating pressure = 1.31×10^5 Pa (acetone)

5.5.2 Fabrication

Fabrication experiments were initiated to demonstrate the feasibility of an aluminum channel core heat pipe panel of the type shown in Figure 5-20. Forming experiments were performed to demonstrate that holes in the core material, which are required for vapor flow, could be aligned properly for corrugation. These experiments were necessary because it is desirable to punch the holes prior to forming. A 0.41 mm (0.016 inch) thick aluminum (5052-H34) sheet material was selected for these experiments. This was considered to be the minimum thickness for the core material, taking into account the requirements for hole punching, forming, and welding.

A single layer of screen is also required on each side of the core material to provide liquid communication between the bottom and top facesheets. Since it is not practical to diffusion bond or sinter aluminum screen to aluminum sheet, it was necessary to develop a resistance spot welding technique. Resistance welding experiments were successfully performed with one layer of 120 by 120 mesh aluminum (5056) screen, 0.094 mm (0.0037 inch) wire diameter, spot welded

to both sides of the aluminum sheet. The spot welds are 3.17 mm (0.125 inch) diameter at a spacing of 12.7 mm (0.50 inch). After welding the core material, 3.17 mm (0.125 inch) diameter vapor holes were punched, and then the material was corrugated as shown in Figure 5-21. Note that the vapor holes are properly lined up with the corrugations.

The next objective was to spot weld the corrugated core to the bottom facesheet and then spot weld to the cover facesheet (Figure 5-20). The problem with this approach was that our resistance welding vendor had informed us that he could not resistance weld the cover facesheet to the core material; the electrodes would be too long and thin for this purpose. This problem was solved by using an electron beam (EB) welding burn-through technique, which was developed on another program.[15] However, the 6061-T6 aluminum alloy, which was originally selected to facilitate machining capillary grooves into the facesheet (Section 5.3.4), was not acceptable for this welding process. Cracking problems associated with fusion welding 6061 aluminum without filler material led to the selection of 5051-H34 aluminum for the cover facesheet material. Moreover, initial welding experiments demonstrated that the material should be thicker than 51 mm (0.020 inch), which was based on stress considerations (Section 5.5.1). For these reasons, the facesheet thickness was increased to 1.27 mm (0.050 inch) and a single layer of 120 by 120 mesh aluminum screen material was spot welded to the inner surface of the cover facesheet, as shown in Figure 5-22, to replace the previously machined capillary grooves. The dimensions of the spot welds are the same as used in making the core material. The bottom facesheet thickness was also retained at 1.27 mm (0.050 inch) in order to utilize already existing grooved material.

The end result was a composite panel constructed as follows. First, the bottom facesheet (grooved) was resistance welded to the corrugated core. The cover facesheet (with screen wick) was then EB welded to the corrugated core using a burn-through weld technique. Next, the end caps and the aluminum/stainless steel fill tube were TIG welded in place. The final step was to seam weld the flanged edges of the panel together. Figure 5-23 is a photograph of the completed panel. Note the appearance of the EB burn-through welds. The intermittent EB welds have a weld length of 63.5 mm (2.5 inches) and a spacing of

E5464

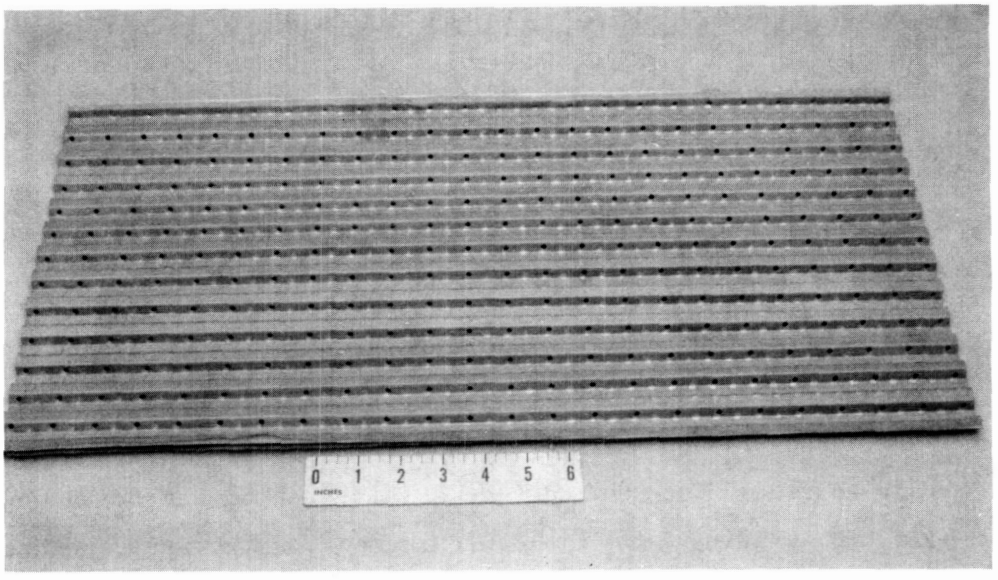

(a) CORE MATERIAL AFTER CORRUGATION

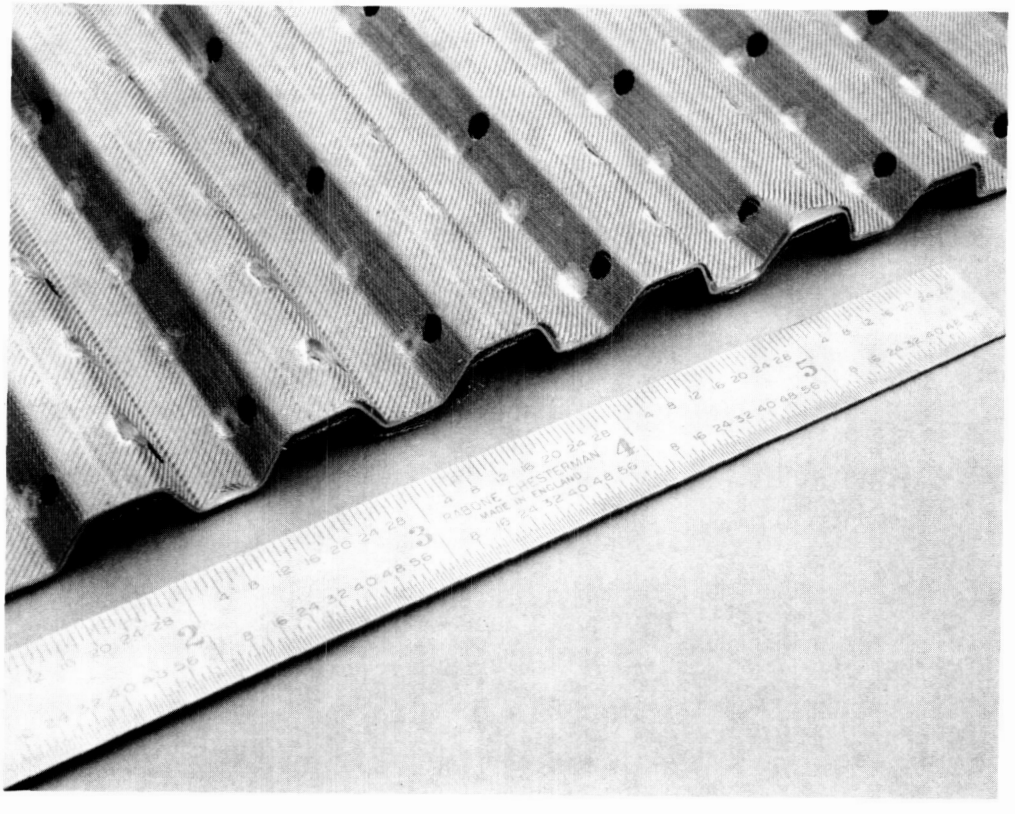

(b) CLOSE-UP OF CORRUGATIONS

Figure 5-21 Corrugated core.

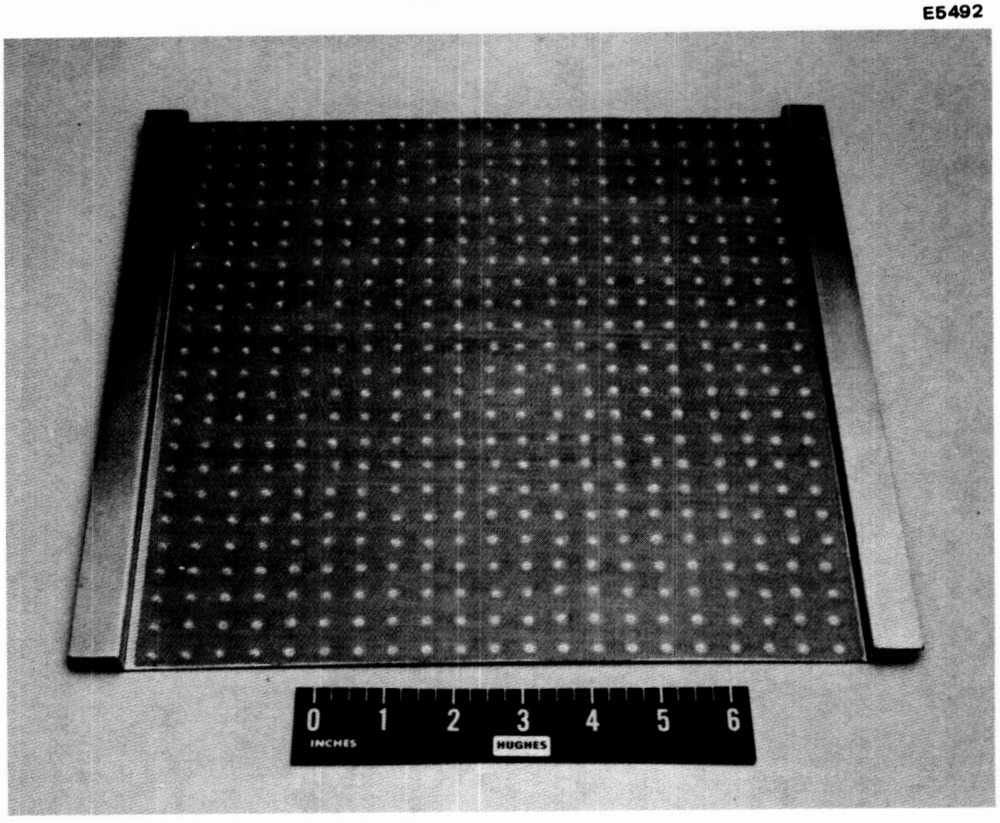

Figure 5-22 Cover facesheet with screen.

E5493

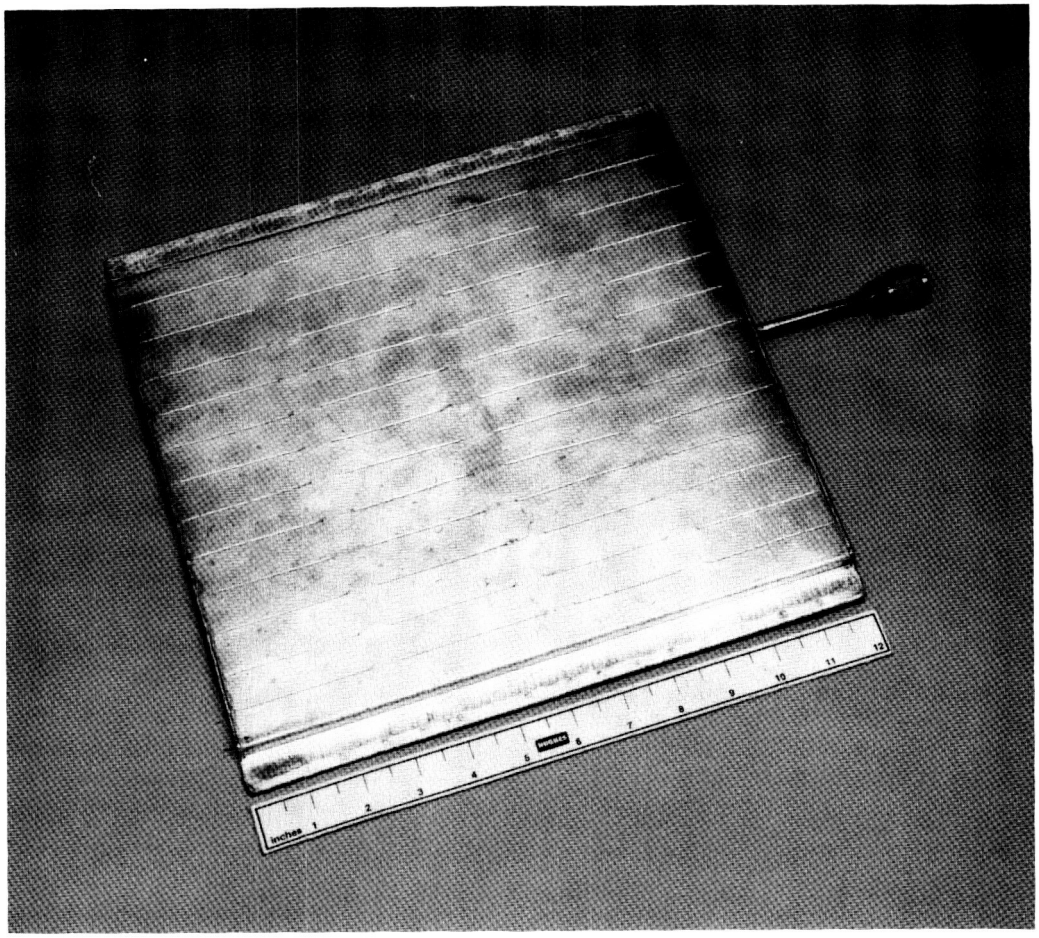

Figure 5-23 Completed channel core panel.

12.70 mm (0.5 inch). These gaps were provided for liquid communication between adjacent liquid-vapor channels. The as-built panel configuration is 0.3 m b- 0.3 m by 10.2 mm thick (12.0 by 12.0 by 0.40 inches) and weighs 9.4 kg/m^2 (1.94 lbm/ft^2), including the weight of the fluid. The dry weight is 8.7 kg/m^2 (1.80 lbm/ft^2).

5.5.3 Thermal Performance Testing

The channel core unit was processed with 65.0 g of HPLC grade acetone. The panel was instrumented per Figure 5-24 and leveled to within ±1.3 mm (0.050 inch). One hundred (100) watts of power was applied to the center heater. Both ambient air and fan cooling were used. The power was increased until an operating temperature of 70°C (158°F) was reached at 325 watts. There was no evidence of dryout at these conditions and the surface temperature varied by only ±0.6°C, as shown in Figure 5-24a. Testing was stopped at 325 watts, however, because the panel was structurally designed for a maximum operating temperature of 70°C (158°F) based on internal pressure. Since the test facility heat sink was limited to this power level, it was not possible to determine the maximum transport capacity of this panel. The test was then repeated with the edge heater tilted 3.17 mm (0.125 inch) above the opposite edge. With a power input of 325 watts into the edge heater, the corresponding temperature data in Figure 5-24b show that surface temperatures varied by only ±1.0°C. Again, testing was stopped at an operating temperature of 70°C (158°F) because of the test facility heat sink limitation.

5.6 SUMMARY

Results from the developmental design phase demonstrated that all designs, channel core, brazed, and formed, would meet the performance requirement of 1000 watts. Design details and tradeoffs are summarized in Tables 5-3 and 5-4 for each design. The formed design is the most inexpensive to fabricate and weighs the least of the three developmental units. It meets both performance and weight ($\leq$7.0 kg/m^2) requirements. The brazed design is limited in panel size because of current vacuum furnace size limits. It would have a poor manufacturing yield based on our results. The major disadvantage of the channel core design is the complexity of fabrication. The panel weight was slightly

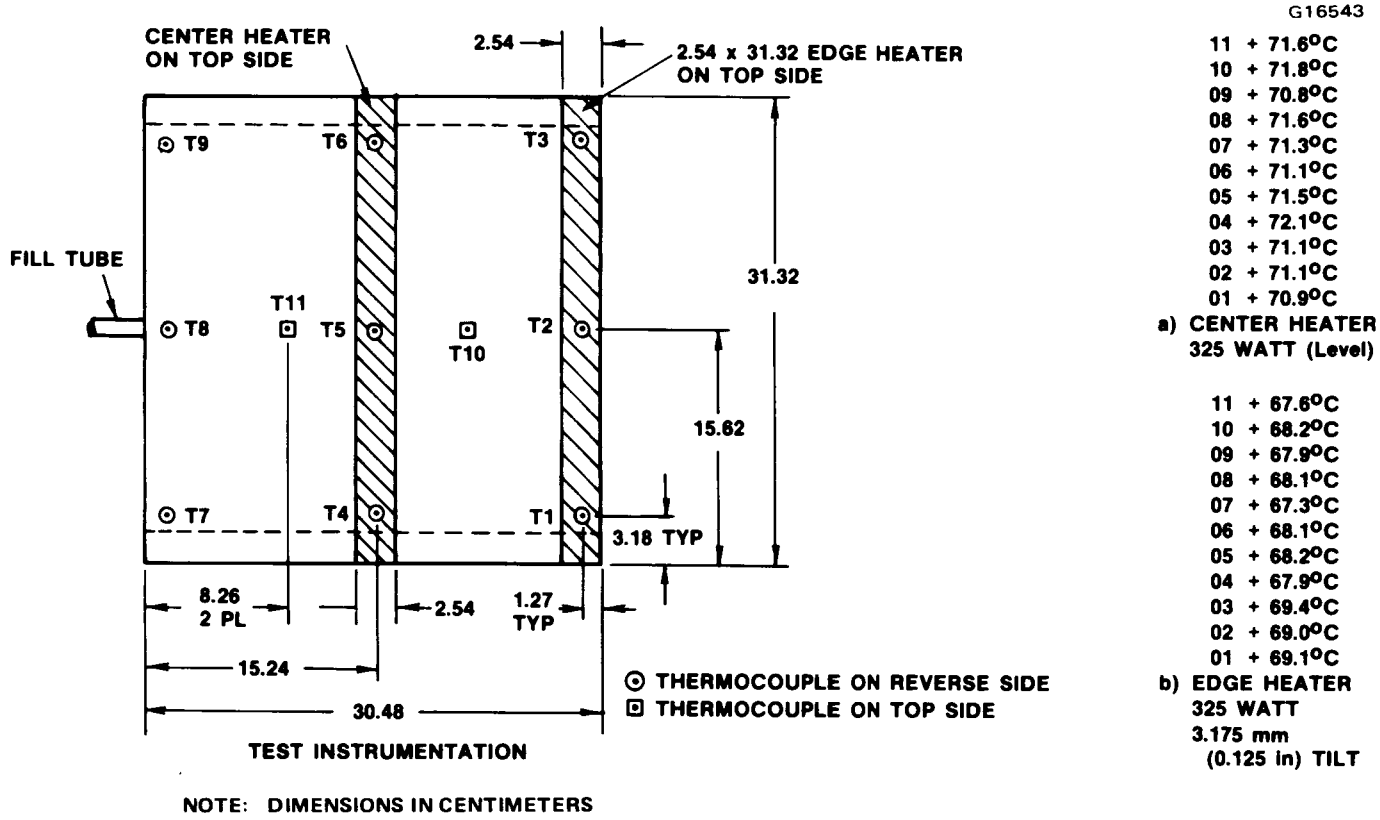

Figure 5-24 Test instrumentation and performance data for channel core panel.

TABLE 5-3

SUMMARY OF DEVELOPMENT UNIT DESIGN DETAILS

Type	Material	Wick	Working Fluid	Nominal Dimensions cm (in.)	Wet Weight kg/m^2 (lbm/ft^2)	Max. Heat Transport* W/m (W/ft)
Brazed	6061, 6101, and 5056 Aluminum	Screen and Foam Metal	Acetone	25.4 x 12.7 x 0.40 (10.0 x 5.0 x 0.16)	7.0 (1.43)	1050 (320)
Formed	6061 Aluminum	Grooves	Acetone	30.5 x 61.0 x 0.38 (12.0 x 24.0 x 0.15)	6.9 (1.41)	394 (120)
Channel Core	6061, 5052 and 5056 Aluminum	Screen and Grooves	Acetone	30.5 x 30.5 x 1.02 (12.0 x 12.0 x 0.40)	9.4 (1.94)	2133** (650)
Honeycomb	316 Stainless Steel	Sintered Screen	Methanol	305.0 x 61.0 x 0.64 (120.0 x 24.0 x 0.25)	9.2 (1.90)	197*** (60)

*Heat transport capacity per unit length for a 61.0 cm (24.0 inch) fin. heated at the centerline; based on thermal convection test results.

**Test facility heat sink limit.

***Extrapolated to 328 W/m (100 W/ft) based on correlated performance prediction model.

TABLE 5-4

DESIGN TRADEOFFS

Type	Advantages	Disadvantages
Brazed	• Not Sensitive to Tilt (Wick Design)	• Low Manufacturing Yield • Limited Size (Due to Furnace Size)
Formed	• Simple to Fabricate (Only Three Parts) • Mounting Holes Can Be Provided at Dimple Locations	• Sensitive to Tilt (Groove Design)
Channel Core	• Potential Lightweight • Highest Heat Transport Capacity • Not Sensitive to Tilt (Wick/Groove Design)	• Heavy Weight Due to Current Manufacturing Requirements • Complexity of Fabrication

in excess of the stainless steel honeycomb panel. However, this was because the burn-through welding technique required the use of thick (heavy) facesheets. With further development, it is felt that the facesheets can be optimized for lighter weight. Core spacing and other materials such as titanium should also be considered for future designs.

Based on the weight and fabrication tradeoffs summarized above, it was concluded that the aluminum prototype panel would consist of ten 0.6 by 0.3 m (24.0 by 12.0 inches) formed design panels. The 10 panels would be welded together, edge-to-edge, to form one 3.0 by 0.6 m (120.0 by 24.0 inches) panel. This modular approach has the advantage of providing redundancy and, therefore, high system reliability.

6.0 ALUMINUM PROTOTYPE PANEL DEVELOPMENT

6.1 DESIGN AND FABRICATION

The design of the 3.0 by 0.6 m (120.0 by 24.0 inch) aluminum prototype panel was based on the formed design development panel described in Section 5.4. The aluminum prototype panel was constructed of ten 0.6 by 0.3 m (24.0 by 12.0 inch) formed panels. The panels were welded together, edge to edge, to form the the 3.0 by 0.6 m aluminum prototype panel.

The formed design panels were fabricated in the same manner as the formed design development panel (Section 5.4). After final welding of each formed panel, mounting slots were machined into the flange of each panel. This was done to facilitate assembly of the ten panels into one 3.0 by 0.6 m aluminum prototype panel. Each formed panel was then manually straightened to remove warpage caused by welding and machining. Next, all of the panels were proof pressure tested at 10 psig for 10 minutes and then were helium leak checked. All units were found to be leak tight to 1×10^{-9} std. cc/sec helium. The ten formed panels were then mounted to an aluminum "T" beam with machine screws for structural support during handling and shipping. The panels were then TIG welded together. To minimize the amount of warpage from the TIG welding, a series of tack welds was used to attach the panels together. Figures 6-1 and 6-2 are photos of the aluminum prototype panel after final assembly. The final panel dimensions are 3.10 by 0.61 m by 3.81 mm thick (122.0 by 24.0 by 0.15 inches) and the panel weighs 7.1 kg/m^2 (1.46 lbm/ft^2), including the weight of the fluid and pinch-off covers. The dry weight is 6.7 kg/m^2 (1.38 lbm/ft^2).

6.2 PROCESSING

After assembly of the 3.1 by 0.6 m (122.0 by 24.0 inch) prototype panel was completed, each of the ten 0.6 by 0.3 m (24.0 by 12.0 inch) formed panels was fitted with a valve and helium leak checked. All ten panels were helium leak tight to 1×10^{-9} std. cc/sec helium. Next, electrical resistance heater tapes were bonded to the panels for use during the burn-in and bakeout process.

E5502

Figure 6-1 Aluminum prototype panel with "T" beam.

E5437

Figure 6-2 Aluminum prototype panel - dimpled surface.

Based on low temperature (-20°) thermal performance testing on the formed design development panel (Section 5.4), it was determined that additional fluid was required for low temperature testing. The fills used for the prototype panel were increased by 10 percent from the optimized (65°C) development panel fill of 38.5 to 42.4 g. This was done to compensate for fluid shrinkage at -20°C.

Each panel was processed by vacuum distillation with 42.5 g of high performance liquid chromatography (HPLC) grade acetone (99.997 percent pure). The panels were then burned in for 12 hours at 65°C. After burn-in, the acetone fills were drained, and each panel was vacuum (1×10^{-6} torr) baked for 2 hours at 100°C. The units were then reprocessed with 42.5 g of HPLC-grade acetone. After final processing, each panel was subjected to a vacuum degassing procedure. The degassing was accomplished by wrapping the panels with thermal insulation and soaking the insulation with liquid nitrogen. When the panels were sufficiently cooled ($\sim -100^{\circ}$C), the valves were opened to vacuum to vent any noncondensable gas.

After processing, the prototype panel was bench tested. During bench testing, it was found that additional fluid had to be added to some of the panels. The extra fluid was required to compensate for variations in groove depth and panel flatness. Because each facesheet was individually machined, some varaition in groove depth did occur. The nominal groove depth was 0.305 mm (0.012 inch) with a tolerance of ±0.051 mm (0.002 inch). Variations in groove depth of 0.254 to 0.356 mm (0.010 to 0.014 inch) can vary the panel fluid fills by 40 percent. Variations in panel flatness can also affect panel fluid fills. On average, the panels are flat to within ±1.27 mm (0.050 inch). Localized low spots can cause groove drainage and fluid puddling. Table 6-1 shows the final fill of each 0.6 by 0.3 m (24 by 12.0 inch) formed panel.

TABLE 6-1

PANEL FILL DATA

Panel No.	Acetone Fill (g)
1	42.4
2	42.4
3	59.7
4	42.4
5	62.7
6	42.4
7	55.0
8	61.3
9	42.4
10	60.5

6.3 THERMAL PERFORMANCE TESTING

After final processing of the prototype panel was completed, the panel was instrumented, and the following series of tests was performed on the prototype panel to characterize its performance:

- High temperature test
- Low temperature test
- Tilt test.

Both the high temperature performance (65°C) and tilt tests were conducted in laboratory ambient air. For low pressure performance testing, the aluminum prototype panel was installed in a low temperature (-20°C) test chamber previously developed for the stainless steel honeycomb panel. The test equipment, methods, and heat transport performance results are described in the following sections.

6.3.1 Test Setup

The test setup which was used for the stainless steel honeycomb panel performance testing was also used for testing the prototype aluminum panel. This test setup is shown schematically in Figure 4-11. As previously described, the heat sink required for low temperature testing at -20°C (-4°F) is provided by six 0.20 m (8.0 inch) wide flanged aluminum extrusions with 25.4 mm (1.0 inch) diameter coolant passages. Three extrusions are placed above the test panel and three below for heat rejection from both sides of the panel. The flanged surfaces of the extrusions facing the test unit were painted with flat black paint. For low temperature testing, the panel was enclosed in a 3.35 m long by 0.76 m wide by 0.61 m high (132.0 by 30.0 by 24.0 inch) Plexiglas chamber. Note that this is not a vacuum chamber. Heat transfer from the heat pipe to the heat sink is by radiation and natural convection. Cooling was provided by flowing gaseous nitrogen from a liquid nitrogen dewar container through the coolant passages of the aluminum extrusions described above.

In high temperature testing, at temperatures up to 70°C (158°F), the top three extrusions were removed for efficient convection and radiation cooling to the laboratory ambient air. The panel is centered approximately 76.2 mm (3.0 inches) from the flanged surfaces of the heat sinks, using a total of eight adjustable plexiglas support legs. Figure 6-3 is a photograph of the test fixture being used for ambient testing. The Plexiglas chamber is located below the test fixture in this photograph. Note that the aluminum "T" beam used for support was thermally isolated from the panel with 12.7 mm (0.50 inch) thick phenolic spacer blocks.

Thirty copper-Constantan (Type T) foil thermocouples were taped directly to the prototype heat pipe panel surface with Kapton tape at the locations shown in Figure 6-4. Each thermocouple was covered with ceramic paper to ensure good thermal contact and to minimize the effect of convection currents on temperature readings. Note that in Figure 6-4 there are three thermocouples on each 0.6 by 0.3 m (24.0 by 12.0 inch) formed panel. One thermocouple is located on the top surface next to the center heater, and the remaining two thermocouples are located on the bottom surface, near the outer edges of the panel.

E5500

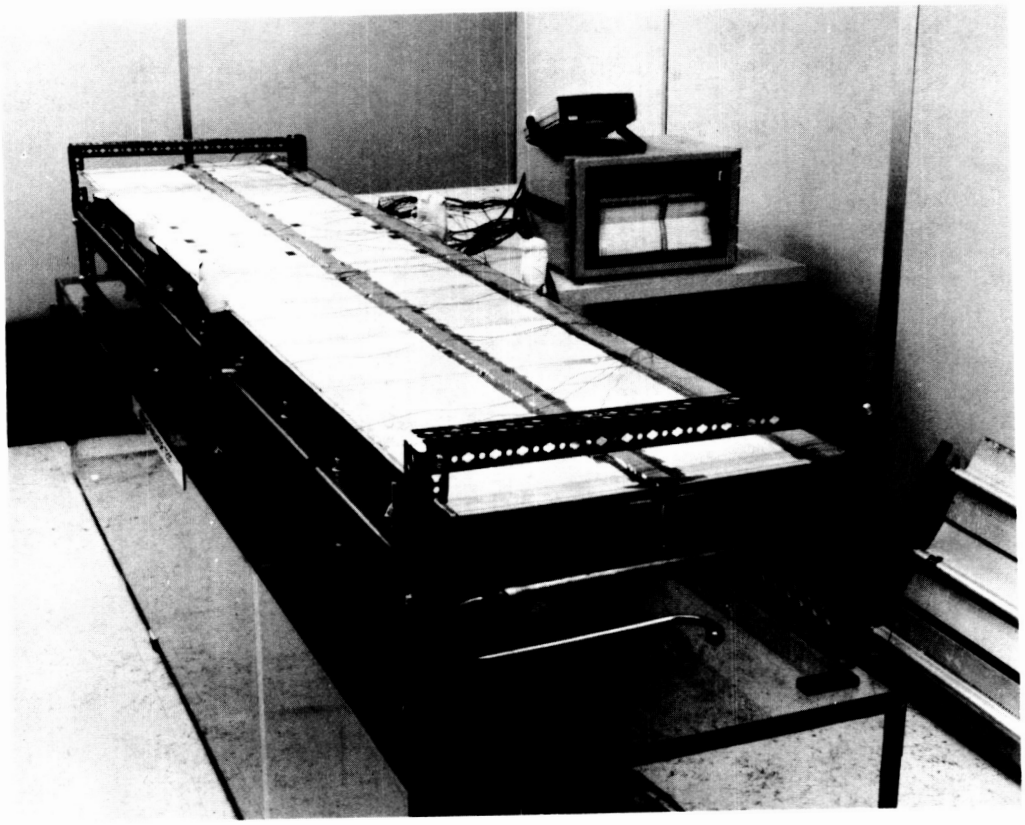

Figure 6-3 Performance test station.

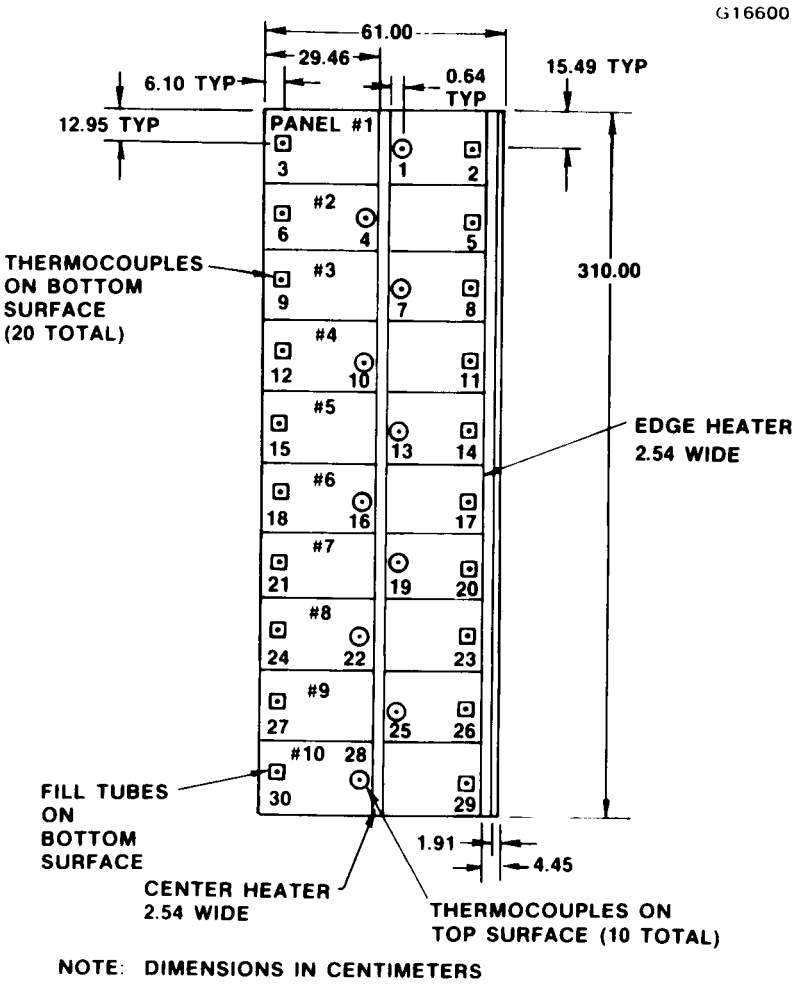

Figure 6-4 Prototype panel heat pipe instrumentation.

Heat input was provided by the center and edge heaters. The center heater was used for both the high and low temperature thermal performance tests. The edge heater was used for tilt testing. The heater assemblies consist of four 6.35 mm (0.25 inch) wide Clayborne Labs heater strips (Part Number E-16-2), wired in parallel. This is equivalent to a 25.4 mm (1.0 inch) wide heater strip. The heaters span the entire length of the panel (Figure 6-4). The center heater simulates a high capacity transport heat pipe or pumped loop. The edge heater was used for tilt testing, which determines the heat pipe's sensitivity to adverse tilts.

6.3.2 High Temperature Performance Testing

For the high temperature test, the panel was leveled to within ±1.27 mm (0.050 inch) in the test fixture with the three top cooling channels removed (Figure 6-3). Input power of 600 watts was initially applied to the center heater (Figure 6-4) with ambient air as the heat sink. The power was then increased in 100-watt increments until 1000 watts was reached with no signs of dryout. Testing was stopped at 1000 watts because of a heat sink limitation. The panel was designed to operate below 70°C. Corresponding temperature data are shown in Table 6-2 and Figure 6-5. Results are also plotted in Figure 6-6, along with computer predictions.

From Table 6-2, it can be seen that individual panel ΔTs varied from a low of 0.1°C to a high of 7.7°C. The average ΔT was 2.3°C. Variations in average panel temperature resulted from air currents in the lab causing uneven convective cooling. Thermal testing in a vacuum environment would eliminate this uneven cooling effect.

To determine the cause of the higher ΔTs, a tilt test was performed on Panel No. 5, which had a ΔT of 7.7°C. The objective was to determine whether fluid or noncondensable gas caused the high ΔT. Panel No. 5 was instrumented per Figure 6-7 and leveled to ±1.27 mm (0.050 inch). Input power of 700 watts was applied to the prototype panel (equivalent to 70 watts for Panel No. 5) with ambient air cooling. After reaching steady state, temperature data for Panel No. 5 were recorded (Figure 6-7). These data show that there is a cold

TABLE 6-2

PROTOTYPE HEAT PIPE RADIATOR HIGH TEMPERATURE PERFORMANCE TEST

POWER: 1000 WATTS

Panel No.	Thermocouple No.	Temperature (°C)	ΔT(°C)	Panel No.	Thermocouple No.	Temperature (°C)	ΔT(°C)
1	1	67.4	0.2	6	16	72.9	1.3
	2	67.5			17	73.9	
	3	67.6			18	74.2	
2	4	70.7	0.1	7	19	74.1	0.2
	5	70.6			20	73.9	
	6	70.7			21	73.9	
3	7	73.0	5.6	8	22	73.2	3.9
	8	67.4			23	69.9	
	9	71.1			24	73.8	
4	10	73.5	0.7	9	25	72.5	0.9
	11	73.1			26	71.6	
	12	73.8			27	72.6	
5	13	74.6	7.7	10	28	70.1	2.1
	14	66.9			29	68.0	
	15	72.9			30	69.9	

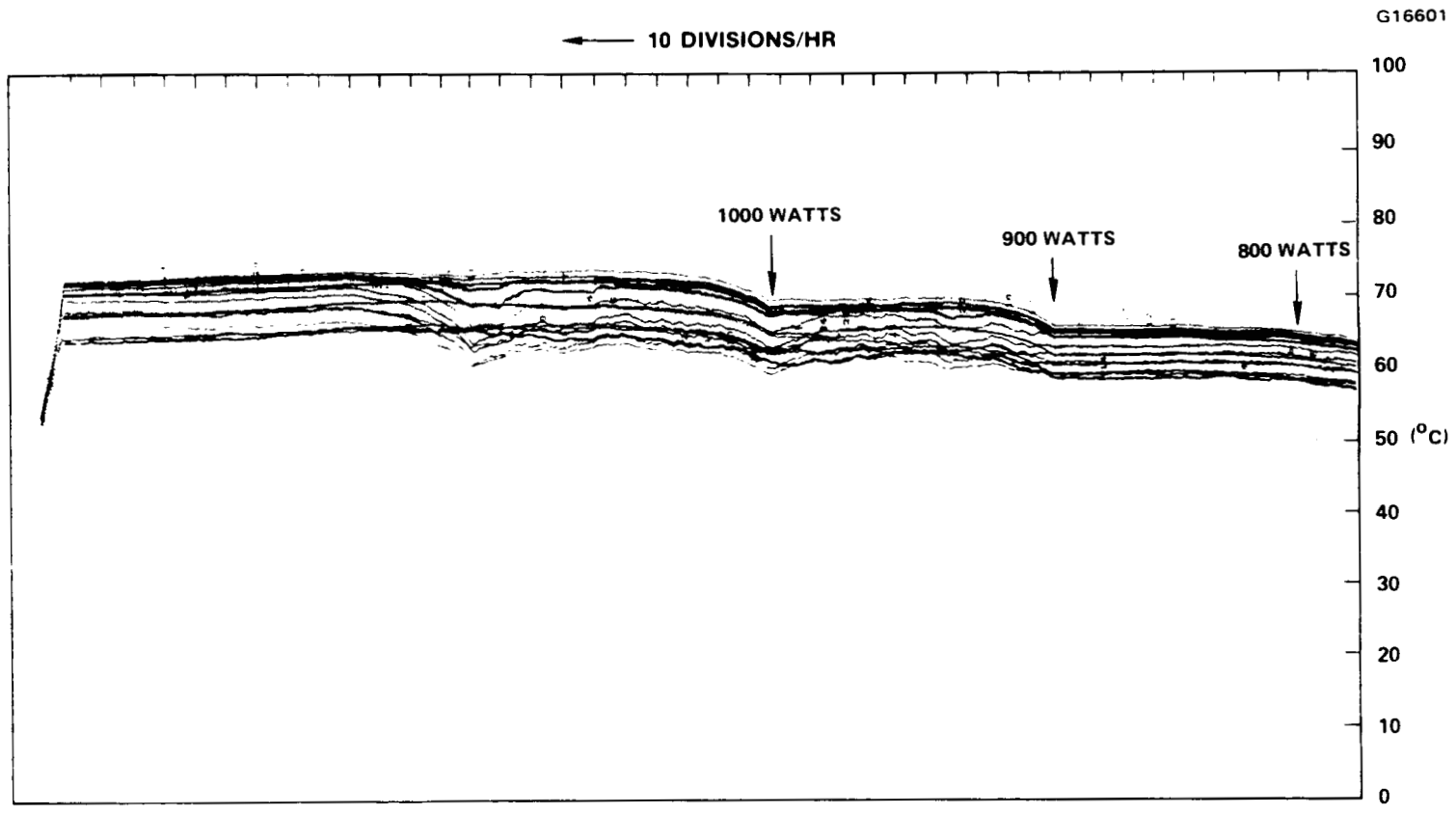

Figure 6-5 High temperature performance test.

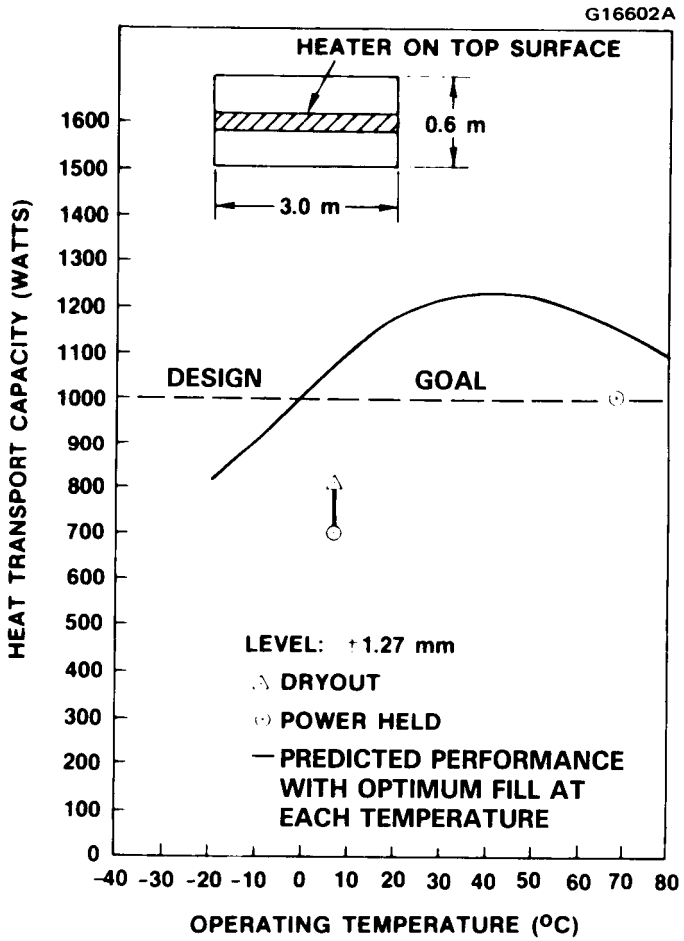

Figure 6-6 Prototype panel thermal performance test results.

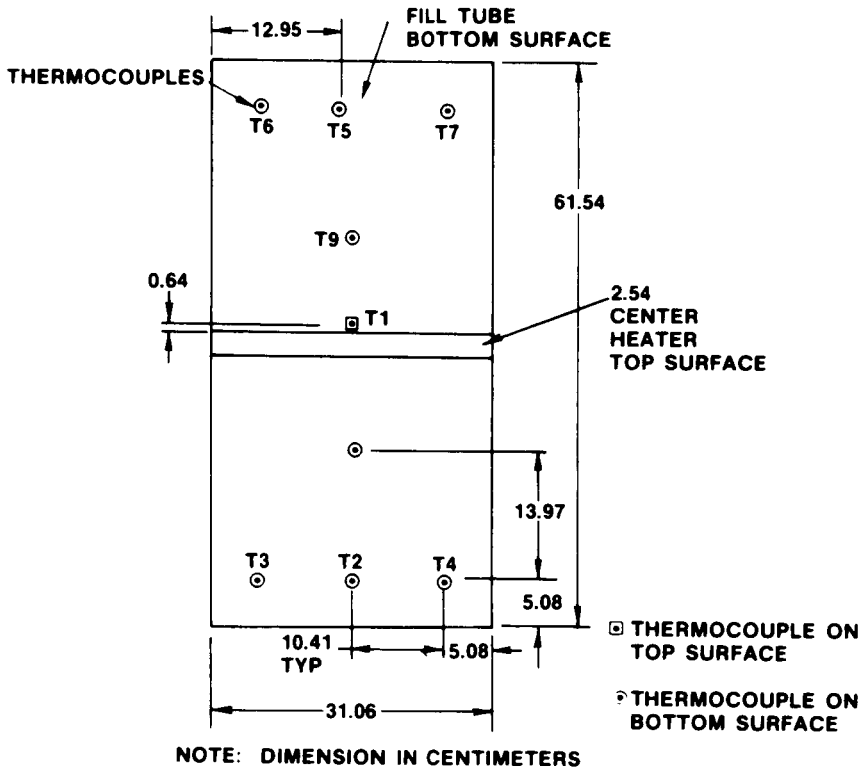

G16603

TEMPERATURE DATA

09	+61.4°C	09	+59.9°C
08	+61.4°C	08	+62.9°C
07	+61.5°C	07	+53.8°C
06	+61.4°C	06	+55.3°C
05	+60.1°C	05	+53.7°C
04	+61.4°C	04	+62.9°C
03	+61.4°C	03	+62.8°C
02	+56.3°C	02	+62.8°C
01	+61.4°C	01	+62.7°C
	700 Watts (LEVEL)		700 WATTS (1/2" TILT)

FLATNESS DATA

09	0.000 IN.
08	-0.020 IN.
07	+0.020 IN.
06	-0.030 IN.
05	0.000 IN.
04	+0.020 IN.
03	-0.070 IN.
02	-0.050 IN.
01	0.000 IN.

Figure 6-7 Excess fluid test panel number 5.

spot at the location of thermocouple No. 2. The panel edge, where thermocouple No. 2 was located, was then lifted 12.7 mm (0.50 inch) above the opposite panel edge to see if any temperature changes would occur. Immediately after lifting the panel, the temperature at thermocouple No. 2 increased by 6°C. This was clear evidence of a fluid puddle. Corresponding flatness data for Panel No. 5 (Figure 6-7) show that the outer panel edges are lower than the middle of the panel. It can be concluded that any localized low spots in the panel will have a tendency to drain the surrounding grooves of fluid and cause a fluid puddle to occur.

6.3.3 Low Temperature Testing

For low temperature testing, the top three coolant channels were installed on the test fixture as previously stated. The test setup was then placed in the low temperature Plexiglas test chamber and leveled to within ±1.27 mm (0.050 inch). Nitrogen vapor from a liquid nitrogen dewar container was then passed through both the top and bottom coolant channels. The flow through the bottom channels was in the opposite direction of flow as compared to the top channels. After cooldown to approximately -20°C (-4°F), 300 watts was applied to the center heater. The power was increased in 100 watt increments until dryout was observed. The panel held 700 watts, and dryout occured at 800 watts. Table 6-3 shows the temperature data recorded at 700 watts. Results are also plotted in Figure 6-6 along with computer predictions.

6.3.4 Tilt Testing

For tilt testing, the panel was first leveled in the test fixture (top cooling channels removed) to within ±1.27 mm (0.050 inch) for the zero tilt condition. Power input of 200 watts was then applied to the edge heater (Figure 6-4) with ambient air cooling. Power was then increased in 50 watt increments until dryout. The panel held 300 watts before dryout was observed at 350 watts. This test was then repeated for 3.17 mm (0.125 inch) and 6.35 mm (0.25 inch) tilts. Results of these tests are plotted in Figure 6-8.

TABLE 6-3

PROTOTYPE HEAT PIPE RADIATOR LOW TEMPERATURE PERFORMANCE TEST

POWER: 700 WATTS

Panel No.	Thermocouple No.	Temperature (°C)	ΔT(°C)	Panel No.	Thermocouple No.	Temperature (°C)	ΔT(°C)
	1	4.4			16	12.6	
1	2	2.1	2.3	6	17	11.8	1.1
	3	2.2			18	11.5	
	4	3.5			19	11.3	
2	5	3.1	1.8	7	20	12.0	0.7
	6	1.7			21	12.4	
	7	6.3			22	12.0	
3	8	-0.5	6.8	8	23	6.6	5.4
	9	1.1			24	10.3	
	10	7.7			25	10.9	
4	11	6.9	0.8	9	26	6.6	4.3
	12	7.5			27	7.4	
	13	11.9			28	7.2	
5	14	5.7	6.2	10	29	0.2	7.0
	15	9.2			30	5.4	

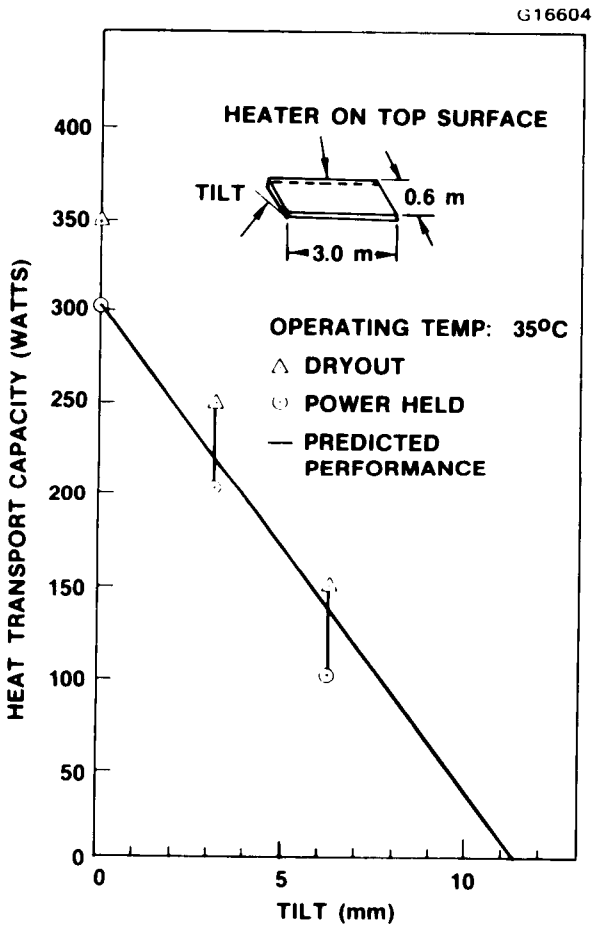

Figure 6-8 Prototype panel tilt test results.

C-2

6.3.5 Burst Pressure Test

The burst pressure test was performed on a 0.6 by 0.3 m (24.0 by 12.0 inch) formed design panel. The panel was identical to the individual panels used in the fabrication of the 3.0 by 0.6 m (120.0 by 24.0 inch) aluminum prototype panel. Prior to testing, the burst unit was helium leak checked, and the panel thickness was measured and recorded at 15 reference locations. The panel was then placed in a safety chamber and was internally pressurized with nitrogen gas.

Pressure was applied in 10 psig increments, holding for 30 minutes at each pressure level, until 100 psig was reached. Then, the pressure was increased in 20 psig increments. After each pressure level, the pressure was released, and the panel was removed from the safety chamber to record any permanent deformations. The burst unit was also helium leak checked to verify that no leaks occurred.

The resistance spot welds failed at approximately 160 psig, as the pressure was being increased from 160 to 180 psig. There was no evidence of permanent deformation prior to burst. This results in a factor of safety of 6.9 for acetone at a maximum temperature of 70°C. Such a large safety factor means that this unit is heavier than necessary. The design can be further refined to achieve even lighter weight panels in the future. Figures 6-9a and 6-9b are photos of the burst unit before and after burst testing.

E5501

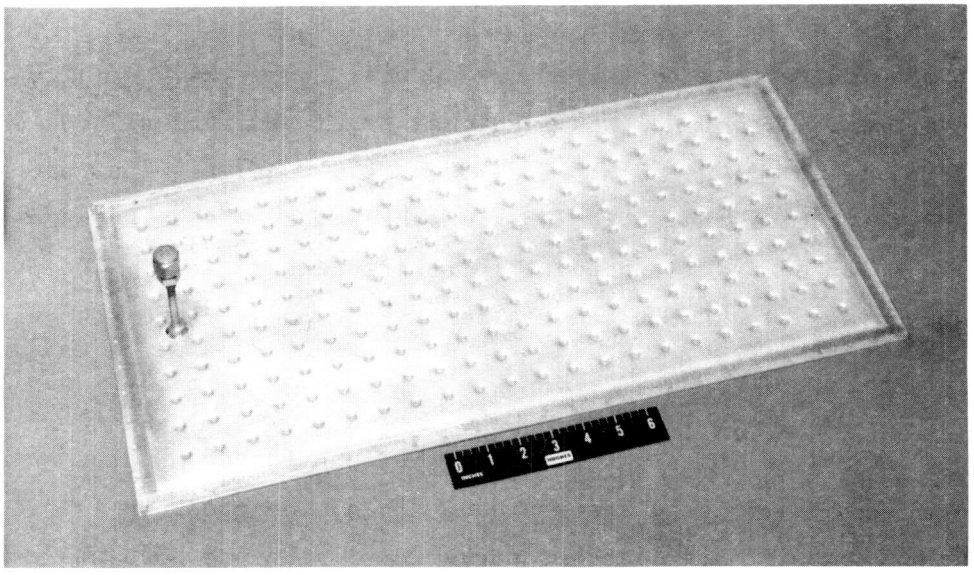

(a) BURST UNIT BEFORE BURST TEST

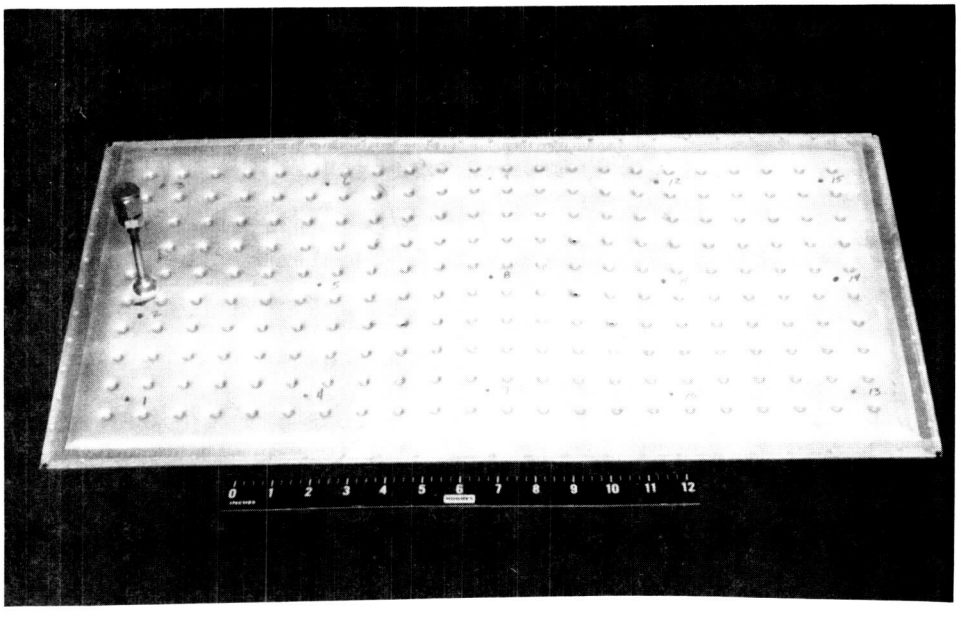

(b) BURST UNIT AFTER BURST TEST

Figure 6-9 Photograph of burst pressure unit.

7.0 CONCLUSIONS AND RECOMMENDATIONS

Both the stainless steel honeycomb and the aluminum heat pipe radiator panels were successfully fabricated and tested. Thermal performance testing demonstrated a fin efficiency of approximately 1.0 for both panels. Table 7-1 is a summary of the stainless steel panel and the aluminum panel developmental results.

A heat transport capacity of 600 watts at 50°C was achieved for the 3.0 by 0.6 m (120.0 by 24.0 inches) stainless steel prototype panel, with methanol as the working fluid. The heat pipe panel was isothermal to within ±1.5°C throughout the entire active surface. However, the heat transport capacity fell short of the design goal of 1000 watts, primarily because the vapor holes were punched in every other crimp of the core ribbon material, rather than every crimp as originally specified. This restricted vapor flow movement and reduced the overall performance. Analysis with a model correlated to the as-built panel test results predicts that the 1000 watt goal can be exceeded by simply including the correct number and distribution of vapor holes in the honeycomb ribbon material.[7,8]

TABLE 7-1

SUMMARY OF PROTOTYPE PANEL HEAT PIPE RESULTS

	Honeycomb Design (Stainless Steel)	Formed Design (Aluminum)
Materials	316 Stainless Steel	6061 Aluminum
Wick Type	Screen	Grooves
Working Fluid	Methanol	Acetone
Nominal Dimensions cm (in.)	305.0 x 61.0 x 0.64 (120.0 x 24.0 x 0.25)	310.0 x 61.0 x 0.38 (122.0 x 24.0 x 0.15)
Wet Weight kg/m^2 (lbm/ft^2)	9.2 (1.90)	7.1 (1.46)
Thermal Performance	Max Transport 600 watts at 50°C (Test results of as-built panel; analysis indicates 1000 W for current design).	1000 watt at 70°C; no dryout observed, heat sink limited

The 3.1 by 0.6 m (122.0 by 24.0 inches) aluminum heat pipe prototype panel held 1000 watts at 70°C with acetone as the working fluid. No dryout was observed because the test facility heat sink limit was reached at 1000 watts. The individual panel ΔTs varied from a low of 0.1°C to a high of 7.7°C. The average panel ΔT was 2.3°C. The prototype aluminum panel meets both performance and weight ($\leq$7.0 Kg/m^2) requirements. Moreover, fabrication and test results indicate that further reductions in weight are possible.

Although the prototype panel heat pipes described in this report were developed as space radiator fins, panel heat pipes have many other applications. As spacecraft heat loads increase, more efficient heat sinking methods are required. The application of heat pipe technology to the design of spacecraft shelves is one area of importance. Panel heat pipes can also be used as isothermal coldplates for space experiments or cooling electronics. Electronic packages can be mounted to the coldplate, which can then be "plugged" into a waste heat thermal bus.

The current effort has demonstrated that the fabrication of lightweight aluminum heat pipe panels is feasible using state-of-the-art technology and equipment. Areas that will require further development before flight designs can be finalized are:

1. Optimize module design
2. Integration methods
3. Life testing.

Optimize Module Design - Before fabrication of a flight-ready aluminum heat pipe radiator fin can begin, the following design parameters must be defined: module size, flatness, interface and fill tube locations, mounting methods, surface finishes, and structural (stiffness) requirements. One of the most important design parameters listed is module size. The current aluminum prototype radiator heat pipe fin consists of ten 0.6 by 0.3 m (24.0 by 12.0 inches) panels combined to form one 3.1 by 0.6 m (122.0 by 24.0 inches) panel. From a cost and logistics point of view, however, it is desirable to have larger heat pipe panels.

Preliminary investigations have shown that individual panels on the order of 0.6 m (24.0 inches) wide by 1.2 to 1.5 m (48.0 to 60.0 inches) long can be achieved with current fabrication techniques. This would significantly reduce the amount of heat pipe processing and assembly time for a given radiator module. Wider fin lengths, greater than 0.6 m (24.0 inches), will require heat pipe panels with improved performance. This can be achieved by the use of deeper grooves or the channel core panel, which has the highest heat transport performance. The use of screen material that is sintered, brazed, or spot welded to the groove facesheets could also improve overall performance for wide heat pipe fins.

As previously described, thermal performance test results showed that variations in panel flatness can cause fluid puddling in 1-g testing. The welding and machining processes cause distortions in the panel surface. For the aluminum prototype panel, all ten 0.6 by 0.3 m (24.0 by 12.0 inches) formed panels were straightened manually. This process was inefficient and lacked precision. As panel sizes are increased, a more efficient and precise method of panel straightening will be required.

Investigations into alternate fabrication methods and materials are recommended for further cost and weight savings. Advanced methods of fabrication, such as roll-bond techniques or chemical milling of grooves, are ways of reducing fabrication costs and allowing even larger (>1.5 m long) module sizes. Also, switching to 7000 series aluminum or graphite reinforced aluminum could reduce weight by as much as 20 percent.

Integration Methods - Mounting of the heat pipe radiator panels to the transport heat pipe will require additional development. Ease of system assembly for on-orbit fabrication and repair will be critical. Attachment methods must be simple, yet provide good thermal contact between the radiator panels and the transport heat pipe. Methods of attachment, such as stud welding of fasteners or drilling of mounting holes, must be developed. Also, required surface finishes, clamping pressures, and use of interstitial materials, such as plated tin and loaded epoxies to reduce thermal resistances, will need to be addressed.

Life Testing - Current literature on aluminum/acetone compatibility is limited. Our experience with the aluminum prototype panel shows promising results. However, a life testing program using aluminum alloys with acetone as the working fluid will be required to verify compatibility. Several life test panels are recommended.

8.0 REFERENCES

1. Ellis, W.E., and Rankin, J.G., "Heat Rejection Development Requirements for Orbital Power Systems," Paper No. 799295, 14th Intersociety Energy Conversion Engineering Conference, August 1979.

2. Oren, J.A., "Study of Thermal Management for Space Platform Applications," NASA CR-165238, December 1980.

3. Oren, J.A., "Study of Thermal Management for Space Platform Applications: Unmanned Module Thermal Management and Radiator Technologies," NASA CR-165307, May 1981.

4. Rankin, J.G., and Marshall, P.F., "Thermal Management System Technology Development for Space Station Applications," Paper No. 831097, 13th Intersociety Conference on Environmental Systems, July 1983.

5. Basiulis, A., and Camarda, C.J., "Design, Fabrication and Test of Liquid Metal Heat-Pipe Sandwich Panels," AIAA Paper No. 82-0903, AIAA/ASME 3rd Joint Thermophysics, Fluids, Plasma and Heat Transfer Conference, June 1982.

6. Tanzer, H.J., "High Capacity Honeycomb Panel Heat Pipes for Space Radiators," AIAA Paper No. 83-1430, June 1983.

7. Tanzer, H.J., Fleischman, G.L., and Rankin, J.G., "Honeycomb Panel Heat Pipe Development for Space Radiators," AIAA Paper No. 85-0978, AIAA 20th Thermophysics Conference, June 1985.

8. Fleischman, G.L., and Tanzer, H.J., "Advanced Radiator Concepts Utilizing Honeycomb Panel Heat Pipes (Stainless Steel)," Interim Technical Report, NASA Contract NAS9-16581, W-30746, August 1985.

9. Rankin, J.G., "Space Station Thermal Management System Development Status and Plans," SAE Paper 851350, July 1985.

10. Astech Division of TRE Corp., Santa Ana, Calif.

11. Tanzer, H.J., "Fabrication and Development of Several Heat Pipe Honeycomb Sandwich Panel Concepts," NASA CR 165962, June 1982.

12. Camarda, C.J., and Basiulis, A., "Radiant Heating Tests of Several Liquid Metal Heat-Pipe Sandwich Panels," AIAA Paper No. 83-0319, January 1983.

13. Chi, S.W., "Heat Pipe Theory and Practice," McGraw-Hill Book Company, New York, 1976.

14. Roark, R.T., and Young, W.C., "Formulas for Stress and Strain," 5th Ed., McGraw-Hill Book Company, New York, 1982.

15. Fleischman, G.L. "High Power Spacecraft Thermal Management," Final Test Report, Air Force Contract F33615-85-C-2557, October 1987.

1. Report No.	2. Government Accession No.	3. Recipient's Catalog No.

4. Title and Subtitle	5. Report Date
Advanced Radiator Concepts Utilizing Honeycomb Panel Heat Pipes	October 1987
	6. Performing Organization Code
7. Author(s)	8. Performing Organizatior Report No.
G. L. Fleischman, S. J. Peck and H. J. Tanzer	W-30746
	10. Work Unit No.
9. Performing Organization Name and Address Hughes Aircraft Company Electron Dynamics Division, P.O. Box 2999 Torrance, CA. 90509-2999	11. Contract or Grant No. NAS 9-16581
	13. Type of Report and Period Covered Final Technical Report June 1982 - June 1987
12. Sponsoring Agency Name and Address National Aeronautics and Space Administration Lyndon B. Johnson Space Center Houston, TX 77058	14. Sponsoring Agency Code

15. Supplementary Notes

Technical Monitor: J. G. Rankin

16. Abstract

The feasibility of fabricating and processing moderate temperature range vapor chamber type heat pipes in a low mass honeycomb panel configuration for highly efficient radiator fins for potential use on the NASA space station was investigated. A variety of honeycomb panel facesheet and core-ribbon wick concepts were evaluated within constraints dictated by existing manufacturing technology and equipment. Concepts evaluated include: type of material, material and panel thicknesses, wick type and manufacturability, liquid and vapor communication among honeycomb cells, and liquid flow return from condenser to evaporator facesheet areas. A thin-wall all-welded stainless steel design with methanol as the working fluid was the initial prototype unit. This unit was 120 x 24 x 1/4 inches, and weighed 1.9 lb_m/ft^2, including the fluid fill. After successful demonstration of the stainless steel honeycomb panel, a lighter weight aluminum panel was designed and fabricated with acetone as the working fluid. It was found that an aluminum panel could not be fabricated in the same manner as the stainless steel panel due to diffusion bonding and resistance welding considerations. Therefore, a formed and welded designed was developed. The prototype unit consists of ten individual 24 x 12 x 0.15 inch panels (modules) that are welded together to form one large panel. The overall panel is 122 x 24 x 0.15 inches and weighs 1.46 lb_m/ft^2, including the fluid fill. These prototype panels have a heat rejection capability of 1000 watts with a fin efficiency of essentially 1.0.

17. Key Words (Suggested by Author(s))	18. Distribution Statement
Heat Pipes Vapor Chambers Space Radiators Spacecraft Thermal Management	

19. Security Classif. (of this report)	20. Security Classif. (of this page)	21. No. of pages	22. Price*
UNCLASSIFIED	UNCLASSIFIED	105	

*For sale by the National Technical Information Service, Springfield, Virginia 22161